Exploring the effect of spermidine on early vascular and reproductive development in methylthioadenosine nucleosidase deficient plant embryos

by

Asuramuni Nimhani Perera

A thesis
presented to the University of Waterloo
in fulfillment of the
thesis requirement for the degree of
Masters of Science
in
Biology

Waterloo, Ontario, Canada, 2019

Authors Declaration

I hereby declare that I am the sole author of this thesis. This is a true copy of the thesis, including all required final revisions, as accepted by my examiners.

I understand that my thesis may be made electronically available to the public.

Abstract

Polyamines (PA) are associated with many critical developmental processes, but their mode of action is not known. Biosynthesis of polyamines, ethylene and nicotianamine produce 5'-methylthioadenosine (MTA) as a by-product. In *Arabidopsis thaliana*, MTA is hydrolyzed to adenine and methylthioribose (MTR) by two forms of 5'-methylthioadenosine nucleosidase (MTN), MTN1 and MTN2 as part of the Yang cycle. *A. thaliana* mutants deficient in *MTN* activity display a complex phenotype that is correlated with accumulation of MTA and an altered polyamine profile. The complete loss-of function *MTN* mutants are lethal. A mutant with approximately 14% residual *MTN* activity (*mtn1-1mtn2-1*) has a pleiotropic complex phenotype including male and female sterility, interveinal chlorosis in young leaves, dark green and twisted mature leaves, reduced auxin transport and vascular abnormalities. A slightly less severe mutant with ~28% residual *MTN* activity (*mtn1-1mtn2-5*) is fertile and has a more moderate phenotype.

Analysis of developing seeds and reproductive organs of the *mtn1-1mtn2-1* mutant revealed its abnormal embryo sac and integument formation as well as undehisced anthers and weak pollen germination. A large scale study conducted to confirm observations made in a previous study showed that exogenous feeding of the polyamine spermidine (Spd) during initial 14 days post germination, can improve the fertility of the severe MTN-deficient mutant. Examining early vascular markers (*AtHB8*) and auxin response reporters (*MP*, DR5) in the severe and moderately deficient *MTN* mutant embryos have shown developmental disruption of vascular tissue and hormone gradients.

The findings presented in this thesis showed the effect of Spd supplementation on MTN-deficient mutants in the areas of reproductive tissue development, ovule and pollen health, embryo vascular development and hormone distribution, as well as vascular bundle arrangement in mature main bolt. Severe mutant plants (*mtn1-1mtn2-1*) supplemented with 100 µM Spd show restored fertility in random branches. The cell arrangement and shape in the integument layers of the *mtn1-1mtn2-1* mutant ovules showed significant improvement and pollen viability is also increased. It is proposed that the partial fertility of branches of adult *mtn1-1mtn2-1* mutant plants is due to the later release of conjugated Spd, acquired at the very early stages during supplementation.

Early vascular marker and auxin response reporter expression in MTN-deficient mutant embryos showed improvement of procambial cell activation and auxin mobility with Spd treatment. Vascular bundle number, shape and arrangement in the main bolt of MTN-deficient mutant plants showed improvements with Spd supplementation. The bundle number was reduced and the arrangement was more symmetrical, restoring a more wild type phenotype. It is possible that Spd supplementation partially restored vascular abnormalities via restoration of auxin distribution at the initial vascular development during embryogenesis.

The eukaryotic translation initiation factor 5A (eIF5A) is implicated in vegetative and reproductive growth and development. Spd supplementation during the early development of the mutants showed improvement in both reproductive and vegetative development. The *mtn1-1mtn2-5* mutants were phenotypically larger and more robust upon Spd supplementation. This is consistent with overexpression mutants of eIF5A. Other eIF5A mutants have displayed male infertility and poor pollen health. The infertility of the MTN-deficient mutant can be attributed to

insufficient availability of active eIF5A due to reduced PA biosynthesis.

Taken together these results suggest the existence of a strong relationship between the MTA induced deficiency of Spd and the reproductive and vascular development of *A. thaliana* MTN-deficient mutants.

Acknowledgements

I would like to thank my research supervisor Dr. Barb Moffatt of the University of Waterloo. First and foremost, I would like to thank you for believing in me and giving me the opportunity to study under your guidance as a Masters student. Your office was always open whenever I ran into a question or a problematic spot in my research work. You provided excellent guidance and constructive criticism during the writing of this manuscript, but continuously and consistently allowed this thesis to be my own work. You always steered me in the right direction, even when I did not see it at the time. You have been a very patient and caring mentor, providing guidance not only in my academic life but also as a role model for my personal life. You have helped me in countless ways when I needed support as a supervisor and as a friend. You have guided me to become a better student and a better person. I learnt how to deal with stressful situations, how to face disappointment and to never ever give up under your tutelage. I cannot express how lucky I am to have had a supervisor like you. I cannot thank you enough!

I would also like to thank the two esteemed experts in my supervisory committee, Dr. Frederique Guinel and Dr. Susan Lolle (not in a particular order). You have guided me with countless valuable information, constructive suggestions and insight provided during our meetings as well as personal communications. Your contribution was immensely helpful in making this project a success! I appreciate every input you have given to make this thesis a reality. Thank you!

I would like to extend my appreciation to all the contributors to the project. Without them this work will not be complete!

- Our collaborator Prof. Edward C. Yeung, from the University of Alberta, Calgary. I

humbly thank you for your extreme generosity in embedding and sectioning my samples using a new and improved method at your lab in Calgary at no cost. I highly appreciate your collaboration and contribution to the project and your willingness to answer any query I had regarding my samples. Your input was extremely valuable in drawing certain conclusions during the course of this project. Without your expert technique, my project would be incomplete. Thank you so much for dedicating your time and energy to make my dream a success.

- Dr. Jaideep Mathur, University of Guelph; Dr. Thomas Berleth, University of Toronto and Dr. Enrico Scarpella, University of Alberta. who kindly provided reporter lines that were used in this project.
- Dr. Ishari Waduwara-Jayabahu, former PhD student of the Moffatt lab and initiator of the MTN project. Thank you for introducing me to the Moffatt lab and also for initiating this wonderful project. Without the mutants you had created my project would not be a reality.
- Maye Saechao and Cherry Chen, former members of the Moffatt lab. Thank you for guiding and training me on various methodologies during my initial months at the laboratory. I learnt a great deal from the both of you starting from how to grow *Arabidopsis* to troubleshooting experimental methods. I enjoyed learning from you and will never forget the lessons you taught me. Your guidance, tips and hints provided valuable information when I started this study. Thank you!
- Shuningbo Ye, Eugene Kovalenko, Ben Trembley former undergraduate students of the Moffatt Lab. Thank you so much for your dedication as undergraduate students during your 499 projects in conducting the preliminary experiments that were used to formulate

my project. Juno's findings on embryo vasculature led to the current work published in this thesis. Eugene and Ben were instrumental in developing the new Spd conjugate lines.

Sarah Schoor and Dr. Simon Chuong from the Chuong lab at the University of Waterloo. Thank you for your valuable feedback at lab meetings and helping me in troubleshooting issues during the course of my research. Dr. Chuong, I have to specially thank you for allowing me to use the fluorescent and dissecting microscopes at your lab. Sarah, words are not enough to say how much I appreciate you going out of the way to show me how things work! Thank you both so much!

Dr. Mungo Marsden and Justin from the Marsden lab at the University of Waterloo. I loved coming and working in the microscopy room of your lab. I could spend hours using your microscopes and still not feel tired. It was nice and cool and quiet. Thank you for trusting me with your very expensive equipment!

Mishi Groh and Adrienne Boon, technicians of the Department of Biology, University of Waterloo. Adrienne, Thank you for introducing me to confocal microscopy! I was thoroughly instructed. You were willing to come down with me to help me whenever I had an issue. Mishi, thanks for being there when Adrienne left. You have been wonderful, both as a technician and a dear friend to me. I will never forget your help during my hunt for baby items during my pregnancy! Thank you so much!

Dr. Kirsten Muller, Associate Dean, Graduate studies. Dear Kirsten, I would not be here today if it was not for you and April. You motivated me, lifted my spirits and gave me hope when I was ready to give up. You showed me how to get help and how to deal with my problems at the time.

The most important thing of all was your attitude. There was no judgment about my situation. You were willing to listen and guide me with no bias. I will never ever forget your help and advice. You knew my fears and showed me how to overcome them and be a better person. You are the reason I stayed motivated. Thank you so much for that!

April Wettig, Graduate Secretary and dear friend. You and Kristen are the motivators who kept pushing me to reach this pinnacle. You were willing to listen as a friend when I was flustered and didn't know what to do. Thank you for being my friend!

Lyn Hoyle, retired greenhouse manager of the Department of Biology, University of Waterloo deserves a special thanking. Thank you for teaching me about the proper care of plants and growth chambers. You were a wonderful greenhouse manager with thorough knowledge regarding pest and disease control of plants. Thank you for all your help and I hope you are enjoying your retirement!

I would also like to thank all the sources of funding which helped me to complete my Master's program: Ontario Graduate Student Scholarship (OGS), the International Masters Student Award (IMSA), Millennium Graduate Bursary from the Graduate Studies and Postdoctoral Affairs Office, Graduate Student Research and Teaching Assistantships from the Department of Biology, University of Waterloo. I would also like to acknowledge the Natural Sciences and Engineering Research Council of Canada (NSERC) grant of the Moffatt lab for providing financial assistance for my research project.

I am very grateful to the academic and non-academic staff and the students of the Department of Biology. It was a wonderful experience to get to know you and work with you. I extend my

thanks to Dr. Dragana Miskovic, Dr. Simon Chuong, Dr. Barb Moffatt and Dr. Susan Lolle for trusting me with TA assignments.

Special thanks go to my dear friends who have supported me in numerous ways and providing encouragement during this period. I thank Ishari and Nandana Jayabahu for motivating me and extending moral support during the entire research period. I would like to extend my thanks to Shyam Dadimuni for sharing his expertise in statistical analysis at the initial stages of the project. Pearl Chang, you have been a motivator, an ear to talk to, a shoulder to lean on and a very good friend. I am lucky to have a friend like you.

A big thank you is extended to my parents who have always guided me to go forward in the right direction. Thank you for everything you have done for me. Thank you for letting me embrace this opportunity, even though I had to travel to the other side of the world, away from you. I will always remember the sacrifices you have made for me. Thank you mom and dad!

Last not but not the least, I thank my husband and my best friend, Priyantha. I have no words to express the gratitude I have for you. You left your job, your family and everything you had built to come to Canada with me. You are the guiding light that never lets me lose focus. I don't know what would I do without you. Thank you for all the sacrifices you made, all the encouragement you gave and for each and every minute you spent taking care of everything so that I could focus on my work. Thank you so much!

Dedication

I dedicate this thesis to two of the most important people in my life,
my husband and my son.

To my husband, Priyantha Mudannayake,
Your immense patience, understanding and unconditional love is like the ocean with no boundaries.
I would not have the strength to go on if it wasn't for you!

To my son, Shevon Mikael Mudannayake,
You came into my life while I was completing one chapter of my life.
You are the beginning of a bright new one.
You are the best son a mother could ever want, and I am blessed to have you in my life!

I am grateful to have a loving husband and a wonderful son and I dedicate this manuscript to the both of you!

Table of Contents

List of Figures

List of Tables

List of Abbreviations

ABA	Abscisic acid
ABRC	Arabidopsis Biological Research Center
ac	Apical cell
ACC	1-aminocyclopropane-1-carboxylic acid
ACL5	ACAULIS5/ Tspm synthase
AdoMet	S-adenosyl-L-methionine /SAM
ami	artificial microRNA
ANOVA	Analysis of variance test
ARF	Auxin response factor
At / *A. thaliana*	*Arabidopsis thaliana*
AtGRP	*A. thaliana* glycine-rich RNA binding protein
AtHB	*Arabidopsis thaliana* homeobox gene
ATP	Adenosine Triphosphate
ATS	Alkaline treatment solution
AuxREs	Auxin response elements
bc	Basal cell
bHLH	Type basic-helix-loop-helix
BR	Brassinosteroids
cDNA	Complementary DNA
cat	Chloramphenicol acetyltransferase
CLE	Clavata 3/ Endosperm surrounding region related
CK	Cytokinin
Col-0	Columbia ecotype
COPR5	Co-operator of PRMT5
Cot / ct	Cotyledon
Cu	Copper
DABS	Decolourized aniline blue solution
DAG	Days After Germination
dH_2O	Distilled water
DHH	Deoxyhypusine hydroxylase
DHS	Deoxyhypusine synthase
DIC	Differential Interference Contrast
DMFO	α-difluoromethylornithine
DNA	Deoxyribonucleic acid
dSAM	decarboxylated *S*-adenosyl methioninamine
eIF5A	eukaryotic initiation factor 5A
ERF	Ethylene response transcription factor

EtOH	Ethanol
eu	expression units
F1	1st filial generation
F2	2nd filial generation
Fe	Iron
G1	1st Spd treated *mtn1-1mtn2-1* mutant generation
G2	offspring of G1 generation
G3	offspring of G2 generation
GA	Gibberellic acid
GC7	N1-guanyl-1,7-diaminoheptane
GFP / *gfp*	Green Fluorescent Protein
GO	Gene Ontology
GUS	*β-Glucuronidase*
HCl	Hydrochloric acid
Hcy	Homocysteine
HD-ZIP III	Homeodomain-leucine zipper transcription factor class III
hyp	Hypophysis
Hypo	Hypocotyl
IAA	Auxin / Indole acetic acid
JA	Jasmonic acid
lacZ	*β-glacatosidase*
Leu	Leucine
Lop1	*LOPPED*
LRR	Leucine-Rich-Repeat
Luc	Luciferase
Lys	Lysine
MEP50	Methylome protein 50
Met	Methionine
MP/mp	*MONOPTEROS*
MS	Murushige and Skoog
MTA	5'-Methylthioadenosine
MTAP	5'-Methylthioadenosine phosphorylase
MTK	5'-Methylthioribose kinase
MTN	5'-Methylthioadenosine nucleosidase
MTR	5'-Methylthioribose
MTR-1P	5'-Methylthioribose 1-phosphate
NA	Nicotianamine
NaCl	Sodium chloride
NAS	Nicotianamine synthase
ODC	Ornithine decarboxylase

PA	Polyamine
PAO	Polyamine oxidase
PAT	Polar Auxin Transport
PCA	Perchloric acid
pd	Protoderm
pe	proembryo
ph	phloem
PIN	*PIN-formed* protein
PRMT	Protein Arginine Methyltransferase
Put	Putrescine
RAM	Root apical meristem
RIOK	Right open reading frame protein kinase
RLK	Receptor-Like Kinases
RNA	Ribonucleic acid
RNA *seq*	RNA sequencing
RT	Room Temperature
SA	Salicylic acid
SAC51	Suppressor of the *ACAULIS5*
SAH	*S*-adenosylhomocysteine/AdoHcy
SAM	*S*-adenosyl-L-methionine /AdoMet /
SAMS	*S*-adenosyl methionine synthase
SEM	Scanning electron microscopy
Spd	Spermidine
SpdS	Spermidine synthase
Spm	Spermine
SpmS	Spermine synthase
sus	Suspensor
TAIR	The Arabidopsis Information Resource
TBO	Toluidine Blue O
T-DNA	Transfer DNA
Tkv	*thick vein*
trn1	*TORNADO1*
Tspm	Thermospermine
UBQ	Ubiquitin
uidA	*β-glucuronidase*
WD45	WD repeat domain 45
WT	Wild Type
xy	xylem
YFP	Yellow Fluorescent Protein
Zn	Zinc

Chapter 1

General Introduction

1.1 Introduction

1.1.1 *Arabidopsis thaliana*

Arabidopsis thaliana is a small flowering plant of the family Brassicacea, a member of the mustard family. It is an annual dicotyledonous herb, a winter weed, native to Eurasia and Africa. The adult plant grows to about 30–60 cm in height. It has one main stem, which is called a "bolt", which emerges around 5-weeks post-germination, demarcating its transition from vegetative to reproductive phase. The main bolt and several secondary bolts arise from a collection of leaves arranged in a flat rosette (Figure 1-1, A). The basal leaves that form the rosette have short petioles and are elliptic in shape extending 20-45 mm in length (Al-Shehbaza and O'Kanehe, 2002). The adaxial surface of the leaf is scattered with simple and stalked 1-forked trichomes. The stem produces a few leaves that are called cauline leaves, which are subsessile or sessile. These leaves are linear, oblong, or elliptic, extending about 10-18 mm (Al-Shehbaza and O'Kanehe, 2002). The *A. thaliana* flower is small, attached to a slender, straight pedicle which is about 3–10 mm long (Figure 1-1, B). The flower has four sepals, four white petals, six stamens and one stigma. The petals and sepals are in typical Brassicaceae arrangement. The six stamens of the flower vary in length and arrangement. The longer stamens are arranged medially and the two shorter stamens are placed laterally. The flower has a superior ovary, with two carpels that enclose ovules. There are about 40–70 ovules per ovary (Al-Shehbaza and O'Kanehe, 2002). The ovary develops into a fruit, which is called a "silique". The siliques are linear and smooth with a distinct mid-vein. They grow to a maximum length of 15-20 mm (Figure 1-1, C). The mature seeds are plump and ellipsoid, light brown to reddish brown in colour and about 300 – 500 µm long (Al-Shehbaza and O'Kanehe, 2002).

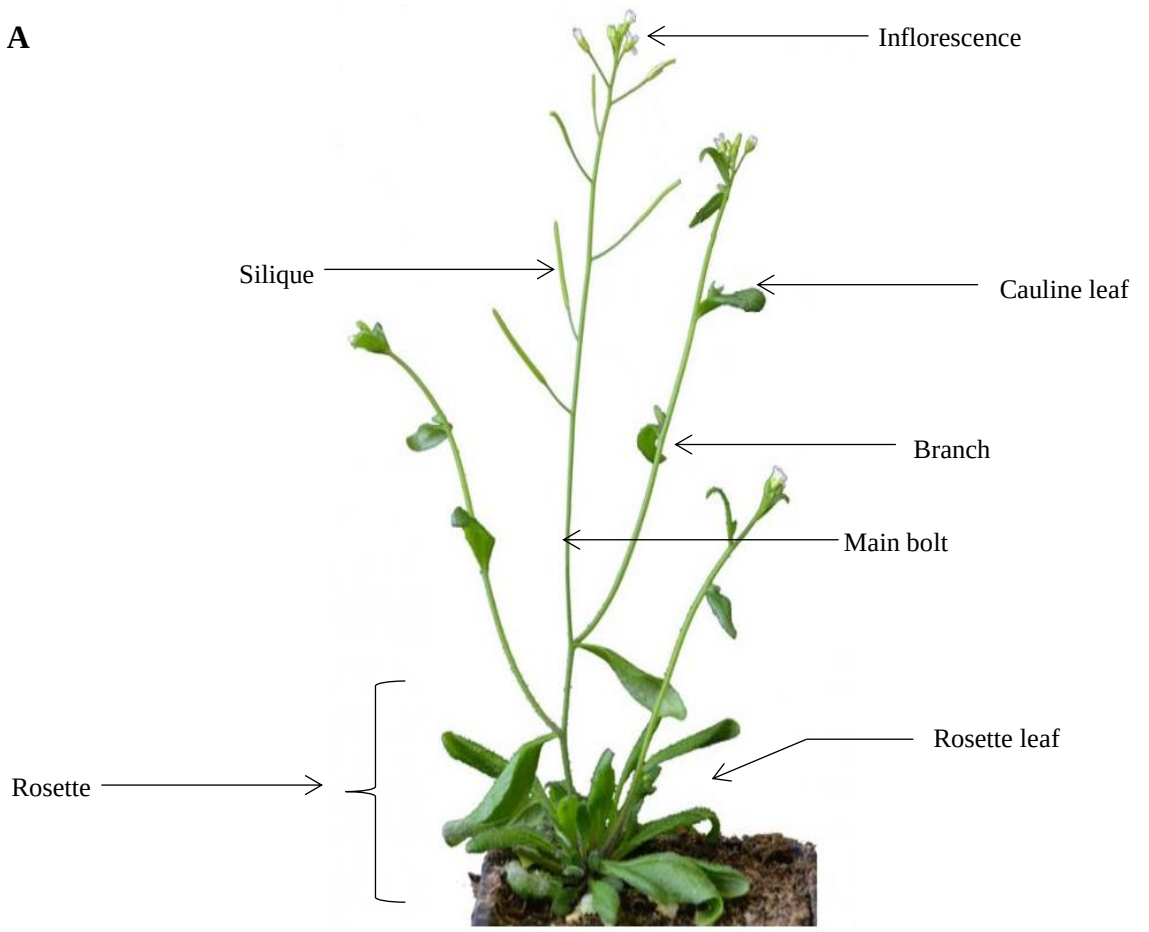
A
Inflorescence
Silique
Cauline leaf
Branch
Main bolt
Rosette leaf
Rosette


B
C

Figure 1-1. Phenotype of the *A. thaliana* plant, flower and fruit of ecotype Columbia.

In A, the adult *A. thaliana* plant is about 5 weeks post germination. The main bolt and one secondary bolt arise from the rosette. The main bolt has two branches and the secondary bolt / stem has none. All secondary stems have a few cauline leaves. The plant has flowers that are arranged in an inflorescence, and fertile fruits / siliques developing along the stem. The lower siliques are more mature than the ones at a higher position.

In B, the *A. thaliana* flower is shown. The flower has four white petals and the stamens carrying the anthers can be seen surrounding the stigma. This flower is a stage 14 flower with open petals and extended stigma.

In C, the fruit of *A. thaliana* is shown. The fruit / silique is narrow and long, with a smooth green surface. The silique in C is a stage 17B silique, which is at full maturity.

Scale bar = 3 mm.

Unlike other members of the Brassicacea family (broccoli, cabbage, turnip, mustard, and canola) which are well known for their agricultural importance, the *A. thaliana* plant has no economic value. However, it has been used widely as a model organism in plant biology, physiology, biochemistry, genetics and molecular biology for more than 40 years (The Arabidopsis Genome Initiative, 2000) because it contains a small genome (135 Mb) with low repetitive sequence content (Kersey et al., 2016), can be transformed using *Agrobacterium tumefaciens*-based vectors and possesses other favorable characteristics such as small size, large number of offspring, and short generation time (six weeks from germination to mature seed production). .

The *A. thaliana* genome was sequenced in 2000 with extensive maps of all 5 chromosomes (The Arabidopsis Genome Initiative, 2000). The complete annotated genome sequence and information on characterized genes as well as their biological processes are freely available to the scientific community through a database at The Arabidopsis Information Resource (TAIR; http://www.arabidopsis.org/index.jsp). The 1001 *A. thaliana* genome project provides a detailed analysis of 1135 genomes of naturally inbred lines / accessions of *A. thaliana* (Alonso-Blanco et al., 2016). These accessions, which are the product of natural selection in response to various environmental and ecological factors, are useful tools for the analysis of complex traits. Seeds for these accessions and thousands of donated mutant lines are available at the two *A. thaliana* stock centers, viz. Arabidopsis Biological Research Center (ABRC), USA, and Nottingham Arabidopsis Stock Centre, Great Britain.

Transfer DNA (T-DNA) mutant lines for most genes and associated expression datasets is a key resource utilized by the scientific community to study the links between the different genotypes and phenotypes in laboratory and field settings (Alonso-Blanco et al., 2016). Several different T-

DNA insertion mutant lines obtained from the ABRC have been used at this (Moffatt) laboratory to describe the physiology of 5′-methylthioadenosine nucleosidase (MTN; EC 3.2.2.9) encoding genes using MTN-deficient mutants in a series of studies (Burstenbinder et al., 2010; Waduwara-Jayabahu et al., 2012).

The altered polyamine (PA) profiles, array of vascular abnormalities and sterility observed in MTN-deficient mutants in the above studies suggested possible link between MTN encoding genes and/or polyamines with vascular development and reproductive function. This research study was formulated to examine the effect of PA, especially of spermidine (Spd), on vascular development and reproductive function using the MTN-deficient mutants of *A. thaliana*.

1.1.2 **Methylthioadenosine nucleosidase**

MTN is an enzyme which catalyzes the hydrolytic cleavage of glycosylic bond in 5'-methylthioadenosine (MTA) to adenine and 5'-methylthioribose (MTR) (Siu et al., 2008; Busrtenbinder et al., 2007; Waduwara-Jayabahu et al., 2012). Two homologues of the MTN enzyme (MTN1 and MTN2) had been identified in *A. thaliana*. Siu et al., (2008) reported that two residues, Leu181/Met168 and Phe148/Leu135 in MTN1/MTN2 in the active site differ between the two enzymes, and might account for the divergence in the specificity of the two MTN enzymes.

MTN contributes to the maintenance of *S*-adenosylmethionine (AdoMet / SAM) homeostasis and is required to sustain high rates of ethylene synthesis (Burstenbinder et al., 2007). In plants, MTA is a common by-product of polyamine (PA), ethylene and nicotianamine (NA) biosynthetic pathways and MTA is used by plants to regenerate methionine (Met) (Giovanelli et al., 1985). However, over-accumulation of MTA is detrimental to plant growth (Burstenbinder et al., 2010;

Waduwara-Jayabahu et al., 2012) and MTN is the only known enzyme to hydrolyze MTA. Thus, MTN deficiency may affect Met availability in plants.

1.1.3 **Methionine**

Met is a sulphur containing amino acid belonging to the aspartate derived amino acid group (Amir et al., 2002). Met cannot be synthesized by mammals, but can be synthesized by plants. Met plays a role in the initiation of mRNA translation and hence is essential for protein synthesis in all organisms. The hydrophobic properties of Met play a role in protein folding and determination of the life-span of proteins (Giglione et al., 2003). In addition, Met serves as the precursor for the synthesis of the AdoMet, the principal universal methyl-donor for methylation reactions (Giovanelli et al., 1985; Ravanel et al., 1998; Burstenbinder et al., 2010). AdoMet serves as a carbon skeleton donor for the synthesis of polyamines, vitamins, co-factors, osmo-protectants and hormones such as ethylene (Droux, 2004; Fontecave et al., 2004; Hesse et al., 2004). Therefore, Met is involved in a variety of metabolic processes including the synthesis of proteins, PAs, Ethylene, NA, and AdoMet, all of which are interconnected. The synthesis of AdoMet accounts for ~80% of Met metabolism, while the synthesis of proteins which consumes the entire Met molecule, uses ~20% of Met. More than 90% of AdoMet is used for transmethylation reactions to produce choline and its derivatives (Burstenbinder et al., 2010). These properties make Met an essential metabolite for primary as well as secondary metabolism of all life forms.

Biosynthesis of Met requires aspartic acid for the main nitrogen/carbon backbone, cysteine for the sulfur moiety and folate for the methyl group (Ravanel et al., 1998). Aspartic acid is converted via β-aspartyl-semi aldehyde into homoserine by two reduction steps of the terminal

carboxyl group. Homoserine is then activated with a phosphate in plants to react with cysteine. This activation requires a molecule of ATP as an energy source. Cysteine is converted to homocysteine by cystathionine γ-synthase and cystathionine β-lyase (Ravanel et al., 1998). The conversion of cysteine to homocysteine is the step that leads to *de novo* synthesis of Met, because homocysteine is next converted to Met by Met synthase via transfer of the methyl group from 5-methyltetrahydrofolate (Ravanel et al., 2004). In addition to catalyzing the conversion of homocysteiene to Met, Met synthase regenerates the methyl group of AdoMet. Furthermore, Met synthase and *S*-adenosylmethionine synthetase form the fundamental components controlling metabolism in the transition from a quiescent to a highly active state during seed germination (Gallardo et al., 2002) of *A. Thaliana*. Thus, Met biosynthesis is important for seed germination and seedling growth in *A. thaliana*.

1.1.4 **Methionine recycling in plants – The Yang cycle**

The *de novo* synthesis of Met is energetically expensive utilizing a single ATP and an amino group transfer (Ravanel et al., 1998; Burstenbinder et al., 2010) as well as sulfur assimilation (conversion of inorganic sulphur compounds such as sulphate into cysteine by plants) is inefficient and energy dependent requiring ATP (Leustek and Saito, 1999). Therefore, plants re-use sulfur metabolites such as MTA to regenerate Met and this involves a cascade of reactions producing the intermediates, 5′-methylthioribose (MTR), 5′-methylthioribose– 1- phosphate (MTR1P) and 2-keto-4-methylthiobutyrate. Studies conducted using *Lemna paucicostata* showed that this pathway contributes to almost one-third of the Met accumulation in protein (Giovanelli et al., 1985). The process of Met salvaging and recycling was comprehensively studied and presented by S.F. Yang in 1979, hence the Met recycling/ salvage pathway is known as the Yang cycle.

The Yang cycle is not an isolated one. It is connected with other biochemical processes such as ethylene, NA and PA biosynthesis reactions (Takahashi & Kakehi, 2010; Waduwara-Jayabahu et al., 2012), which produce MTA as a byproduct (Figure 1-2). The MTA enters the Yang cycle via depurination by MTN to produce adenine and MTR (Sauter et al., 2013); the latter is phosphorylated to 5'-methylthioribose 1-phosphate (MTR1P). Eukaryote cells use a single-step reaction catalyzed by MTA phosphorylase (MTAP; EC 2.4.2.28) to produce MTR1P. Most bacteria and eukaryotes (protozoa and plants) do this in two steps involving MTN activity which results in MTR and adenine formation, followed by MTA kinase (MTK; EC 2.4.2.27) mediated phosphorylation of the MTR (Figure 1-2). Lack of MTN enzyme activity results in over accumulation of MTA in different organs leading to detrimental growth effects (Waduwara-Jayabahu et al., 2012; Sauter et al., 2013).

Although a steady supply of AdoMet is required for methylation reactions as well as for the continued production of ethylene, NA and PAs (Danchin, 2016), the Yang cycle is not essential for the ethylene, NA and PA biosynthesis to be sustained as evidenced by the fact that *A. thaliana* MTK knock-out mutants are indistinguishable from Wild Type (WT) plants (Burstenbinder et al., 2010).

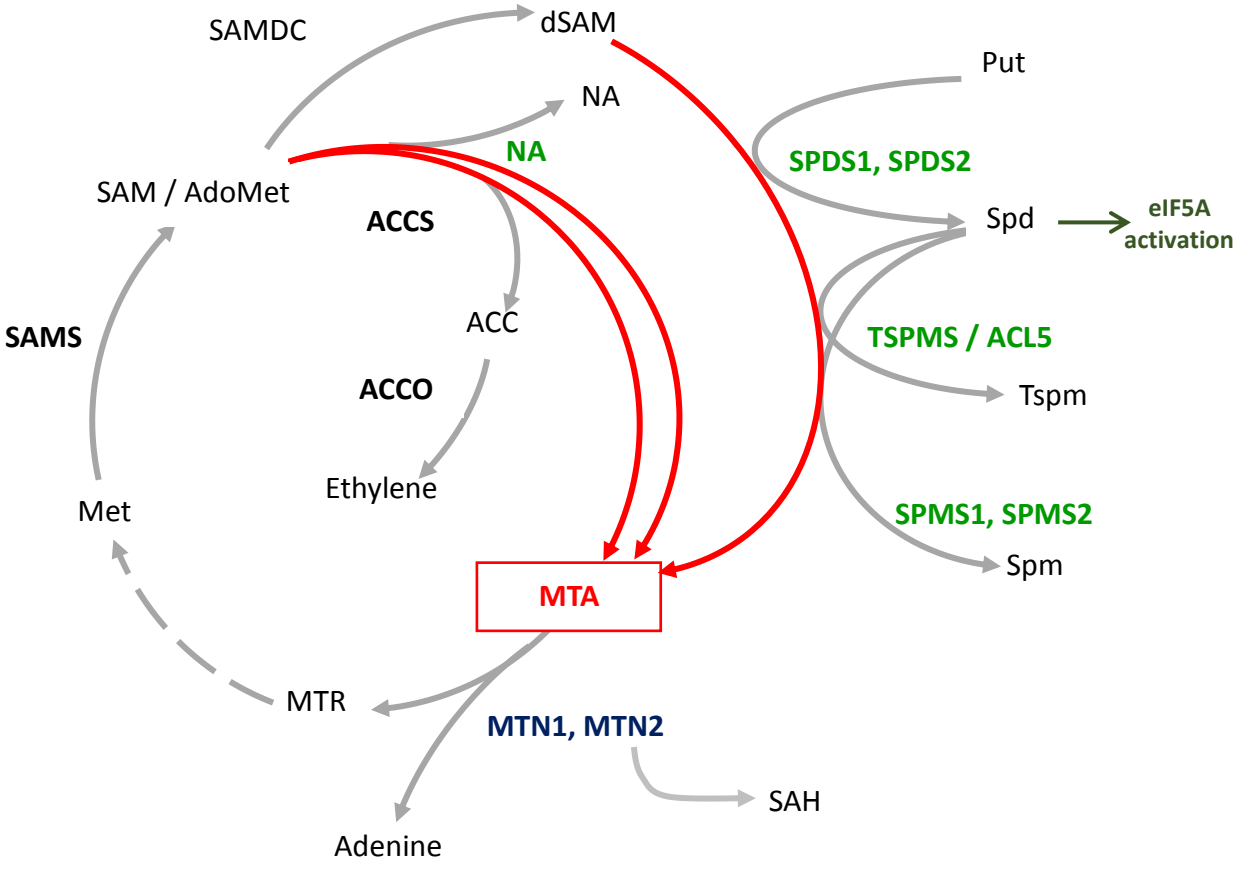
SAMDC
dSAM
Put
NA
NA
SPDS1, SPDS2
SAM / AdoMet
ACCS
Spd
eIF5A
activation
ACC
SAMS
TSPMS / ACL5
ACCO
Tspm
Ethylene
Met
SPMS1, SPMS2
Spm
MTA
MTR
MTN1, MTN2
SAH
Adenine

Figure 1-2. Biochemical reactions producing methylthioadenosine (MTA)

Ethylene, nicotianamine (NA) and polyamine biosynthesis (putrescine (Put), spermidine (Spd), spermine (Spm) and thermospermine (Tspm)) produce MTA as a by-product. The 5'-methylthioadenosine nucleosidase (MTN) enzyme catalyzes the reaction of converting MTA to 5′-methylthioribose (MTR) and adenine.

Spd is produced from Put by Spd synthase (SPDS1 and SPDS2) enzymes. Spd is the precursor for both Spm and Tspm. The Spm production is catalyzed by two synthases, Spm synthase 1 and 2. Tspm is produced by Tspm synthase / ACL5. Spd is essential for the activation of eukaryotic translation initiation factor 5A (eIF5A). One of the two MTN enzymes (*MTN2*) which catalyze the conversion of MTA to MTR, also acts on *S*-adenosylhomocysteine (SAH) as a substrate *in vitro*. *S*-adenosylmethionine (AdoMet / SAM) synthase (SAMS) converts Met to AdoMet which is the primary precursor for ethylene, nicotianamine and polyamine biosynthesis.

(Modified from, Waduwara-Jayabahu, 2011).

1.2 *A. thaliana* methylthioadenosine nucleosidase genes

The *A. thaliana* genome contains two genes encoding MTN; these are annotated as *MTN1* (At4g38800) and *MTN2* (At4g34840). There are three other related sequences: At4g24330, At4g24350, At4g28940, but bioinformatics analysis suggests that these MTN-related genes have likely evolved to have different substrates based on their expression profiles and phylogenetic relatedness (Paul Brogee and Andrew Doxey, personal communication). The coding regions of the two annotated *MTN* genes share a 73% nucleotide identity and a 64 % amino acid sequence identity (Waduwara-Jayabahu et al., 2012).

In vitro assays of MTN activity in crude extracts of four-day-old seedlings and rosette leaves of three-week-old plants grown on media showed that *MTN1* is responsible for 80% of the MTN activity (Burstenbinder et al., 2010). MTN1 is also transcribed to a much higher extent and more broadly throughout the plant, than MTN2. This leads to the conclusion that the metabolism of MTA is mediated primarily by this isoform. Kinetic characterization of MTN1 and MTN2 showed that MTN1 is completely inactive towards *S*-adenosylhomocysteine (SAH), while MTN2 can utilize SAH as a substrate to a limited extent *in vitro* (14% affinity relative to MTN1; Siu et al., 2008).

Analysis of microarray and RNA sequencing (RNA *seq*) data (Winter et al., 2007) revealed very high expression level of the *MTN1* gene in several organs of *A. thaliana*: the cotyledons (1098.39 ± 75.95 eu) and root (1597.03 ± 36.61 eu) of developing seedlings, the entire rosette (1030.96 ± 67.15 eu) after transitioning, flower bud sepals at stage 12 and 15 (1062.06 ±30.17 eu and 1378.11 ± 26.89 eu), transition shoot apex (1207.53 ± 25.06 eu) and immature seeds (1086.39 ± 33.95 eu). The rest of the organs had lower levels of *MTN1*, but these levels were significantly

higher than the corresponding *MTN2* expression values (Figure 1-3 A & B). The *MTN2* gene expression levels in the seedling and developing plant were considerably lower than *MTN1*. The highest *MTN2* expression level was observed in mature pollen (145.06 ± 11.74 eu), which was still lower than *MTN1* (1405.18 ± 100.34 eu).

Analysis of *A. thaliana* leaf tissue using translatome technology (King and Gerber, 2016) has revealed that *MTN1* is preferentially expressed in phloem and guard cells whereas *MTN2* is expressed in epidermal cells and phloem cells (Pommerrenig, et al., 2011; Winter et al., 2007). The availability of sulfur containing by-products in the phloem promotes the expression of Met recycling genes in the vasculature (Zierer et al., 2016).

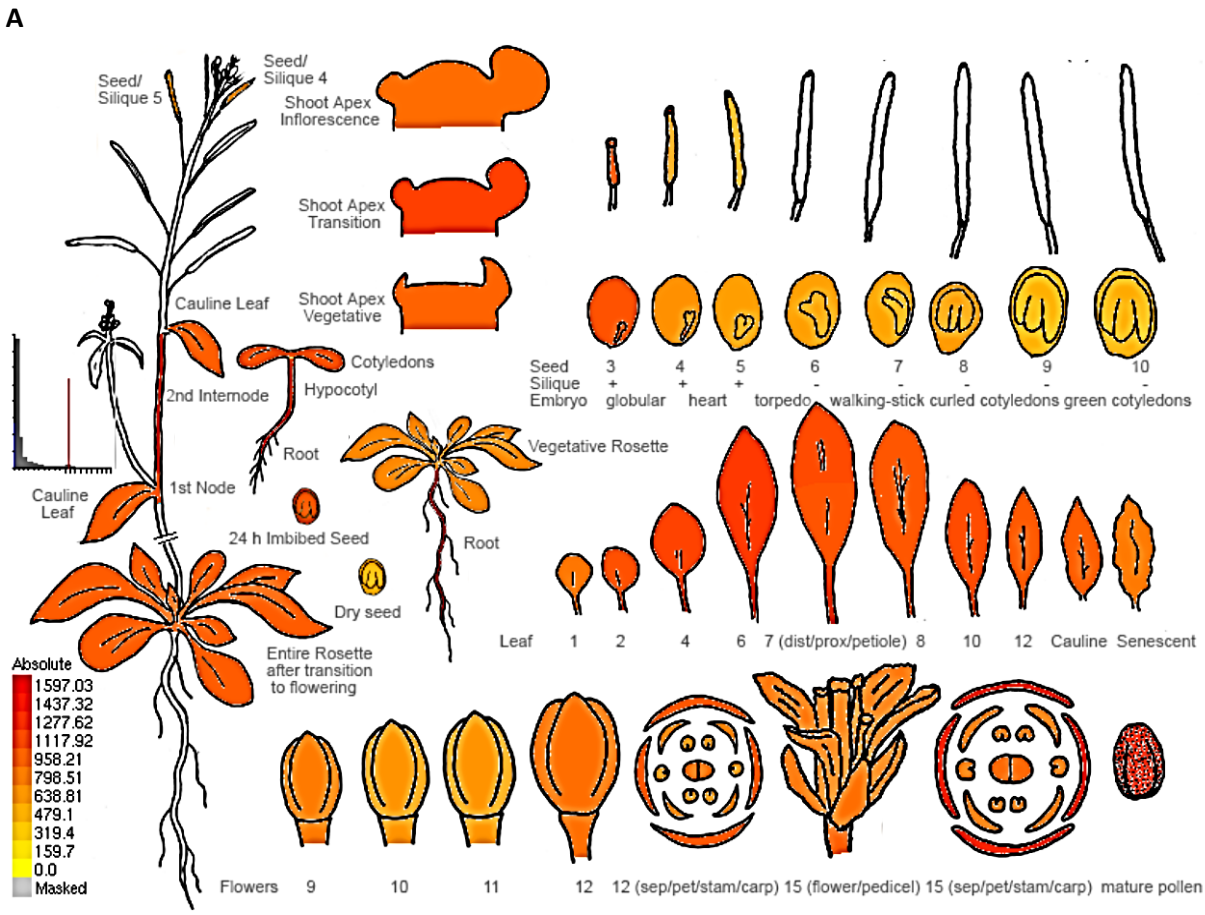
A
Seed/
Silique 5
Seed/
Silique 4
Shoot Apex
Inflorescence
Shoot Apex
Transition
Shoot Apex
Vegetative
Cauline Leaf
Cotyledons
Hypocotyl
2nd Internode
Root
1st Node
Cauline
Leaf
24 h Imbibed Seed
Dry seed
Entire Rosette
after transition
to flowering
Vegetative Rosette
Root
Absolute
1597.03
1437.32
1277.62
1117.92
958.21
798.51
638.81
479.1
319.4
159.7
0.0
Masked
Seed 3 4 5 6 7 8 9 10
Silique + + + - - - - -
Embryo globular heart torpedo walking-stick curled cotyledons green cotyledons
Leaf 1 2 4 6 7 (dist/prox/petiole) 8 10 12 Cauline Senescent
Flowers 9 10 11 12 12 (sep/pet/stam/carp) 15 (flower/pedicel) 15 (sep/pet/stam/carp) mature pollen

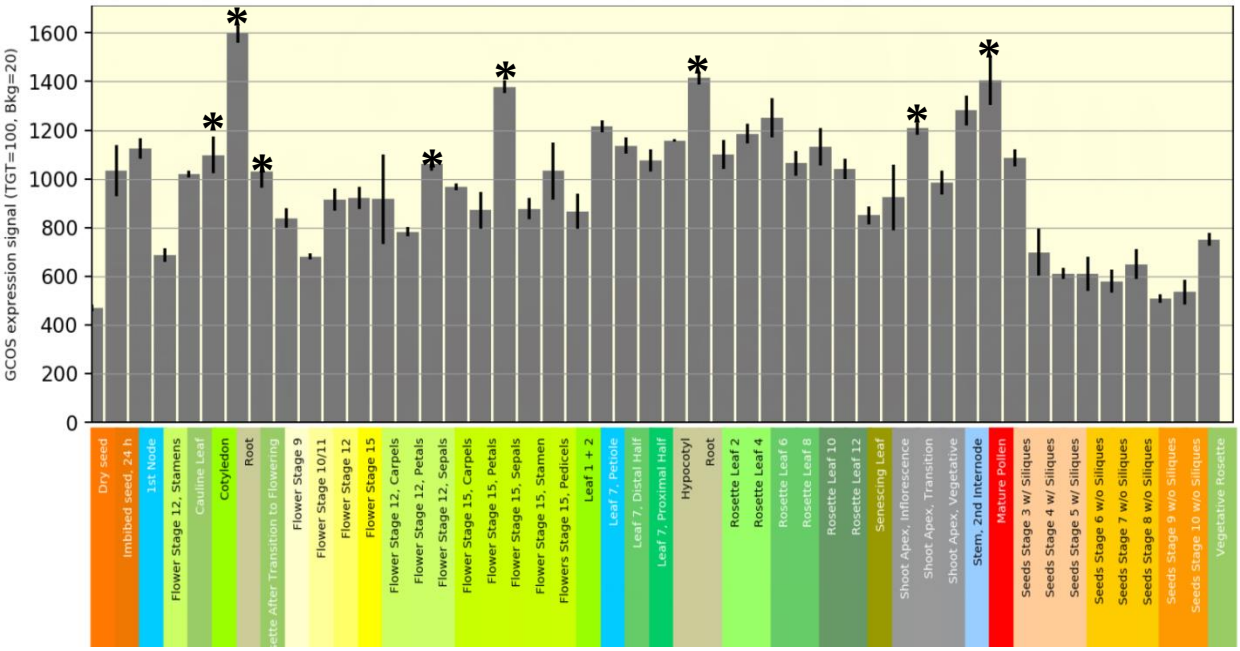
GCOS expression signal (TGT=100, Bkg=20)
0
200
400
600
800
1000
1200
1400
1600
Dry seed
Imbibed seed, 24 h
1st Node
Flower Stage 12, Stamens
Cauline Leaf
Cotyledon
Root
Flower Stage 9
Flower Stage 10/11
Flower Stage 12
Flower Stage 15
Flower Stage 12, Carpels
Flower Stage 12, Petals
Flower Stage 12, Sepals
Flower Stage 15, Carpels
Flower Stage 15, Petals
Flower Stage 15, Sepals
Flower Stage 15, Stamen
Flowers Stage 15, Pedicels
Leaf 1 + 2
Leaf 7, Petiole
Leaf 7, Distal Half
Leaf 7, Proximal Half
Hypocotyl
Root
Rosette Leaf 2
Rosette Leaf 4
Rosette Leaf 6
Rosette Leaf 8
Rosette Leaf 10
Rosette Leaf 12
Senescing Leaf
Shoot Apex, Inflorescence
Shoot Apex, Transition
Shoot Apex, Vegetative
Stem, 2nd Internode
Mature Pollen
Seeds Stage 3 w/ Siliques
Seeds Stage 4 w/ Siliques
Seeds Stage 5 w/ Siliques
Seeds Stage 6 w/o Siliques
Seeds Stage 7 w/o Siliques
Seeds Stage 8 w/o Siliques
Seeds Stage 9 w/o Siliques
Seeds Stage 10 w/o Siliques
Vegetative Rosette

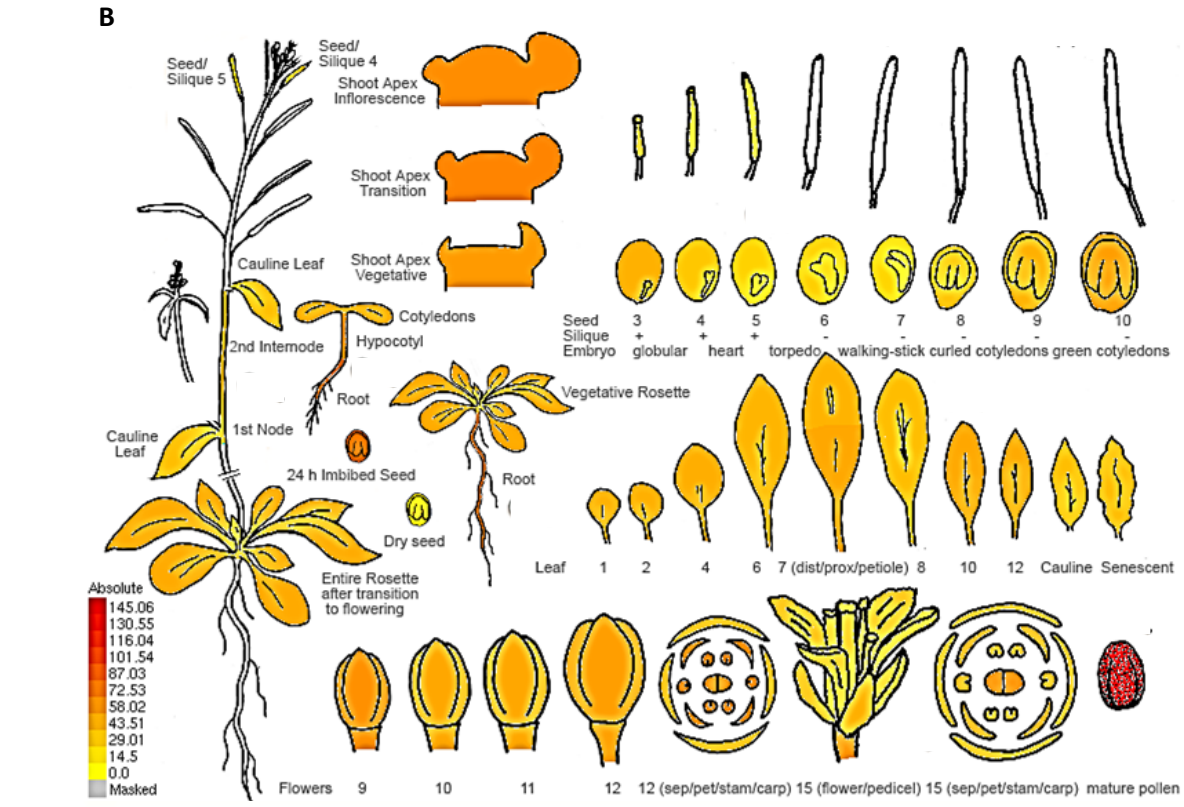
B
Seed/
Silique 5
Seed/
Silique 4
Shoot Apex
Inflorescence
Shoot Apex
Transition
Shoot Apex
Vegetative
Cauline Leaf
Cotyledons
Hypocotyl
2nd Internode
Root
1st Node
Cauline
Leaf
24 h Imbibed Seed
Dry seed
Vegetative Rosette
Root
Entire Rosette
after transition
to flowering
Absolute
145.06
130.55
116.04
101.54
87.03
72.53
58.02
43.51
29.01
14.5
0.0
Masked
Seed
Silique
Embryo
3
+
globular
4
+
heart
5
+
torpedo
6
-
walking-stick
7
-
curled cotyledons
8
-
9
-
green cotyledons
10
-
Leaf 1 2 4 6 7 (dist/prox/petiole) 8 10 12 Cauline Senescent
Flowers 9 10 11 12 12 (sep/pet/stam/carp) 15 (flower/pedicel) 15 (sep/pet/stam/carp) mature pollen

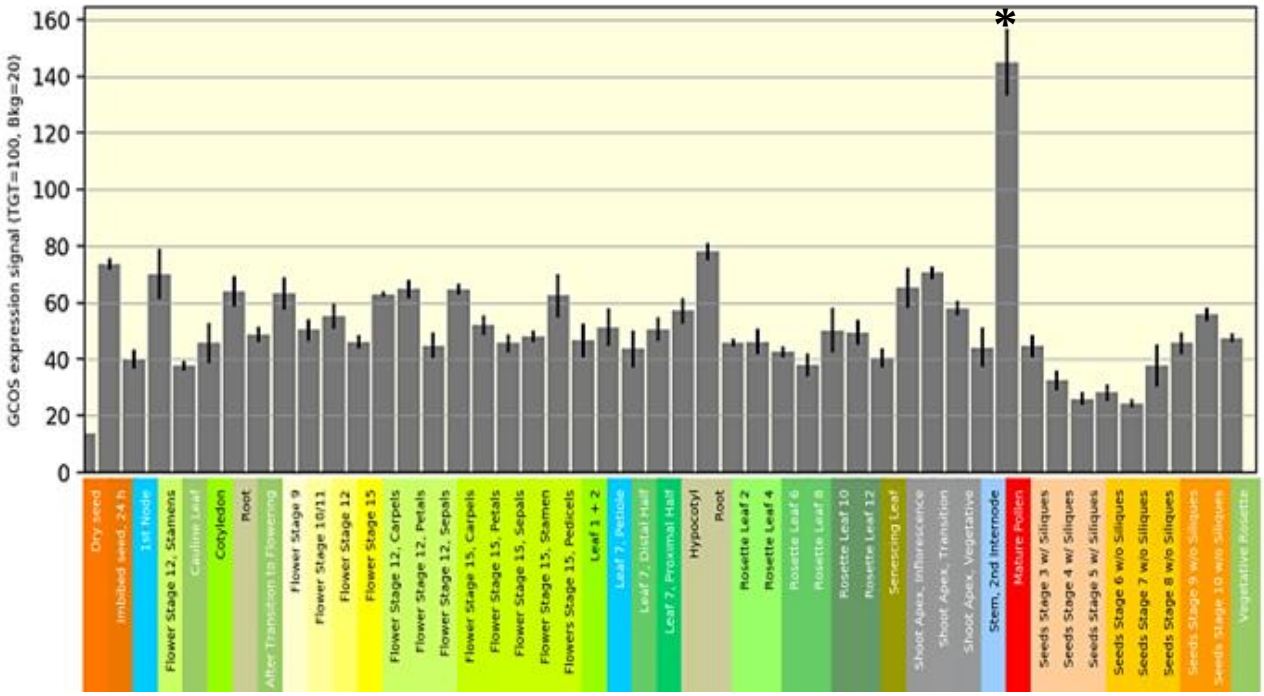
GCOS expression signal (TGT=100, Bkg=20)
160
140
120
100
80
60
40
20
0
*
Dry seed
Imbibed seed, 24 h
1st Node
Flower Stage 12, Stamens
Cauline Leaf
Cotyledon
Root
After Transition to Flowering
Flower Stage 9
Flower Stage 10/11
Flower Stage 12
Flower Stage 15
Flower Stage 12, Carpels
Flower Stage 12, Petals
Flower Stage 12, Sepals
Flower Stage 15, Carpels
Flower Stage 15, Petals
Flower Stage 15, Sepals
Flower Stage 15, Stamen
Flowers Stage 15, Pedicels
Leaf 1 + 2
Leaf 7, Petiole
Leaf 7, Distal Half
Leaf 7, Proximal Half
Hypocotyl
Root
Rosette Leaf 2
Rosette Leaf 4
Rosette Leaf 6
Rosette Leaf 8
Rosette Leaf 10
Rosette Leaf 12
Senescing Leaf
Shoot Apex, Inflorescence
Shoot Apex, Transition
Shoot Apex, Vegetative
Stem, 2nd Internode
Mature Pollen
Seeds Stage 3 w/ Siliques
Seeds Stage 4 w/ Siliques
Seeds Stage 5 w/ Siliques
Seeds Stage 6 w/o Siliques
Seeds Stage 7 w/o Siliques
Seeds Stage 8 w/o Siliques
Seeds Stage 9 w/o Siliques
Seeds Stage 10 w/o Siliques
Vegetative Rosette

Figure 1-3. Expression pattern of MTN1 and MTN2 genes in *A. thaliana*

The (A) *MTN1* (At4g38800) and (B) *MTN2* (At4g34840) gene expression levels in seedlings, seeds and the developing plant.

In A, the expression pattern of *MTN1* is shown. The cotyledons, seedlings root, the transitioning plant rosette and shoot apex, stage 12 and 15 flower bud sepals, immature seeds show highest expression levels (deep red colour in schematic, * in the expression chart for *MTN1*).

In B, the expression pattern of *MTN2* is shown. All the expression values of *MTN2* expression are lower than *MTN1* (A). The highest MTN2 expression is seen in mature pollen, but this is still lower than *MTN1 (** in the expression level chart for *MTN2*)

(Adapted from eFP browser expression level chart, Winter et al., 2007. Accessed on 6th January 2019).

1.2.1. The MTN-deficient mutants: PA profile, Growth and Reproduction

The collection of T-DNA sequence-indexed mutants is a valuable resource that is used for *in vivo* characterization of gene function in plant biology. Burstenbinder et al. (2010) studied a set of MTN-deficient single mutants for the characterization of the *A. thaliana MTN* genes. Three T-DNA insertion single *MTN* mutants; *mtn1-1* (T-DNA insertion in the third intron of the *MTN1* gene: SALK_085385), *mtn2-1* (*AtMTN2*: SALK_071127; insertion in the fourth exon) and *mtn2-5* (SALK_022510: insertion in the promoter) were used for this study.

All the single mutants had a WT phenotype (Burstenbinder et al., 2010), but, when grown on MTA-supplemented media, they had altered polyamine profiles as the primary defect, with increased levels of putrescine (Put) and Spermine (Spm). This result suggests that the altered PA profile was due to the high availability of MTA in the media. Three-week-old *mtn1-1* mutant seedlings grown on MTA-supplemented media (500 µM) had shorter root lengths compared to WT and *mtn2-1*mutants. This observation is evidence to the higher contribution of *MTN1* than *MTN2* to the metabolism of MTA. Shoot fresh weight measurements of WT, *mtn1-1*, *mtn2-1* did not vary significantly from each other when grown on complete, 100µM or 500 µM sulfate or Met supplemented media (n=50). The measurements taken from four-day-old seedlings revealed that ethylene and NA levels were not altered (Burstenbinder et al., 2010). These results suggest that the effect of *MTN* gene mutations of the single mutants on ethylene and NA biosynthesis was not significant at this early stage in development.

Based on the findings of Burstenbinder et al. (2010), a series of MTN-deficient double mutants were created at the Moffatt lab to examine the outcome of simultaneous reduction of both *MTN* genes (Waduwara-Jayabahu, 2011). The double mutants were created using single T-DNA

insertion and artificial microRNA (amiRNA) lines in the Col-0 background (Figure 1-4). The *mtn1-1mtn2-1*double mutant is a knock-down mutant, with *MTN1* contributing to the residual MTN activity. Attempts to create complete knock-out mutants were unsuccessful due to embryo lethality (Waduwara Jayabahu, 2011).

The MTN enzyme activity assays conducted using crude extracts of floral buds of MTN-deficient single mutants, indicated that floral buds have the highest MTN-specific activity (Burstenbinder et al., 2010). The *mtn1-1mtn2-1* mutant plant buds had 14% residual MTN activity (1.21 ± 0.27 nmol mg^{-1} protein min^{-1}in WT) indicating a significantly reduced ability of the mutants to hydrolyze MTA (Waduwara-Jayabahu et al., 2012). The *mtn1-1mtn2-5* double mutant buds showed 28% residual MTN activity compared to WT and were fertile and more WT-like phenotypically (Waduwara Jayabahu, 2011).The difference between the *mtn1-1mtn2-1* and *mtn1-1mtn2-5* mutants is the site of TDNA insertion T-DNA in the *MTN2* gene. The *mtn1-1mtn2-1* mutant carries the insertion in the 4^{th} exon whereas the *mtn1-1mtn2-5* carries the insertion in the promoter region (Figure 1-4). The manner in which the difference in the insertion site of the T-DNA affect the observed differences in *MTN* activity and phenotypic characteristics of the plant warrants further investigation.

The *mtn1-1mtn2-1* mutant is male and female sterile; it was recovered from the self-progeny of plants that are homozygous mutant for one *MTN* gene and heterozygous for the other (i.e., an F2 population from a cross of the two single mutants). The *mtn1-1mtn2-5* mutant is maintained as a homozygous double mutant and seed stocks are updated regularly with ease as it is fertile. The two different F1 parent plants (i.e., *mtn 1-1 mtn 1-1 MTN* 2 *mtn 2-1* and *MTN1 mtn 1-1 mtn 2-1 mtn 2-1*) did not differ phenotypically nor did the double mutants arising from them despite the

genetic difference of the parents. Therefore, part of this research is designed to detect developmental differences that might exist in *mtn1-1mtn2-1* from the two different F1 parents.

Ectopic expression of the *MTN1* cDNA under a constitutive promoter in the *mtn1-1mtn2-1* background restored the WT phenotype confirming that the pleiotropic phenotype of *mtn1-1mtn2-1* was indeed a result of the MTN deficiency (Waduwara-Jayabahu et al., 2012). The *mtn1-1mtn2-1* mutants with restored WT phenotype still lacked MTN2 activity indicating *MTN1* alone was sufficient to recover the normal growth. Under normal conditions, MTN2 has low expression levels compared to *MTN1* (Figure 1-3) and these results confirmed *MTN1* is the larger contributor to MTN activity.

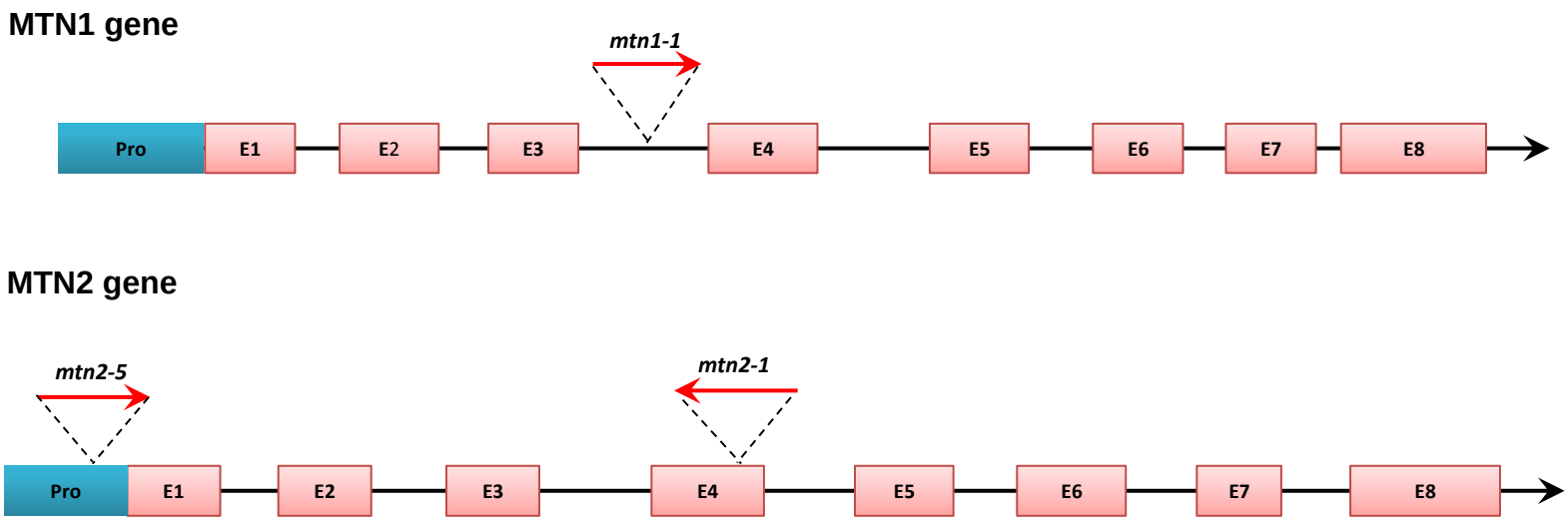

Figure 1-4. T-DNA insertion positions for the *MTN1* and *MTN2* genes in *A. thaliana*

The *mtn1-1* contains an insertion in the 3rd intron, while the *mtn2-1*, and *mtn2-5* contain an insertion in the 4th exon and the promoter, respectively. The *mtn2-1* T-DNA insertion is in the reverse orientation relative to transcription of the gene.

To evaluate the extent of the effects of MTN deficiency on plant growth and reproduction both plate-based and soil-based growth assays were conducted, monitoring development defects of *mtn1-1mtn2-1* in comparison to the WT parent (Waduwara-Jayabahu, 2011). Observations were made according to the developmental milestones described by Boyes et al. (2001). Data on true leaf development, metabolite content of rosette leaf samples and floral buds of plants two weeks after bolting were analyzed. Defects in male and female reproductive organs were evaluated in stage 14 flowers as described by Smyth et al. (1990). White light microscopy, scanning electron microscopy (SEM) and laser scanning confocal microscopy were used for phenotypic developmental analysis of stem cross sections and reproductive tissue.

The developmental profiling revealed that the *mtn1-1mtn2-1* mutant develops no obvious phenotypic defects until the formation of the first true leaves, after which a wide array of abnormalities become evident particularly after the transition from the vegetative to the reproductive phase. The WT seedlings produced a first true leaf greater than 1 mm ten days after germination (DAG), but the *mtn1-1mtn2-1* seedlings took 12 DAG to reach this stage. The first true leaf and the second true leaf of the *mtn1-1mtn2-1* seedlings did not emerge simultaneously as occurs in the WT. Instead, the second true leaf was slightly delayed in emergence making it a very early phenotypic marker for the identification of *mtn1-1mtn2-1* double mutants. The first true leaves of *mtn1-1mtn2-1* seedlings also displayed interveinal chlorosis, which is most notable in emerging young leaves when seedlings were grown on half-strength Murashige and Skoog ($^1/_2$ MS) media (Murashige and Skoog, 1962). The interveinal chlorosis gradually disappeared when seedlings were transplanted into soil in most cases.

The targeted profiling of Met metabolites revealed statistically significant ($P< 0.05$) MTA increases in *mtn1-1mtn2-1* mutants in the inflorescences and rosette leaves relative to the WT,

consistent with MTN deficiency. *S*-methyl-5'-thioadenosine phosphorylase (MTAP; EC 2.4.2.28) is a glycosyltransferase that utilizes MTA as a substrate in humans (Nobori et al., 1996). Introduction of a cDNA, encoding human MTAP gene activity (UBQ10::hMTAP) into the MTN-deficient mutant resulted in a normal phenotype, confirming accumulation of MTA is the basis of the pleiotropic phenotype of this mutant (Waduwara-Jayabahu, 2011).

The *mtn1-1mtn2-1* mutants developed abnormal rosette leaves with an increase in the number of secondary veins and thicker mid-veins (Waduwara-Jayabahu, 2011) which appear to be associated with an increased number of xylem, phloem and cambial cells. These leaf characteristics were very similar to those of the thermospermine-deficient mutants *tkv* (Clay and Nelson, 2005) and *acaulis5* (*acl5*; Hanzawa et al., 1997; Kakehi et al., 2008). In the case of *tkv*, the increased xylem was attributed to the reduced polar auxin transport (Clay and Nelson, 2005) as vascular differentiation of true leaves follows the position specified by auxin (Scarpella et al., 2006).

Assuming that the *mtn1-1mtn2-1* mutant might have polar auxin transport (PAT) deficiencies, a synthetic auxin-responsive promoter (DR5) directing expression of Green Fluorescent Protein (DR5*rev::*GFP) was introduced to the mutant lines and WT to evaluate auxin availability in stem cross-sections (Friml et al., 2003). However, results on DR5*rev*::GFP expression in stem cross sections was not conclusive (Waduwara-Jayabahu, 2011). The auxin mobility in the stems warrants further investigation, yet, could not be included in the research presented in this thesis due to time constraint.

Reproductive characteristics of the sterile *mtn1-1mtn2-1* double mutant showed that development arrests when siliques are 2-3 mm in length. Occasionally, a mutant plant will produce a silique

containing a few non-viable seed-like structures. SEM and light microscopy observations of the reproductive organs have indicated that *mtn1-1mtn2-1* sterility was associated with improper degeneration of callose in mature anthers, indehiscent anthers, sticky and misshapen pollen, poor pollen tube growth, and abnormal or delayed ovule maturation (Waduwara-Jayabahu, 2011). The exact developmental time point when the pollen and ovule development is arrested was not clear. The research study presented in this thesis was designed to identify possible developmental time-points when this arrest would occur.

1.3. Effect of Polyamines

Polyamines are small polycationic molecules associated with a wide variety of biological processes. They are ubiquitously found in all organisms and, in the case of plants, found in tissues that are actively growing. They are found to be involved in a myriad of developmental processes such as cell signaling and membrane stabilization (Tabor and Tabor, 1984) embryo and reproductive development, stem elongation, as well as responses to biotic and abiotic stress (Takahashi & Kakehi, 2010; Alcázar & Tiburcio, 2014; Minocha et al., 2014; Rangan et al., 2014).

Higher plants contain the polyamines Put, Spd, spermine (Spm) and Tspm (a structural isomer of Spm), in free or conjugated forms soluble in the cytosol. The soluble conjugated PAs exist as hydroxycinnamic acid amides while the insoluble PAs occur in bound forms (Rangan et al., 2014). The level of PAs within plants is maintained by tight regulation of not only PA synthesis genes but also of the expression of PA catabolizing genes (Rangan et al., 2014).

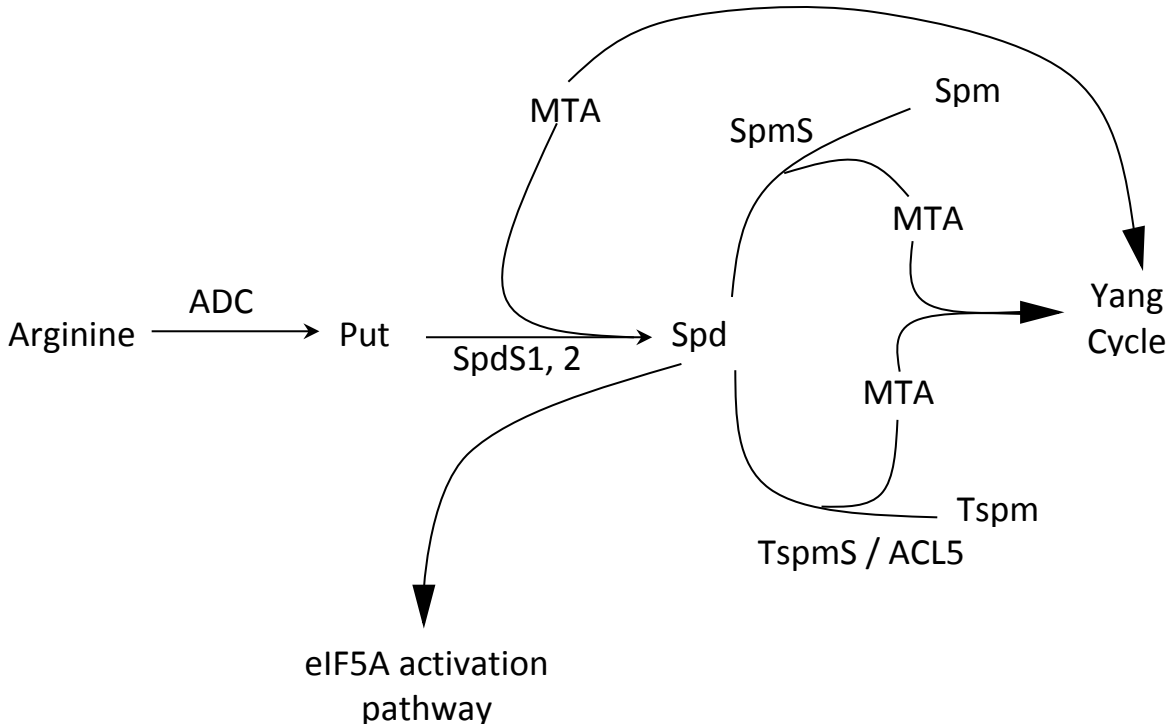

Figure 1-5. Polyamine biosynthesis reactions

The amino acid arginine is carboxylated by arginine decarboxylase (ADC) to produce the precursor polyamine putrescine (Put). Put produces spermidine (Spd) via spermidine synthase (Spds) 1 and 2 and a molecule of 5′-methylthioadenosine (MTA) is produced as a by-product. Spd is the precursor of both spermine (Spm) and thermospermine (Tspm), produced by enzymatic actions of spermine synthase (SpmS) and thermospermine synthase (TspmS / ACL5), respectively. Each reaction produces a single molecule of MTA as a by-product. All the MTA molecules produced during polyamine biosynthesis enter the Yang cycle and are converted to methylthioribose (MTR) and adenine by MTN. The Spd is also a part of the eukaryotic translation initiation factor 5A (eIF5A) activation pathway, where it contributes to the 1st and critical step of activation.

Putrescine is a diamine, the simplest PA and the precursor for the subsequent PAs that are produced (Nguyen et al., 2015). The PA biosynthesis in *A. thaliana* initiates with the conversion of arginine to putrescine by arginine decarboxylase (ADC, EC 4.1.1.19); Put is converted in turn to triamine Spd by Spd synthase (SpdS, EC 2.5.1.16). Spd is the precursor of two other polyamines, Spm and Tspm; their synthesis is catalyzed by spermine synthase (SpmS, EC 2.5.1.22) and Tspm synthase (TspmS / ACL5, EC 2.5.1.79), respectively. Each polyamine synthase reaction produces a single molecule of MTA, which enters the Yang cycle by being converted to MTR and adenine by MTN.

Spd is involved in autophagy (Eisenberg et al., 2009), RNA transcription (Denver and Ivanov, 2018; Frugier et al., 1994) translation (Dever and Ivanov, 2018), and also associated with plant growth regulation (Garcia-Jimenezet al., 1998) and the activation of the eukaryotic translation initiation factor 5A (eIF5A) (Dever and Ivanov, 2018; Chattopadhyay et al, 2003). The activation of eIF5A is dependent on the availability of Spd as shown by studies in yeast (Chattopadhyay et al., 2003; Nishimura et al., 2005). The inactive eIF5A is modified by an amino butyl moiety originating from Spd (Figure 1-6).

The *A. thaliana* genome contains two genes encoding Spd synthase; *SPDS1* and *SPDS2*. *A. thaliana* mutants deficient in Spd synthesis were first identified by Imai et al. (2004), who used two Spd synthesis T-DNA mutants having mutations in both *SPDS1* and *SPDS2* genes (*spds 1-1* and *spds 2-1*, respectively) for their research. The *spds1-1* mutant is a null while *spds2-1* has slightly leaky expression. These mutants had a normal phenotype whereas the double mutant, which has a small amount of Spd, was embryo lethal due to lack of maternal carryover of Spd (Imai et al., 2004). The embryo lethal phenotype was rescued by transformation with the WT *SPDS1* gene (Imai et al., 2004) emphasizing the importance of Spd in embryo development.

A. thaliana mutants that are unable to synthesize either Put or Spm are embryo lethal (Alcázar & Tiburcio, 2014). The Spd-mediated activation of eIF5A is one of the key functions of Spd as shown in experiments of yeast grown in Spd-limiting conditions (Chattopadhyay et al., 2008; Kang and Hershey, 1994). A recent review by Tiburcio et al (2014) discusses the absolute dependence of eIF5A on the freely available Spd for activation; the lack of free Spd leads to loss of cell viability (Kang and Hershey, 1994; Tiburcio et al., 2014).

Tassoni et al. (1996) reported the availability of free and conjugated polyamines in different organs of *A. thaliana*, and revealed that Spd is the most abundant polyamine, with the highest level detected in developing *A. thaliana* flowers. Spd is also the most abundant covalently bound or conjugated polyamine in the perchloric acid (PCA)-soluble fraction, and is highest in cotyledons. While the level of other polyamines is generally low in all organs, in the PCA-insoluble fraction of flowers, Spd and Put conjugates show higher levels (Tassoni et al., 1996; Tassoni et al., 2000). Germination and growth of *A. thaliana* seeds on solid media supplemented with 0.5 mM Spd lead to a 30% increase in leaf mass and production of a well-developed root system in the adult plant. At concentrations greater than 0.8 mM, the root growth was inhibited. The results also indicated that these growth conditions lead to increases in the levels of free and conjugated Spd in both soluble and the insoluble fractions (Tassoni et al., 2000).

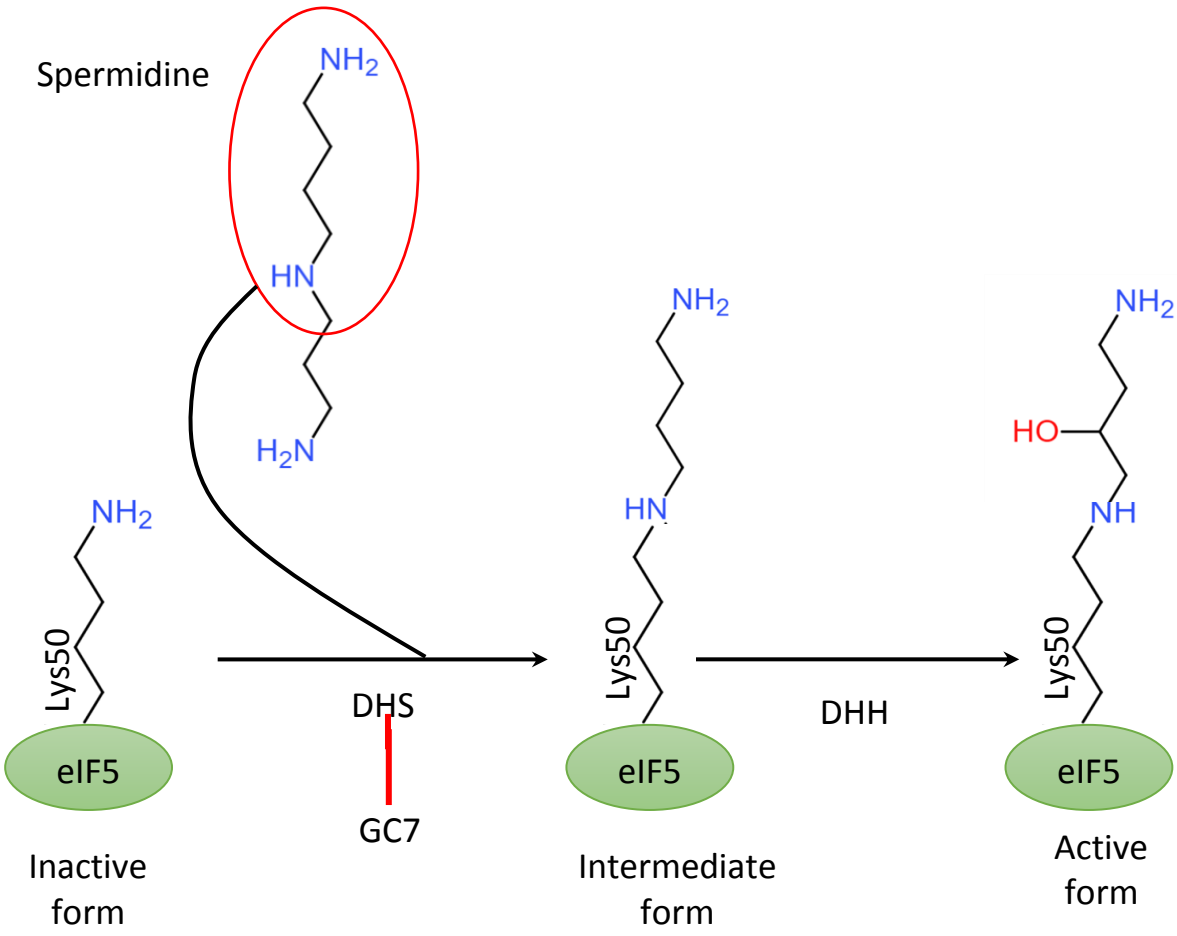

Figure 1-6. The eukaryotic translation initiation factor 5A (eIF5A) activation pathway

The enzyme deoxyhypusine synthase (DHS) transfers an amino butyl moiety (red circle) from spermidine (Spd) to the lysine residue (Lys50) of the inactive precursor eIF5A. The intermediate form is hydrolysed by deoxyhypusine hydroxylase (DHH) to produce the active eIF5A protein. N1-guanyl-1, 7-diaminoheptane (GC7) is a DHS inhibitor that prevents eIF5A activation in the 1st step.

(Adapted from Hauber et al., 2010)

The Spd effects described above are somewhat consistent with those observed when *A. thaliana* MTN-deficient mutant seeds were germinated and grown on Spd-supplemented media for 14 days by Waduwara-Jayabahu et al., (2012). Waduwara-Jayabahu (2011) hypothesized that the application of Spd might reverse some abnormalities during growth of the mutant, and conducted a pilot experiment of feeding Spd exogenously to MTN-deficient mutant seeds using Col-0 as a WT. Partial restoration of fertility in the otherwise infertile *mtn1-1mtn2-1* mutant was observed (Waduwara-Jayabahu et al., 2012). In the study reported in this thesis, exogenous feeding of Spd to MTN deficient mutant seeds was carried out in large scale to validate the preliminary results reported by Waduwara-Jayabahu et al., (2012).

1.4. Effect of Nicotianamine (NA)

Nicotianamine (NA) is a metal chelator present ubiquitously in higher plants (Takahashi et al., 2003). NA chelates metal ions of Fe (II), Fe (III), Cu (II) and Zn (II) which are important micronutrients for the healthy growth of plants. The nicotianamine bound metal ions are associated with NA transporters (Chu et al., 2010) for the mobility throughout the plant. The concentration of NA in both xylem and phloem is nearly 20 μM and 130 μM, respectively; suggesting that the transport of metals by NA occurs via both the xylem and phloem with a higher mobility in the phloem within the plant as shown by studies conducted using castor bean and tomato (Pich & Scholz, 1996).

NA biosynthesis involves conjugating three molecules of AdoMet (Higuchi et al., 1999) which produces three molecules of MTA (Dreyfus et al., 2009) as a byproduct. The *mtn1-1mtn2-1* mutant has an over-accumulation of MTA leading to the feedback inhibition of NA synthase (NAS) activity resulting in very low NA levels (Waduwara-Jayabahu et al., 2012). The

concentration of NA in mutant shoots and roots ranged between 20 - 500 nM / g of fresh weight. The highest NA levels were detected in the inflorescence (268 ± 58 pmol mg FW^{-1}) of 5-6 week old WT, as compared to the lower NA content (106 ± 50 pmol mg FW^{-1}) in rosette leaves. The *mtn1-1mtn2-1* mutant inflorescences had 34% less NA content than those of WT and NA was undetectable in the rosette leaves.

NA mutants of other plant species have also been studied extensively to understand the complex relationships between metal transport and development. Ling et al (1999) reported on a NAS mutant of *Solanum lycopersicum* (tomato), *chloronerva*, which has a complex phenotype including sterility, dark green mature leaves and leaf interveinal chlorosis. The interveinal chlorosis is an indication of iron (Fe) deficiency (Li and Lan, 2017; Ling et al., 1999). Analysis of the mature *chloronerva* mutant leaves revealed that those had an excess of Fe. Since the application of NA to leaves of the mutant reduced the iron content to a level of the WT, and the addition of NA to nutrient solution inhibited Fe uptake by roots of the mutant as well as of the WT, Ling (1990) concluded that NA directly or indirectly regulates the iron uptake in plants, and that in the absence of or reduced NAS activity, the resultant lowered NA leads to poor translocation of Fe. In addition to problematic translocation of Fe, the NAS mutant had defects in Cu translocation in the xylem, stressing the need for NA for proper translocation of metal ions (Ling et al., 1999).

Klatte et al., (2009) generated a quadruple NAS mutant (*nas4x-2*) knocking-out the expression of all the NAS genes in *A. thaliana*; the mutant produced no detectable NA, was male and female sterile with defective pollen and ovule development as well as had severe leaf chlorosis (Klatte et al., 2009). The intermediate mutant (*nas4x1*) also displayed interveinal chlorosis associated with Fe deficiency, a clear indication of reduced NAS activity.

The pleiotropic phenotype of the severe *mtn1-1mtn2-1* double mutant shares certain characteristics with *chloronerva*: appearance of interveinal chlorosis in first true leaves as early as 10 days post germination (Figure 1-7), presence of dark green leaves in the mature plant, and sterility in the plant (Waduwara-Jayabahu et al., 2012).

The *nas4x1* mutant displayed mild chlorosis during vegetative phase, which turned severe during transition to the reproductive phase (Klatte et al., 2009). The chlorotic symptoms in the *mtn1-1mtn2-1* mutant seedlings during vegetative phase fade upon maturity suggesting a slightly higher level of NAS activity in the *mtn1-1mtn2-1* mutants than in the *nas4x1* mutant.

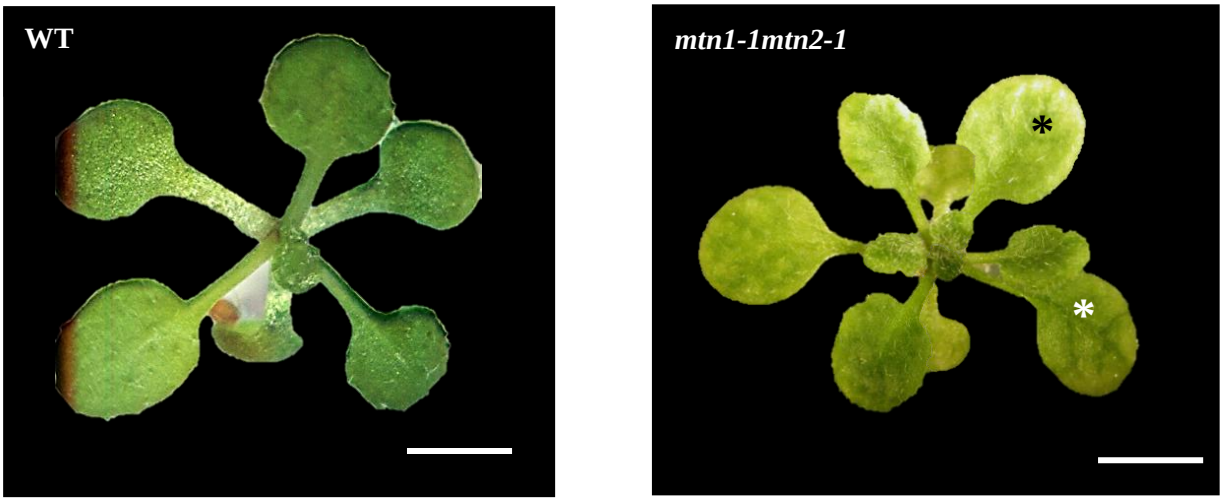

Figure 1-7. Interveinal chlorosis of the *mtn1-1mtn2-1* mutant plant

WT and *mtn1-1mtn2-1* mutant plants grown on half-strength Murashige and Skoog (½ MS) media for 14 and 20 days, respectively. The WT seedling shows typical coloring of the leaves and the seedling is slightly larger. The mutant seedling is lighter-colored and shows interveinal chlorosis (*), an indication of Fe deficiency.

Scale bar = 10 mm.

Other studies (Schuler et al., 2012) have shown that NA is responsible for the transport of Fe to sink organs such as young leaves and flowers; the lack of Fe transport to flowers results in improper pollen production as well as problematic pollen tube growth. Analysis of gene expression levels in flowers and seeds of the *nas4x1* mutant showed that reduced Fe may trigger developmental distress and modify Fe uptake and distribution (Klatte et al., 2009).

Taken together, these findings lead to the hypothesis that sterility of the MTN-deficient plants is at least partially associated with reduced NAS activity. Investigations into Fe supplementation in MTN-deficient mutants and monitoring gene expression levels at floral organs and seeds, as well as monitoring the reproductive characteristics are necessary to test this hypothesis.

1.5. Other factors associated with plant reproduction and growth

Other factors that are associated with plant reproduction and growth are protein arginine methyl transferase (PRMT) and eukaryotic translation initiation factor 5A (eIF5A). Mutants in PRMT5 (EC. 2.1.1.319) and eIF5A have pleiotropic phenotypes indicating effects on growth and development (Deng et al., 2010; Nishimura et al., 2005).

1.5.1. Protein Arginine Methyltransferase 5 (PRMT 5)

Methyl transferases are a group of enzymatic proteins that transfer a methyl (CH_3) group from a donor molecule to an acceptor molecule. The addition of a methyl group to the arginine residue of a protein allows recognition by specific binding partners (Bedford & Clarke, 2009). The post-translational methylation process is essential for the regulation of important biological processes such as transcription, RNA processing, DNA repair and signal transduction (Hernando et al.,

2015). The PRMT5 is a type I / II methyltransferase, involved in the formation of monomethylearginine and symmetric dimethylarginine based on the position of the methyl residue (Bedford & Clarke, 2009).

A. thaliana PRMT5 (*AtPRMT5*) mutants with reduced PRMT5 function displayed an array of pleiotropic phenotypes including delayed flowering, growth retardation, production of dark green and curled leaves as well as reduced sensitivity to vernalization (Hernando et al., 2015; Deng et al., 2010). AtPRMT5 enzyme methylates a wide group of substrates including histone and non-histone proteins. Mass spectroscopy measurements showed 15% of the proteins were RNA binding or processing factors such as *A. thaliana glycine-rich RNA binding protein 7* (*AtGRP7*) and *AtGRP8* (Deng et al., 2010). Furthermore, AtPRMT5 regulates the splicing of pre-mRNA of certain flowering-time regulatory genes. The loss of function or reduced function of AtPRMT5 leads to delayed flowering (Deng et al., 2010).

Marjon et al. (2016) examined whether MTA had an inhibitory effect on mammalian methyltransferases, especially on PRMT5, using *in vitro* biochemical assays with MTA supplementation. PRMT5 measurements showed strong inhibitions of PRMT5 and PRMT4 by MTA. Further experiments on the effects of MTA on cell lines deficient in methylthioadenosine phosphorylase (MTAP; a key enzyme in the methionine salvage pathway) confirmed that the activity of PRMT is impaired by MTA (Marjon et al., 2016). In addition, PRMT5 co-complexes such as RIO kinase (RIOK1), WD repeat domain 45 (WD45) / methylome protein 50 (MEP50) and co-operator of PRMT5 (COPR5) were susceptible in MTAP-depleted cells due to the over-accumulation of MTA in these cell lines (Marjon et al., 2016; Mavrakis et al., 2016).

The MTN-deficient *A. thaliana mtn1-1mtn2-1* mutant has a higher than normal MTA content.

Based on the findings of Marjon et al. (2016) and Mavrakis et al., (2016), this MTA might impair AtPRMT5 activity of the MTN-deficient mutants. The phenotype of the *mtn1-1mtn2-1* mutant is similar to those of the PRMT5 loss-of-function mutants in several respects including: delayed flowering, growth retardation, dark green curled leaves, sterility, fasciation and vascular deformities. Further investigation into the levels of AtPRMT5, its co-complexes, as well as other interacting partners within the MTN-deficient *mtn1-1mtn2-1* mutant is warranted. As a follow-up investigation of this study, the changes in expression levels with Spd and Tspm treatments could be examined to assess the effect of MTN deficiency on PRMT5 activity.

1.5.2. Eukaryotic Translation Initiation Factor 5A

The eukaryotic translation initiation factor 5A (eIF5A) is functionally and structurally conserved across all kingdoms (Feng et al., 2007). Loss-of-function mutants of eIF5A in yeast and *A. thaliana* showed severe detrimental development defects such as abnormal cell proliferation, cell division and cell death (Saini et al., 2009; Feng et al., 2007), indicating the importance of functional eIF5A.

Nishimura et al (2005) examined the independent effects of polyamines and eIF5A on cell proliferation in plants using inhibitors for polyamine biosynthesis and eIF5A activation. The α-difluoromethylornithine (DMFO) which significantly reduces Put and Spm was used as a polyamine biosynthesis inhibitor; activation of eIF5A was reduced by the deoxyhypusine (DHS) inhibitor *N1*-guanyl-1, 7-diaminoheptane (GC7). Although GC7 treatment reduced active eIF5A levels (Figure 1-6) it did not influence the polyamine levels. Suppression of active eIF5A with GC7 along with DMFO treatment resulted in inhibited cell growth. The reduction of Put and Spd levels became significant after 12h post incubation, while the decline of activated eIF5A became significant only after the polyamine levels dropped. The rate of cell proliferation was reduced

when both the polyamine and eIF5A levels were lowered indicating the intricate regulation of cell proliferation via polyamines and eIF5A. However, the individual contribution of each to the proliferation reduction was not clear (Nishimura et al., 2005). The importance of polyamines and eIF5A in development and growth is found throughout the literature but the exact mechanisms involved are yet to be elucidated. Future experiments designed to investigate the effect of the MTN-deficiency in *PRMT5* and *eIF5A* mutants can be based on the findings of the research presented in this thesis.

In addition to the altered PA profile and sterility, the MTN-deficient *mtn1-1mtn2-1* mutant displayed an array of vascular abnormalities (Burstenbinder et al., 2010) as well. Hence this study was designed to examine the contributory factors to changes in vasculature.

1.6. Plant vascular development

The plant vascular system comprises three distinct types of conductive tissue: the xylem, which transports water and minerals; the phloem which transports aqueous photo assimilates and the meristematic tissue or the cambium and procambium (Fukuda, 2004). The vascular tissue is differentiated from provascular cells as interconnected continuous cell files (Mattsson et al., 1999; Fukuda, 2004). In addition to transporting the nutrients, signaling molecules and water, the vascular tissue provides a rigid physical support to maintain the plant in an upright position (Mattssonn et al., 1999; Yang and Wang, 2016).

The development of the vascular tissue can be observed in all major organs during early development stages, as the provascular cells differentiate and align together to form well organized continuous, narrow cell lines (Foster et al., 1952). The cells that differentiate into

vascular cells (procambial cells) are continuously produced by both shoot and root apical meristems of adult plants (Fukuda, 2004), giving rise to xylem and phloem precursor cells.

During differentiation, cell-to-cell communication as well as long distance communication is important. Long distance communication occurs via the use of signaling molecules and is vital for the continued production of vascular tissue (Fukuda, 2004; Notaguchi & Okamoto, 2015). The xylem and phloem precursor cells differentiate into specific cells that make up the complex and well defined vascular tissue (Fukuda, 2004; De Rybel et al., 2016). The phloem precursors differentiate into phloem sieve elements, parenchyma cells, companion cells and phloem fibers, while the xylem precursors differentiate into xylem fibers, parenchyma cells and tracheary elements.

The vasculature of an adult plant is pre-established in the embryo and differentiates at predictable positions and times during development. However, in response to local signals these arrangements can be altered (Fukuda, 2004). The root vascular tissues develop from four provascular initial cells that undergo several rounds of oriented, periclinal cell divisions to create a patterned vascular bundle by the end of embryogenesis (De Rybel et al., 2014). The establishment of provascular cells is less complex in the embryos, than in the adult. The regulatory networks for provascular cell initiation as well as the development of the provascular strands in the early leaf primordia and developing leaves has been studied extensively in *A. thaliana* (DeRybel et al., 2014; Fukuda, 2014; Scarpella et al., 2010; Scarpella et al., 2004; Baima et al., 2001; Baima et al., 1995), but not much is known of the molecular mechanism of phloem cell differentiation.

1.6.1. Phytohormones

As indicated previously, MTN-deficient mutant *mtn1-1mtn2-1* and *mtn1-1mtn2-5* showed abnormalities in vascular development (Waduwara-Jayabahu et al., 2012). Plant growth and development is directed by a combination of endogenous and environmental signals. Intrinsic factors that influence vascular differentiation include the plant growth regulators and signaling components. Plant growth regulators are fundamental to the processes involved. They are tightly controlled and homeostasis is maintained to achieve a well-balanced growth of the plant because they control the growth and development of a plant as well as the developing embryos it carries, regulating virtually all levels of development to a degree (Gray, 2004; Yadegari & Drews, 2004).

Phytohormones are signal molecules produced within plants, and occur in extremely low concentrations. They include auxin, cytokinin (CK), gibberellins (GAs), abscisic acid (ABA), ethylene, brassinosteroids (BRs), salicylic acid (SA), jasmonic acid (JA) and strigolactones.

Diverse hormone pathways consist of many signaling components that link a specific hormone perception to the regulation of downstream genes. The signaling components that function as key regulators of vascular development include leucine rich repeats (LRR), Receptor-Like Kinases (RLK), and the Clavata 3/ Endosperm surrounding region (CLE) peptide (Torii, 2004; Zhou et al., 2011). The homeodomain transcription factor (HD-ZIP III) family directs the gene expression underlying the spatial information necessary for regulating procambial cell specification and proliferation (Baima et al., 2001).

The plant hormones auxin and BRs are both involved in promoting cell expansion (Nemhauser et al., 2004). These two hormone regulatory pathways are interlinked and studies have shown that elevated auxin levels result in a 40% up-regulation of BR-induced genes (Nemhauser & Chory,

2002; Goda et al., 2004; Nemhauser et al., 2004). Further experiments showed that auxin and BR are involved in hypocotyl elongation in *A. thaliana* seedlings (Nemhauser et al., 2004).

The auxin and CK activity within the growing plant is conserved as a dynamic balance. The auxin / CK ratio is carefully maintained in many areas of development such as metabolism, transport and signaling (Schaller et al., 2015). The formation and development of the root apical meristem is controlled primarily by the auxin and CK balance in this tissue (Schaller et al., 2015). The root growth is determined by the rate of cell division and differentiation. The core factors that determine this rate are auxin and CK (Schaller et al., 2015; (Dello Ioio et al., 2007).

The ethylene and JA pathways are involved primarily in defense against plant pathogens. Ethylene promotes maturation and senescence and JA stimulates plant defense pathways. The Ethylene response transcription factor 1 (ERF1) is one of the key interaction nodes for both the ethylene and JA pathways, further confirming the evidence of plant hormones working in a carefully balanced homeostasis (Lorenzo et al., 2003).

Although there are many growth regulators that play crucial parts in vascular development of the plant, Waduwara-Jayabahu et al (2012) suggests an impaired auxin flow in the *mtn1-1mtn2-1* mutant. Plant growth and development is controlled by a dynamic balance between the phytohormones auxin and CK. The *mtn1-1mtn2-1* mutants' pleiotropic phenotype includes vascular and fertility related issues. Therefore, the experiments conducted for the study reported in this thesis mainly focused on the plant hormone auxin and a few other downstream genes that respond to auxin flow and their response to the polyamine Spd. Examination of the effects of other phytohormones were beyond the scope of this study and will have to be carried out in future, based on the findings of this research.

1.6.2. Auxin

The plant hormone auxin is a major regulator of apical dominance, tropic responses, embryogenesis, vascular patterning and phyllotaxis, cell division and elongation, lateral root formation, apical dominance, leaf and flower development (Spicer et al, 2013; Michniewicz et al, 2007). Auxin is produced at the apical meristems (root and shoot) of the plant (Armengot et al., 2016).

Throughout the past many researchers have focused on the distribution of auxin in plants. The biochemical and physiological data that had been generated so far suggest that the auxin distribution in a plant is accomplished via two very distinct transport pathways which are both spatially and physiologically separated (Michniewicz et al., 2007).

The spatial distribution of auxin within the plant is achieved by PAT, which influences the degree of gene regulation by auxin gradients. The polar movement of auxin through the plant occurs via the vascular system in the stems providing long range auxin mobility. This movement is tightly regulated and is only part of a multimodal auxin transport network system (Bennett et al., 2016). Bennett et al (2016) proposed a model called the connective auxin transport (CAT). This model presents that CAT is localized and allows tissue to be modulated by the information brought in by PATs.

The identification of PAT inhibitors (Katekar & Geissler, 1980; Scanlon, 2003; Amijima et al., 2014) led to the discovery of the importance of auxin transport and the development of different mutants (Katekar & Geissler, 1980; Scanlon, 2003; Amijima et al., 2014). Indole acetic acid (IAA) is a natural auxin that is produced in the shoot apical meristem (SAM) and the expanding leaves. IAA is transported basipetally and laterally in the shoot while the root auxin is

transported acropetally and basipetally (Figure 1-8). Auxin transport within the plants is mediated by specific cellular transport proteins (Lomax et al., 1995) and the directionality of the auxin flow has been attributed to a polar distribution of efflux carriers (*Arabidopsis PINFORMED* / AtPIN FORMED / PIN) in the cell membranes (Rubery & Sheldrake, 1974; Schuetz et al., 2013). The use of PAT specific inhibitors causes the formation of local aggregates of vascular cells and discontinuous veins in newly developed leaves in growing plants (Mattsson et al, 1999). The PAT inhibitors were less effective in the inhibition of the vascular pattering of seedlings grown in inhibitor supplemented media, suggesting that the role of auxin in vascular patterning occur at early embryonic stage (Mattsson et al., 1999). Procambial cells are pre-determined in cotyledons at the embryonic stage. These pre-procambial cells are activated via auxin gradient to become xylem precursors during vascular patterning (Berleth and Jurgens, 1993).

The major players of PAT are the PIN auxin efflux carriers. The PAT is mediated by PIN3, PIN4, and PIN7 during embryonic stages, and the PINs are located in the plasma membrane at the basal end wall in both procambial cells and xylem parenchyma cells (Fukuda, 2004; Schuetz et al., 2013). The polarized auxin flow is caused by the asymmetrically localized PIN1 protein, leading to the formation of continuous columns of procambial cells (Fukuda, 2004). PINOID, a serine/threonine kinase, is also implicated in the asymmetrical transport of AtPINs, as the PINOID mutant shows similar phenotype to the PIN1 mutant and as PINOID is expressed in xylem precursor cells and parenchyma cells (Benjamins et al., 2001). *A. thaliana* pattern forming *GNOM* gene directs PINs to the appropriate apical basal membranes while the PINOID phosphorylates the PINs determining the exact location providing an auxin gradient for vascular differentiation (Richter et al., 2010).

A model proposed by Dengler et al. (2006) explains auxin mobility and examines the relationship between the internal vascular bundle arrangements and the vasculature of lateral organs leading to phyllotaxis. The model explains how the auxin moves away and also towards the shoot apical meristem, and how it is concentrated in points that identify the future positions of the leaf primordia via PIN proteins. The PIN proteins re-distribute to the center of the meristem once the leaf primordia commence development, and align in a narrow line connecting the cells forming the procambial cell line for the future mid-vein (Dengler, 2006; Scarpella et al., 2006). The model proposed by Bennett et al (2016) suggests that CAT mediates communication between PAT and the surrounding tissues. Their results show a gradient of auxin transporters across the stems. The majority of PATs controlled by PIN1 at one end and the ABCB19/1 expressing pith cells at the other end with the PIN4 /PIN 7 expressing parenchyma cells in-between (Benette et al., 2016). This model tries to explain how cross communication between internodes within the plant occur. They suggest PIN3, PIN4 and PIN7 auxin transporters arranged laterally across the stem facilitate communication between PAT and CAT.

Baima et al (2014) proposed another model for the positive and negative feedback regulation of auxin and vascular development by various transcription factors. Transcription of the HD-ZIP III family genes *ATHB8* and *ATHB15* occurs strictly in the procambial or xylem precursor regions (Baima et al., 1995; Fukuda, 2004; Baima et al., 2014), and is activated by MONOPTEROS (MP); *MP* which in turn is activated by auxin flow. The antagonistic relationship between these transcription factors are seen when overexpression of *ATHB8* or down regulation of *ATHB15* increases proliferation of xylem cells.

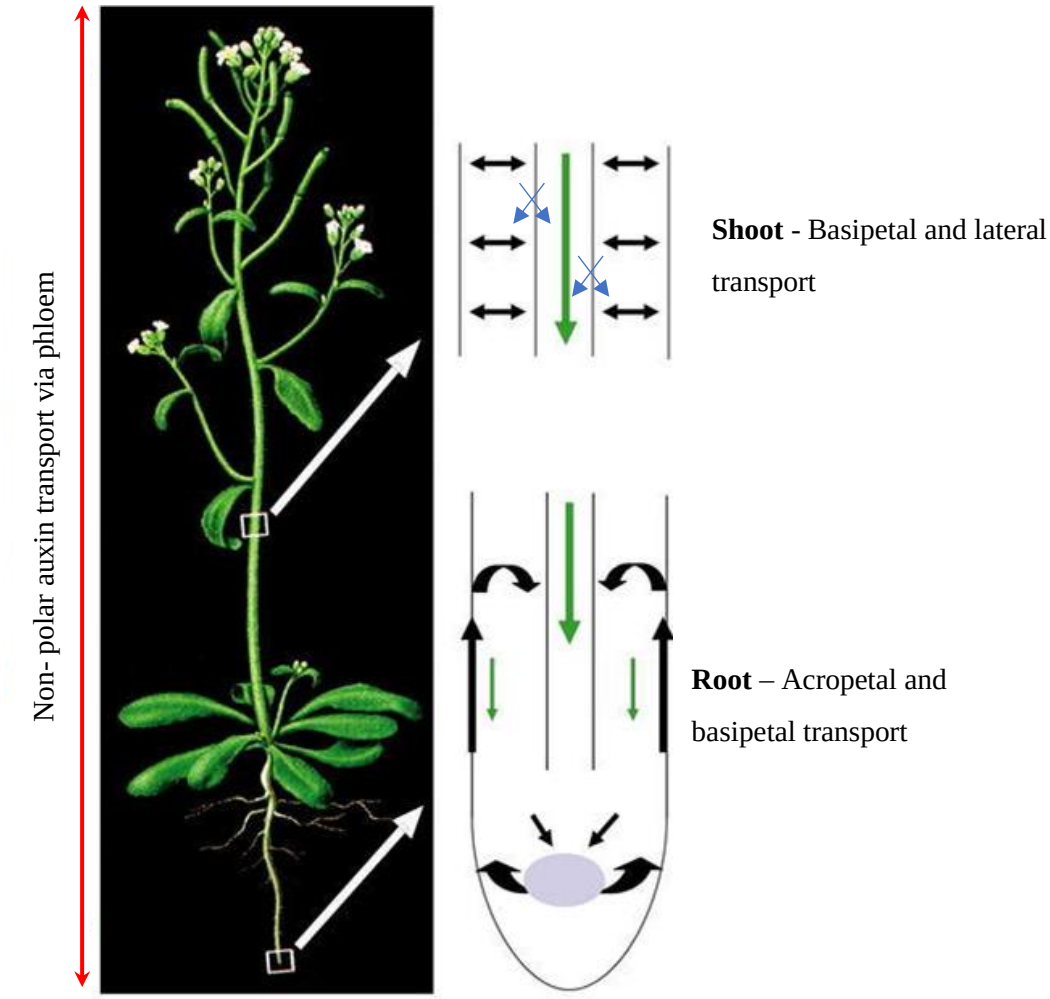

Figure 1-8. Schematic for polar and non-polar auxin transport in *A. thaliana*

The fast non-polar auxin distribution throughout the plant is via the phloem (red arrow). The slow polar auxin transport (PAT) is shown in green and black arrows. Blue arrows indicate connective auxin transport (CAT), which communicate signals brought over by PAT to neighboring tissue.

(Adapted from Michniewicz et al, 2007 and Bennett et al., 2016)

The TARGET OF MONOPTEROS5/LONESOME HIGHWAY (TMO5/LHW) basic helix-loop-helix (bHLH) transcription factor heterodimer is a rate-limiting regulator of periclinal cell divisions. *MONOPTEROS (MP)* is activated by the flow of auxin through the procambial cells, ensuring the continuation of vascular formation throughout the plant. MP in turn activates HD ZIP III genes such as AtHB8 allowing these cells to differentiate into vascular stem cells. Mutants of MP display defects in auxin signaling, such as failure to establish vascular stem cells (Hardtke, 1998), similar to other auxin transport mutants such as *pin1*, *trn1*/(TORNADO1), and *lop1*/(LOPPEDED), which are severely defective in vein formation as well (Carland & McHale, 1996; Gälweiler et al., 1998; Cnops et al., 2000). Defective vein development is also observed in auxin–insensitive mutants (*bodenlos*) which cannot recognize auxin (Hamann et al., 2002) as well as when normal plants are treated with PAT inhibitors such as 1-N-naphthylphthalamic acid (Mattsson et al., 1999).

1.6.3. Cytokinin

Cytokinins (CKs) are another important phytohormones that regulates diverse plant growth and developmental processes including female gamete and embryo development, seed germination, cell division, formation and maintenance of procambial cells, regulation of plant meristem activity, morphogenesis in shoots and roots as well as floral development (Werner et al., 2001). The CK biosynthesis genes are expressed in areas of continuous growth such as root apical meristem and root vascular bundle (Mähönen et al., 2000). CKs are mobilized via the vascular system to other regions of the plant. Generally, cytokinin transport is acropetal via the xylem sap, but there is no real polarized transport (Le Bris, 2017). Mähönen et al (2000) reported *WOODEN LEG (WOL)* gene is required for the asymmetrical cell division needed for phloem and procambium establishment. The *CRE1/AtHK4* gene, encodes a histidine kinase which act as a

CK receptor (De Leon et al., 2004). Studies in *WOL* mutants showed reduced number of procambial cells in embryos while the vascular system in roots consisted of only xylem tissue. This shows that CK functions through *WOL/CRE1/AtHK4* and is necessary for the maintenance of procambial activity (Mähönen et al., 2000). These CK receptors work together with histidine-containing phosphotransfer factors and response regulators. In *A. thaliana*, there are 22 response regulators (*ARR1–ARR22*) under two distinct subtypes: type A, with 10 members and type B, with 11 members (Nguyen et al., 2015). The type A members are CK inducible, with only a receiver domain, while the type B are not CK-inducible and have both receiver and output domains. The *ARR7* and *ARR15* are expressed ectopically in the central and peripheral zones of *mp* mutants but not in WT. These findings suggest that *ARR7* and *ARR15* are targets of MP-mediated auxin signaling in the central zone while being CK suppressors (Su et al., 2011).

Cell specification during embryogenesis is under the control of auxin and CK. The asymmetric distribution of auxin via PIN proteins during apical –basal axis formation is the first crucial step during embryo patterning (Möller and Weijers, 2009). During root meristem development, meristematic cell division is induced by auxin and the differentiation of meristematic cells by inhibiting auxin signaling is carried out by CK (Su et al., 2011). In the shoot, the opposite occurs, where the CK promotes shoot meristematic cell proliferation while auxin trigger organogenesis by inhibiting CK biosynthesis (Su et al., 2011). This antagonistic and dynamic relationship between auxin and CK in the shoot and root meristems is the key regulator for cell proliferation and differentiation.

1.7. Molecular Tools for studying gene expression

Genetic manipulation of plants has been around for quite some time in the scientific world and the amount of data on different plant genes is accumulating at a rapid rate. The creation and screening of mutants for the purpose of understanding fundamental biological processes is not a novel idea anymore. Conventional screening methods based on phenotypic characteristics as well as the use of selectable markers such as those for antibiotic or herbicide resistance is still being used. However, more efficient screening and observation at a cellular or tissue level provides better resolution. A couple of the most widely used screening tools are luminescent markers and reporter genes (Jansson, 2003). The introduction of these markers or reporters into plants is facilitated by; micro projectile bombardment, microbial vectors, microinjection, electroporation and transfection, transgenic lines carrying reporter genes. Reporter genes are widely used in molecular biology to study gene expression; they are also used as markers for transformants. Using reporter genes is a non-destructive method for observing and identifying tissues with minimal manipulation of the samples (Huttly, 2009). The use of fluorescent reporters is preferred by many molecular biologists, as the gene expression can be observed in real-time and there is minimal damage to the sample.

1.7.1. Reporter genes

In molecular biology, a reporter gene is a functioning segment of a gene that is attached to a regulatory region of a gene of interest in a bacteria, cell culture, animal or plant. Reporter genes are employed to obtain an enhanced view of gene expression at the sub-cellular, cellular and tissue levels (Ziemienowicz, 2001). The gene that is chosen as a reporter has certain characteristics that will assist in identifying whether the gene of interest has been taken up by the organism or if it is expressed in a particular tissue type. The genes for chloramphenicol

acetyltransferase (*cat*), β-glacatosidase (*lacZ*), β-glucuronidase (*uidA*), luciferase (*luc*), green fluorescent protein (*gfp*) are some of the commonly used reporters used to assess gene expression, protein localization and protein trafficking at inter- and intra-cellular levels (Ziemienowicz, 2001). Reporter genes can be designed as transcriptional (tagging a gene promoter with a reporter) or translational fusions (tagging the protein product with a reporter). The study reported in this thesis used hormone response reporters as well as pre-vascular markers that express a fluorescent signal to observe auxin mobility and pre-vascular cell determination.

1.7.2. *Arabidopsis thaliana HOMEOBOX 8 (AtHB8)* gene reporter

Genes belonging to the homeodomain protein family (HD-ZIP) are important for cell differentiation and cell development in plant systems. Several studies conducted using meristem mutants of *A. thaliana* (*KNOTTED1*; *KN1*; Hake et al., 1992) and cell identity mutants (*GLABRA2*; Rerie et al., 1994) have shown altered leaf morphology and abnormal trichome initiation, respectively. Isolation and characterization of homeodomain proteins in *A. thaliana* (AtHB) had been carried out to further understand the putative genes that regulate plant development (Sessa et al., 1993; Baima et al, 1995; Scarpella et al., 2004). Baima et al., (1995) characterized the expression of the *A. thaliana HD-ZIP III homeobox 8 gene (AtHB8*) by *in situ* mRNA analysis and showed that the gene was transcribed in procambial cells of the developing embryo, as well as in other developing organs and during the regeneration of vascular strands. They further showed that in seedlings, the *AtHB8* gene is first transcribed in the procambial regions of the first true leaves (Figure 1-10). Additional studies (Baima et al., 1995) have confirmed that the expression of *AtHB8* is in preprocambial cells. The *AtHB8* expression promotes vascular differentiation (Baima et al., 2001; Baima et al., 2014). Scarpella et al (2004)

examined *AtHB8* expression during true leaf development and documented the remarkable consistency of its expression during vascular patterning, making it an ideal marker for assessing provascular tissue development (Figure 1-9).

According to the model proposed by Baima et al. (2001, 2014), *AtHB8* gene expression and the expression of several other HD-ZIP III genes are induced by MP, which is regulated by auxin flow in the xylem procambial cells, leading to xylem differentiation (Su et al., 2011). Chromatin immunoprecipitation assays revealed that AtHB8 interacts with ACL5 and BUD2, two enzymes involved in Tspm synthesis (Carlsbecker et al., 2010; Baima et al., 2014). The positive feedback loop of auxin flow influences MP, and in turn activates *HD-ZIP III* genes in procambial precursor cells leading to xylem vessel cell determination (Ohashi-Ito & Fukuda, 2010).

The *A. thaliana* MTN-deficient *mtn1-1mtn2-1* homozygous mutant has severe vascular development abnormalities, including asymmetric arrangement and increased number of vascular bundles, indicative of altered xylem differentiation and development. Investigation of the impact on the phloem tissue of the mutant should be carried out in future research. Since the fate of the cells becoming xylem precursor cells is determined during embryonic development, observing vascular development during embryonic stages will provide information of when and to what degree the vascular development is impaired in MTN-deficient mutants. Therefore, embryos excised from the MTN-deficient mutants (*mtn1-1mtn2-1* and *mtn1-1mtn2-5*) were examined for early vascular development during the course of this research.

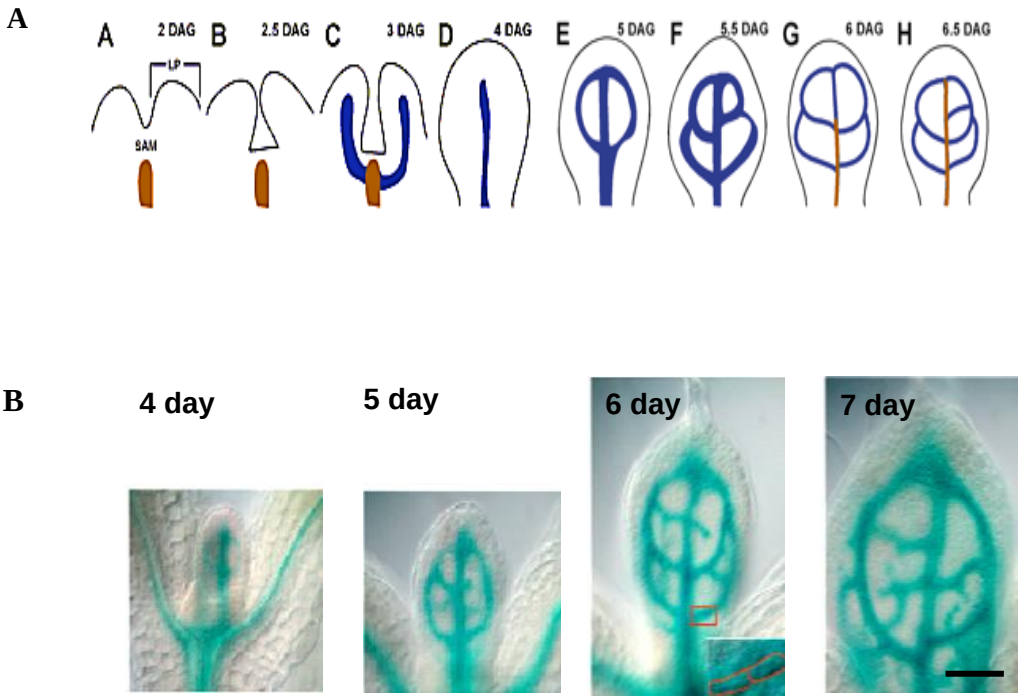

Figure 1-9. *A. thaliana* vein development in first true leaf

A- Schematic diagram of the vascular development in the first true leaf of *A. thaliana*. Brown line depicts meristem tissue and blue lines indicate provascular tissue. (Adapted from Scarpella et al., 2004).

B - The GUS activity of *AtHB8::GUS*, in the leaf primordia and first true leaf of *Arabidopsis thaliana* in 4, 5, 6 and 7 days after germination. The inset in 6 day after germination is a close up of the vasculature. The outlined cells in the inset are elongated procambial cells.

Scale bar: 100 µm. (Adapted from Baima et al., 2014).

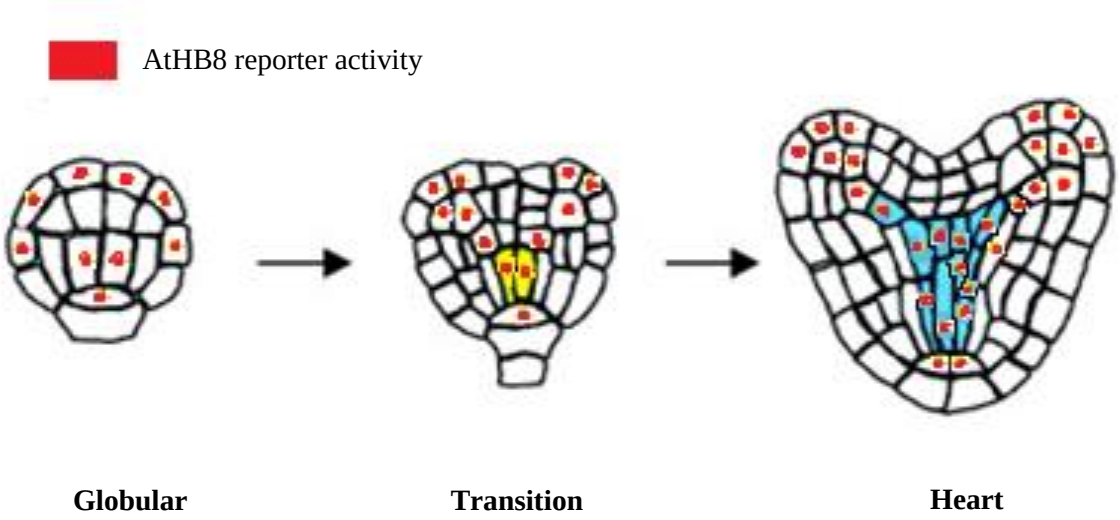

Figure 1-10. The *AtHB8* gene expression patterns in developing *A. thaliana* embryos

(A) Schematic diagram of cell fate during embryonic development of *A. thaliana* from globular stage (left) to heart stage (right). The two central cells are highlighted in yellow in the transition stage embryo. These cells divide longitudinally and transversely to become the procambium (blue) in the heart stage embryo. (Adapted from Ohashi-Ito and Fukuda, 2010).

1.7.3. Auxin response reporters

Several reporters are being used to monitor auxin responses and availability of auxin. The earliest reporter was developed based on Auxin response elements (AuxREs) first identified in studies of a soybean gene that was transcriptionally induced within minutes of auxin application (Liao et al., 2015; Liu et al, 1994). Subsequent analysis of the promoter led to the creation of the DR5 auxin reporter which consists of seven tandem repeats of the auxin responsive TGTCTC element fused to a minimal promoter upstream of the coding region for *β-glucuronidase* (GUS) (Ulmasov et al., 1997). The GUS coding region was later replaced with GFP and YFP to create fluorescent reporters of auxin maxima in plants (Zhou et al., 2014).

Another synthetic auxin response reporter based on DR5 activity was generated by Liao et al. (2015) for better sensitivity and precise identification of auxin gradients in plant tissue. Since the AuxREs of the DR5 reporter had a medium binding affinity leading to limited sensitivity, to improve the function and sensitivity of the DR5 reporter, the original nine repeats of AuxREs in the DR5*rev* promoter were replaced with a novel binding site (TGTCGG). This new reporter was named DR5*v*2, and showed a much broader and precise expression pattern than that of DR5 reporter. In early embryos, the expression levels of both DR5 and DR5*v*2 were comparable. However, at later maturing growth stages such as heart and torpedo, new expression domains in DR5*v*2 were present. These new domains were more evident in embryonic cotyledon and vasculature than DR5 (Liao et al., 2015).

Liao et al. (2015) developed a second reporter based on the DII-VENUS reporter for semi-quantitative analysis of auxin-input in plant tissue. The DII-VENUS reporter is an Aux/IAA based auxin signaling sensor (Brunoud et al., 2012). The VENUS yellow fluorescent protein is

fused to the Aux/IAA auxin-interaction domain (DII) which is an auxin dependent degradation domain, in-frame. Therefore, the absence of fluorescence signal indicated auxin accumulation (Liao et al., 2015). This construct is able to provide information on relative auxin distribution at a cellular level in different tissues. The new reporter developed by Liao et al (2015), is a combination of DII fused to n3xVENUS and a mutated DII_VENUS (mDII) with an ntdTomato. The construct is driven by the ribosomal promoter *RPS5A*, which is active in most dividing cells (Liao et al., 2015). The new reporter was named R2D2 (Ratiometric version 2 of D2's). Liao et al (2015) reports that the auxin input detected by R2D2 during early embryogenesis is consistent with observations made with other auxin response reporters such as DR5 and DR5*v*2.

During *A. thaliana* embryogenesis, PIN 7 is the first PIN protein to be expressed in the zygote. The expression is localized in the apical side of the basal cell, enabling auxin transport into the apical cell based on auxin gradient (Möller and Weijers, 2009). The PIN1 expression shows polarity in the 32-cell stage and is localized to the provascular cell basal membranes next to the hypophysis, and is thought to transport auxin into the hypophysis (Figure 1-11, B III). PIN 4 expresses late in the embryonic development where expression is seen in the uppermost cell of the hypophysis in the heart stage. The DR5 expression is seen in the apical cell and in the proembryo and then later in the hypophysis as well as the apical cell domains of the embryo (Möller and Weijers, 2009) which are the future cotyledon tips (Figure 1-11 A, B and C).

A

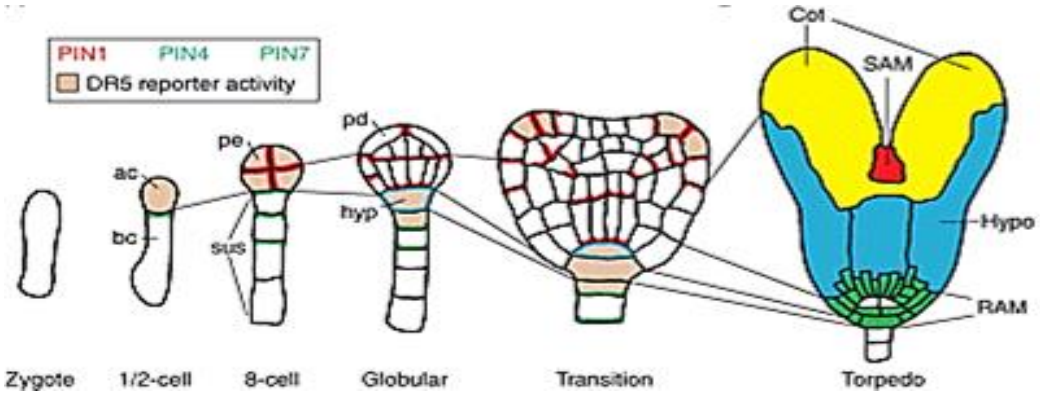
PIN1
PIN4
PIN7
DR5 reporter activity
ac
bc
pe
sus
pd
hyp
Cot
SAM
Hypo
RAM
Zygote
1/2-cell
8-cell
Globular
Transition
Torpedo

B

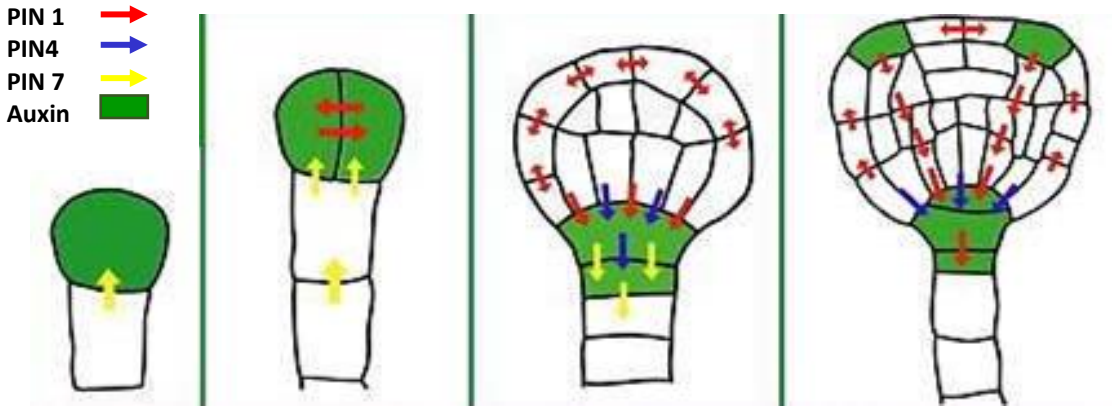
PIN 1
PIN4
PIN 7
Auxin
I
II
III
IV

C

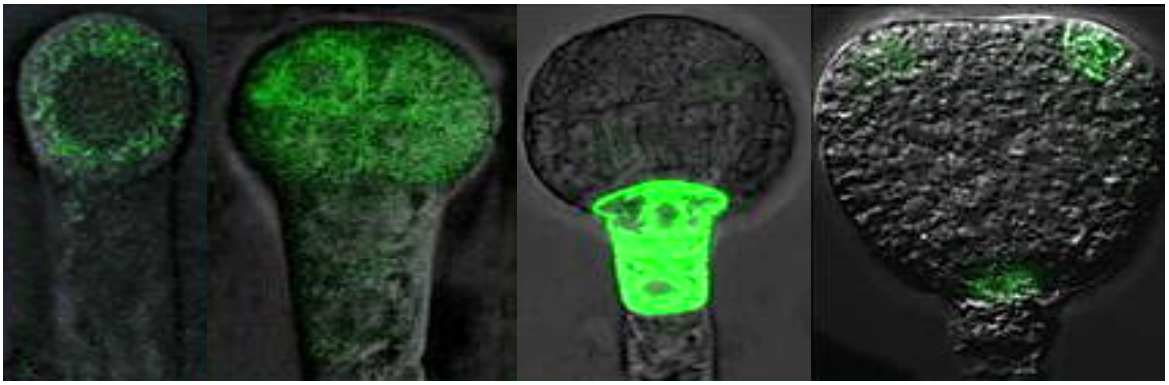
I
II
III
IV

Figure 1-11. The auxin distribution and auxin response reporter expression patterns in the developing *A. thaliana* embryos

A) Schematic diagram of PIN1, PIN4, PIN7 and DR5 expression in developing *A. thaliana* embryo. The zygote develops into two cells; the apical cell (ac) and the basal cell (bc). The apical cell shows DR5 activity (pink) indicating the presence of auxin. At the 8-cell stage, the basal cell has formed the suspensor (sus), which anchors the embryo to the seed. The apical cell has further divided into eight cells and formed the proembryo (pe), which shows PIN1 expression with no polarity and DR5 activity. The globular embryo has PIN1 activity in the protoderm (pd) while PIN4 is expressed in the hypophysis cell (hyp). DR5 activity is observed in the hypophysis indicating auxin maxima. In the transition stage, PIN1 expression is in the apical half of the embryo. PIN4 expression is now seen at the hypophysis and the future root apical meristem (RAM). The DR5 expression is concentrated to the future cotyledon tips and the bottom of the embryo. The coloured regions of the torpedo stage embryo show RAM in green, the hypocotyl (Hypo) in blue, the cotyledons (Cot) in yellow and the shoot apical meristem in red. (Adapted from Möller and Weijers, 2009).

(B) Schematic diagram of PIN1, PIN4, PIN7 and auxin distribution in developing *A. thaliana* embryo from the one-cell stage to the transition stage. PIN7 (yellow) is expressed from the earliest stages and PIN1 (red) and PIN4 (blue) start to express at globular stage. The arrows depict the auxin flow mediated by each PIN protein. The polarity of PIN localization changes during the embryo development. The accumulation of auxin (green) correlates with the PIN expression in the apical cell and developing pro-embryo (II), the basal part of the globular embryo and the upper suspensor cell / hypophysis (III), the future cotyledon tips and future root apical meristem (IV). (Adapted from Michniewicz et al, 2007).

(C) DR5::GFP expression pattern depicting auxin distribution marked by activity of auxin responsive promoter DR5 in pre-globular, globular and transition stage embryos. (Adapted from Friml et al., 2003).

Indirect visualization of auxin gradient achieved by the use of DR5 promoter driven reporter constructs (Figure 1-11 C), which allow visualization of where and when the PAT is disrupted in the developing embryo. Considering the model of PAT via PIN proteins (Möller and Weijers, 2009), use of such reporters in the MTN-deficient mutant backgrounds (*mtn1-1mtn2-1* & *mtn1-1mtn2-5*) will disclose if this disruption is one of the major causes of the disordered vascular development. The CAT is localized allowing tissue to modulate and be modulated by PAT signals (Bennett et al., 2016). Problematic PAT will produce a reduction of signal to distal tissue, and the CAT will not function efficiently. Tissues will be misguided due to lack of proper information and produce unprecedented, pleiotropic results as observed in the *mtn1-1mtn2-1* mutant.

1.7.4. *Monopteros* reporter

MP is expressed during embryonic growth stages, and responds to auxin flow and in-turn modulates the activation of AtHB8. This gene is an auxin response factor and is known as MONOPTEROS (At1g19850) gene.

Mayer et al. (1991) discovered that four genes, including the *Auxin response factor 5 (ARF5) / MP* gene, are involved in the apical-basal pattern formation. Mutations in the *MP* gene stop the development of the hypocotyl, radicle and root meristem, which are components of the basal pattern. These results suggest the requirement of the *MP* gene in the early embryo development stages, when the apical-basal pattern formation takes place (Mayer et al, 1991).

Baima et al (2014), proposed that *MP* is an inducer of the HD ZIP III genes (*AtHB8*, *Rev*, etc.) in provascular cells, leading to xylem vessel differentiation under the influence of an auxin gradient. Many ARFs are widely expressed, whereas *MP* (*ARF5*) is expressed in the lower level

of the pro-embryo (Figure 1-12, A). Rademacher et al. (2011) reported that during embryo development at the heart shape stage, ARF5/MP is expressed in domains of vascular tissue formation. This is consistent with the model proposed by Baima et al. (2014), invoking MP in activation of HD ZIP III genes for vascular development.

This relationship between MP and vascular development in the embryo is important to study the development of vasculature in the *mtn1-1mtn2-1* mutant, which displays many developmental deformities, including irregular vascular development, increased number of vascular bundles and high degree of fasciation. Observing the MP expression in the developing embryos of the MTN-deficient mutants will help in identifying the cause of disrupted vascular development. The study presented in this thesis investigated whether the *MP* expression is disrupted in the early development stages of the mutant embryos.

The examination of auxin response reporter (DR5*rev*::GFP) expression in MTN-deficient mutant embryos (*mtn1-1mtn2-1* and *mtn1-1mtn2-5*) was carried out in this research project. To validate the observations obtained from auxin response reporter expression patterns in embryos arising from the Spd-treated and non-treated plants this second reporter (MP::GFP) was employed. To visualize whether the *MP* expression is disrupted in the early development stages of the mutant embryos, the fluorescent-tagged reporter gene was introduced into the MTN-deficient mutants and the expressions of the reporter was monitored.

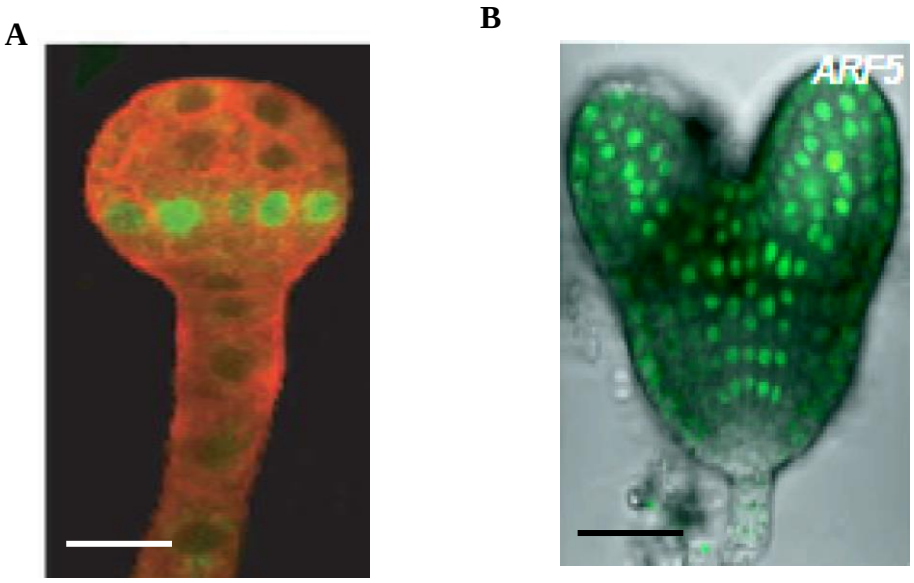

Figure 1-12 Expression of *ARF5/ Monopteros* in *A. thaliana* embryos

(A) Expression of auxin response factor (ARF) in pro-embryo, globular stage of *A. thaliana*. *ARF5 / MONOPTEROS* is expressed in lower levels (green signal). (Adapted from Rademacher et al., 2011). Scale bar = 20 µM

(B) *ARF5 / MP* expression pattern in heart stage embryo of *A. thaliana*. The expression is seen throughout the embryo (green signal). (Adapted from Rademacher et al., 2011). Scale bar = 100 µM

1.8. Objectives

1.8.1. General objective:

This research was formulated with the overall objective of assessing the effect of Spd-supplementation on the reproductive and vascular development of MTN-deficient *A. thaliana* mutants.

1.8.2. Specific objectives:

The specific objectives of this research were to examine the effect of Spd-supplementation on *mtn1-1mtn2-1* and *mtn1-1mtn2-5* mutants with special reference to the following:

a. Compare the changes in vasculature of adult mutant plants to the wild type.
b. Evaluate vascular development in developing embryos of the mutants.
c. Examine the growth, development and functions of reproductive organs of the two mutant types (*mtn1-1mtn2-1 and mtn1-1mtn2-5*).
d. Assess the auxin distribution and activation of auxin response reporters in embryos.

Chapter 2

The effect of Spd feeding on vasculature and fertility of MTN-deficient mutants

2.1 **Introduction**

A. thaliana mutant plants deficient in MTN displayed an array of abnormalities in vegetative phenotypes and reproductive development, of which, the abnormalities in vasculature, male and female fertility, developmental progression as well as interveinal pigmentation were some of the key features (Burstenbinder et al., 2010; Waduwara-Jayabahu et al., 2012). In most plants including *A. thaliana*, MTN hydrolyzes MTA to MTR and adenine. The MTR enters the Met recycling pathway (Yang cycle) (Giovanelli et al., 1985; Sauter et al., 2013), which recycles sulphur containing metabolites to Met. The Met recycling pathway is universal and found in all organisms (Giovanelli et al., 1985).

A. thaliana mutant *mtn1-1mtn2-1* showed accumulation of MTA which leads to feedback inhibition of MTA synthesizing reactions (Waduwara-Jayabahu et al., 2012). The analysis of the PA profiles of the homozygous MTN-deficient mutant *mtn1-1mtn2-1* revealed a significant increase of putrescine (Put), while the spermine (Spm) levels were lower than those of the wild type (WT), although spermidine (Spd) levels were not significantly different (Waduwara-Jayabahu, 2011). Polyamines are associated with numerous biological processes including the hypusination and activation of eukaryotic translation initiation factor 5A (eIF5A, Chattopadhyay et al., 2008), mobility of nucleic acids, growth and development as well as stress response (Minocha et al., 2014).

Waduwara-Jayabahu (2011) hypothesized that altered PA profile leads to changes in other interacting pathways and the plant attempts to compensate the imbalance. The polyamine Spd is important for embryonic growth as shown by Imai et al. (2004). Studies in *Drosophila melanogaster DAD11* gene mutants have shown that Met, AdoMet and methionine sulfoxide are

important factors for achieving normal fecundity (Chou et al, 2014). Waduwara-Jayabahu (2011) examined whether the application of Spd would reverse some reproductive abnormalities in the adult plants. Exogenous supplementation of Spd to MTN-deficient *mtn1-1mtn2-1* mutant seeds was carried out using the *A. thaliana* ecotype Columbia as a WT control in the pilot experiment, and partial restoration of fertility was observed. This experiment was repeated in large scale to validate the result at the beginning of the study reported in this thesis. This study also used two different mutants from the series of MTN deficient double mutants created by Waduwara-Jayabahu et al. (2012); a severe mutant, *mtn1-1mtn2-1* and a less severe mutant *mtn1-1mtn2-5*. One of the main focuses of the research presented in this thesis was investigating the effect of short-term feeding of Spd (14DAG) on vascular and reproductive development of the MTN-deficient mutants. Two approaches were used to examine the effect of Spd feeding on mutant plants: 1) microscopy and 2) reporter gene expression in WT and mutant genetic backgrounds.

A. thaliana mutants having severe deficiencies in MTN activity (*mtn1-1mtn2-1*), showed increased number of vascular bundles with higher number of xylem and phloem cells in individual bundles than the WT, and abnormal reproductive development (Waduwara-Jayabahu et al., 2012). Vascular and reproductive development in plants is regulated by several hormones of which auxin, CK and BR are the key players involved in cell division and elongation (Nemhauser & Chory, 2002; Goda et al., 2004; Nemhauser et al., 2004). The abnormal development of the mutant vasculature and reproductive structures suggests that the homeostasis of these three hormones is disrupted in the plant.

Polyamine activity is closely connected with hormonal activity in plants (Liu et al., 2013). For example, the plant hormones auxin and gibberellin induce polyamine synthesis (Bagni & Serafini-Fracassini, 1985), while auxin and polyamines are both associated with growth

regulation and development (Hove et al., 2015). The research described in this thesis was mainly focused on the phytohormone auxin.

Auxin plays a key role in plant growth and development (Zhao, 2010). The differentiation of plant cells into tissues is dependent on cell identity and positional signaling (Hove et al., 2015). The fate of a cell is adjusted based on its relative positioning to others from the information gathered via cell-to-cell communication (Hove et al., 2015). Auxin signaling and transcription factors such as WUSCHEL-RELATED HOMEOBOX (WOX) are associated with tangential cell division during embryonic stage (Costanzo et al., 2014). Tangential cell division is important for adding length to a developing organ. These factors mediate the cell division from a similar cluster of primary cells to differentiate into two distinctly different cell identities (Breuninger et al., 2008). The *mtn1-1mtn2-1* mutants displayed characteristics of altered cell identity and problems in positional signaling in the vegetative state of the plant (Waduwara-Jayabahu et al., 2012).

According to the available models on auxin mobility (flux-based and concentration-based, Berkel et al., 2013), if the mutant had problematic auxin signaling during early developmental stages, the auxin mediated cell-cell communication would be malfunctioning leading to issues in longitudinal and radial patterning. During angiosperm embryogenesis, several essential domains of the developing plant including its polar axis, domains that will be organized into other parts of the plant body (e.g. apical and basal meristem, cotyledons, root, hypocotyl) and the primary tissue and organ systems are established (Jürgens, 2001). The apical-basal patterns of the embryo is organized along the longitudinal axis defining the root and shoot poles, and the radial axis involving the development of the ground tissue, the vascular tissue and the outer epidermis (Mayer et al., 1991; Baima et al., 1995). Examination of auxin mobility and vascular pattern

initiation during embryo stages of the MTN-deficient mutants may shed some light on the auxin distribution and cell activation issues. Examining auxin response reporter expression and reporters of axin dependent genes for cell activation in the MTN-deficient mutant backgrounds is an ideal first step. Fluorescent tagged reporters for auxin response and procambial cell activation genes are some of the tools that can be used for this purpose. In the study reported in this thesis, fluorescent tagged reporters for auxin response and procambial cell activation genes were used and the reporter expressions in the embryos arising from plants not treated with Spd and Spd-treated mutant plants (*mtn1-1mtn2-1* and *mtn1-1mtn2*-5) were observed to elucidate the effect of Spd-supplementation on auxin distribution and cell activation issues during development of the mutants.

Waduwara-Jayabahu et al. (2012) suggests auxin mobility issue in earlier research carried out using the MTN-deficient mutants (*mtn1-1mtn2-1* and *mtn1-1mtn2-5*). The main focus of this research study presented in this thesis was infertility of the *mtn1-1mtn2-1* mutant, vascular initiation during embryo development of both MTN-deficient mutants and auxin distribution at the embryonic stage of the mutants (*mtn1-1mtn2-1* and *mtn1-1mtn2-5*). Several hypotheses were formed during the development of the research presented in this thesis to test for the effect of Spd on the problematic vascular development and infertility of the mutants: The *mtn1-1mtn2-1* homozygous mutant embryos have problematic auxin distribution and cell activation; The *mtn1-1mtn2-5* mutant embryos have less problematic auxin distribution and better cell activation; The Spd supplementation to the mother plant (*mtn1-1mtn2-1* heterozygote and *mtn1-1mtn2-5*) will overcome the problematic auxin flow and cell activation in the embryos.

2.2 **Materials and methods**

2.2.1 **Chemicals**

All general chemicals used were of analytical grade or higher, purchased from Sigma Aldrich, Oakville, ON, Canada; Bioshop, Burlington, ON, Canada; BioBasic, Markham, ON, Canada; VWR, Mississauga, ON, Canada; or Thermofisher Scientific, Canada. Microscopy reagents were from Canemco and Marivac (Gore, Quebec, Canada).

2.2.2 **Plant material and growth conditions**

The T-DNA insertion lines for the *MTN1* (At4G38800) and *MTN2* (At4G34840) genes were originally obtained from The Arabidopsis Information Resource (TAIR), by Dr. Waduwara-Jayabahu, for her PhD project. These single T-DNA insertion lines *mtn1-1* (SALK_085385), *mtn2-1* (SALK_071127) and *mtn2-5* (SALK_022510) were used to generate the double mutant lines *mtn1-1mtn2-1* and *mtn1-1mtn2-5* by Waduwara-Jayabahu. These double mutant lines were used for this study.

The *mtn1-1mtn2-1* homozygous mutant is male and female sterile. Therefore, it was recovered from segregating (F_2) populations arising from two different F1 parent genotypes: MTN1*mtn1-1 mtn2-1mtn 2-1* and *mtn1-1mtn1-1* MTN2*mtn 2-1*. The *mtn1-1mtn2-5* mutant is fertile, and was maintained as a homozygous double mutant.

Seeds were surface sterilized by exposure to chlorine gas created by mixing bleach and hydrochloric acid (100ml Bleach (Cholorx ®) + 4ml Concentrated HCl for 1.5 hr in the fume hood), prior to being placed on ½ Murashige-Skoog (MS) medium buffered with 0.5 mM MES. The media pH was adjusted to 5.3 with 1 M KOH. The media was prepared with no sucrose and was solidified with 0.8 % (w/v) agarose (Murashige and Skoog, 1962).

2.2.2.1 **Spermidine supplementation**

For the Spd-supplemented media, Spd was added from a sterile aqueous stock of 100 mM (maintained at -20^{o}C) to sterilized 50^{o}C media to get final working concentration of 100 µM Apart from this treatment all the other growth conditions were maintained similarly for the Spd supplemented mutants, non-supplemented mutants and WT.

2.2.2.2 **Plate-based and soil based growth conditions**

Seed sowing was done in a laminar flow cabinet using aseptic technique. Seeds were placed in a 1cm^2 grid, with one seed per 1cm^2, and 50 seeds per plate. After seeding, the plates were sealed with breathable tape (Micropore^{TM}, 3M Deutschland GmbH, Health Care Business, Germany), to facilitate gas exchange. The seeded plates were incubated in the dark at 4^{0}C for 48 h for seed stratification. Following stratification, the seeded plates were transferred to a tissue culture chamber (TC7, Conviron, Winnipeg, Canada) for 14 days under continuous light: 24h at 21^{0}C with photosynthetically active radiation (~120 µM m^{-2}s^{-1} PAR) provided by fluorescent lights. Seedlings were then transplanted to 5 cm square pots containing a 1:1 soil mixture of Sunshine LC1 mix (coarse, propagation mixture) and Sunshine LG3 mix (fine, germination mixture) (SunGro Horticultural Inc., Washington, USA). The seedlings were sprayed with a transplant fertilizer solution [10:52:10 (N: P: K) fertilizer mix (Plant products Co Ltd, Brampton, Canada)] to facilitate root growth. The flats containing 32 pots each were moved to a growth chamber and were covered with a clear, plastic dome to regulate humidity and acclimatize the seedlings growth chamber conditions over a period of one week. The growth chamber (E16, Conviron, Winnipeg, Canada) was maintained under long day conditions: 16h at 22^{0}C with 150 µmol m^{-2}s^{-1} PAR. The plants were watered every two days and fertilized with 21:7:7 (N: P: K) fertilizer mix (Plant products Co Ltd, Brampton, Canada) once a week until maturity.

This methodology was followed for growing WT and *mtn1-1mtn2-5* mutant plants. However, an additional selection step was needed when growing the *mtn1-1mtn2-1* mutant, as it was obtained from a segregating population. After the seeded plates were moved to the tissue culture chamber following stratification, the growth of the F2 seedlings was monitored for signs of delayed true leaf emergence and interveinal chlorosis. Around the 10^{th} day post germination, the *mtn1-1mtn2-1* double mutants were identified based on the interveinal chlorosis of their true leaves. The double mutant *mtn1-1mtn2-1* seedlings that were phenotypically identified were marked on the back of the plate. These seedlings were allowed to grow for another 4 days (14 days post germination) in the tissue culture chamber. The genotypes of these seedlings were verified by PCR as described in 2.2.5. At 14 days after germination, the identified *mtn1-1mtn2-1* seedlings were transplanted to soil (Sunshine mix LC1:LG3, 1:1) as explained in the above methodology. In addition, a few of the non-homozygous *mtn1-1tmn2-1* seedlings were transplanted to soil at 14 days post germination for identification of heterozygous plants for *mtn1-1mtn2-1* homozygous embryo recovery at maturity.

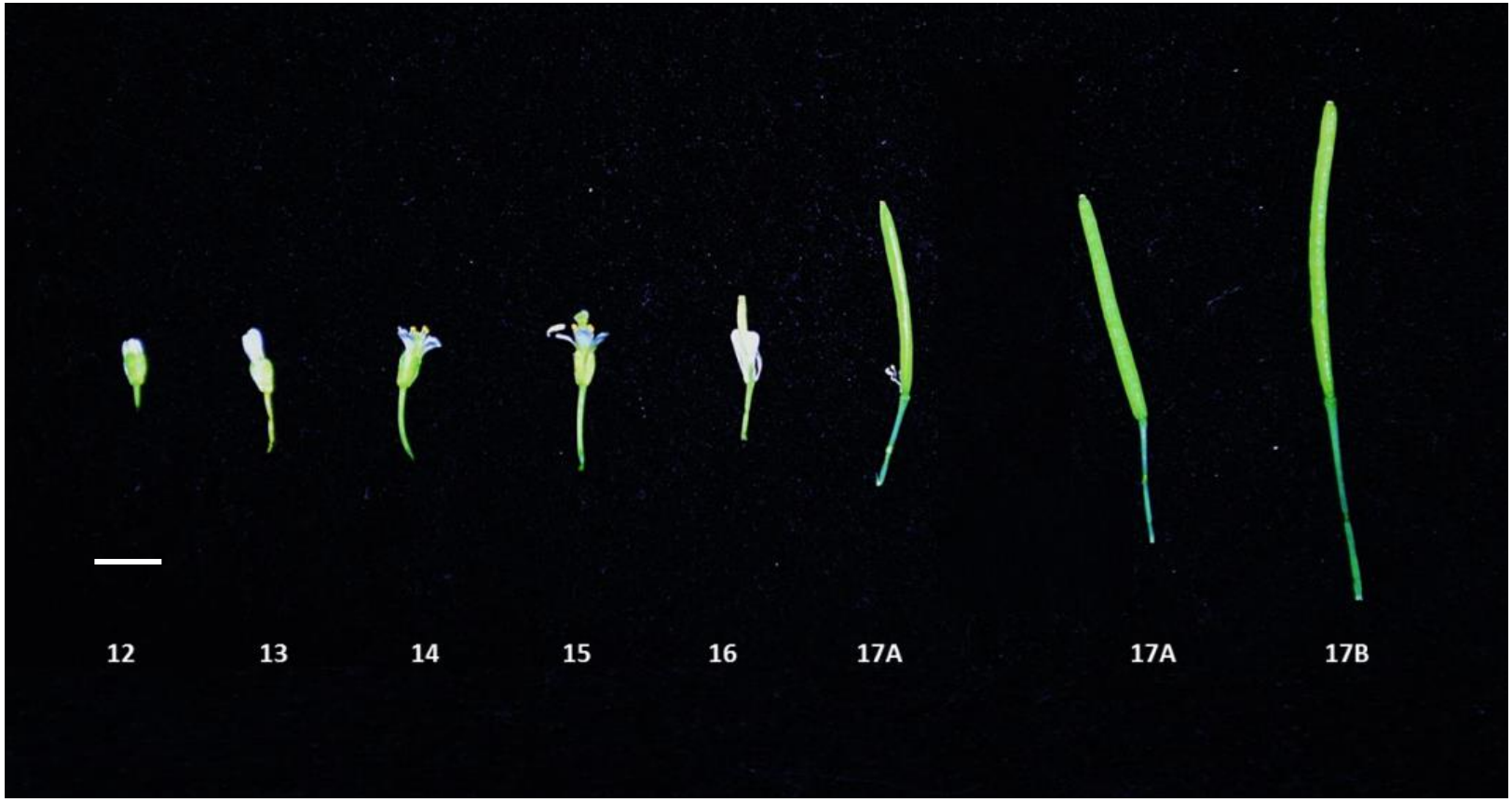

Figure 2-1. Summary of flower and fruit development stages of *A. thaliana*

The flowers and developing fruit / siliques were obtained from healthy, 6-week-old WT plants. The flowers and siliques are arranged and classified according to the guidelines by Smyth (1990).

Scale bar = 3 mm

2.2.3 **Embryo harvesting and dissection**

Embryos were collected from healthy, 5-6 week-old adult plants of WT, *mtn1-1 mtn2-5* and heterozygous *mtn1-1mtn2-1* adult plants. The heterozygous *mtn1-1mtn2-1* seedlings were identified via PCR based genotyping, after they were transplanted to soil at 14 days post germination. The confirmed heterozygous seedlings were allowed to mature to produce flowers and siliques. Siliques (stage 17A and 17B, Smyth et al., 1990; see Figure 2-1) were harvested from healthy, flowering 5-6 week old plants (WT, *mtn1-1mtn2-5* and *mtn1-1mtn2-1* heterozygote) for embryo dissection. A dissecting microscope (NIKON SMZ 1500), 2 x 25 gauge insulin needles, fine #5 forceps and microscope slides (conventional and depression slides) were used for the dissection.

The selected siliques were placed lengthwise on double-sided tape attached to a conventional microscope slide. An insulin needle was used to gently open the silique down its length and the forceps helped to gently tease it open along the valves, exposing the developing seeds within. The developing seeds were transferred to a depression slide containing embryo dissection solution ($^1/_2$ MS + 0.04 mg / L-glutamine + 3% (w/v) sucrose) (Gazzarrini et al., 2004). The seeds were moved around to break the surface tension, allowing them to sink to the bottom.

While viewed through the 10x magnification of the dissecting microscope, the embryo was excised using the insulin needles. Specifically, a small cut was made on the distal round end of the seed (opposite the funiculus attachment, Figure 2-2 F, arrowhead) using the straight edge of the needle. The flat side of the needle was then used to gently palpate the seed, to dislodge the embryo attached at the micropylar end. This was done very carefully, to prevent creating pressure that would crush the embryo. The dislodged embryo popped out of the opening made at

the distal end, along with a cloud of endosperm. The embryos were not always easily dislodged, especially those at the earlier growth stages (i.e. globular and heart stage). In such situations, the developing seed was cut lengthwise to expose the micropylar end, where the embryo was nestled. The needles were used very carefully to separate the embryo from the surrounding tissue.

Isolated embryos were transferred using a P200 micropipette to a fresh depression slide containing the dissection solution. This transfer was done to free the embryos of any surrounding tissue debris. This 'wash' step was repeated three times.

An additional fixation step followed by five washes was employed for embryos expressing GFP to retain the fluorescence (Nybo, 2012). These embryos were incubated at 4^{o}C for five min in 2% (w/v) paraformaldehyde solution made from a 20% (w/v) stock solution, followed by 5 washes in 1x PBS (8 g NaCl + 0.2 g KCl, 1.44 Na_2HPO_4, 0.24 g KH_2PO_4, 1 L H_2O; pH = 7.4 with HCl). The fixed embryos were mounted with fresh dissecting solution on an 8-well cover slide for confocal microscopy.

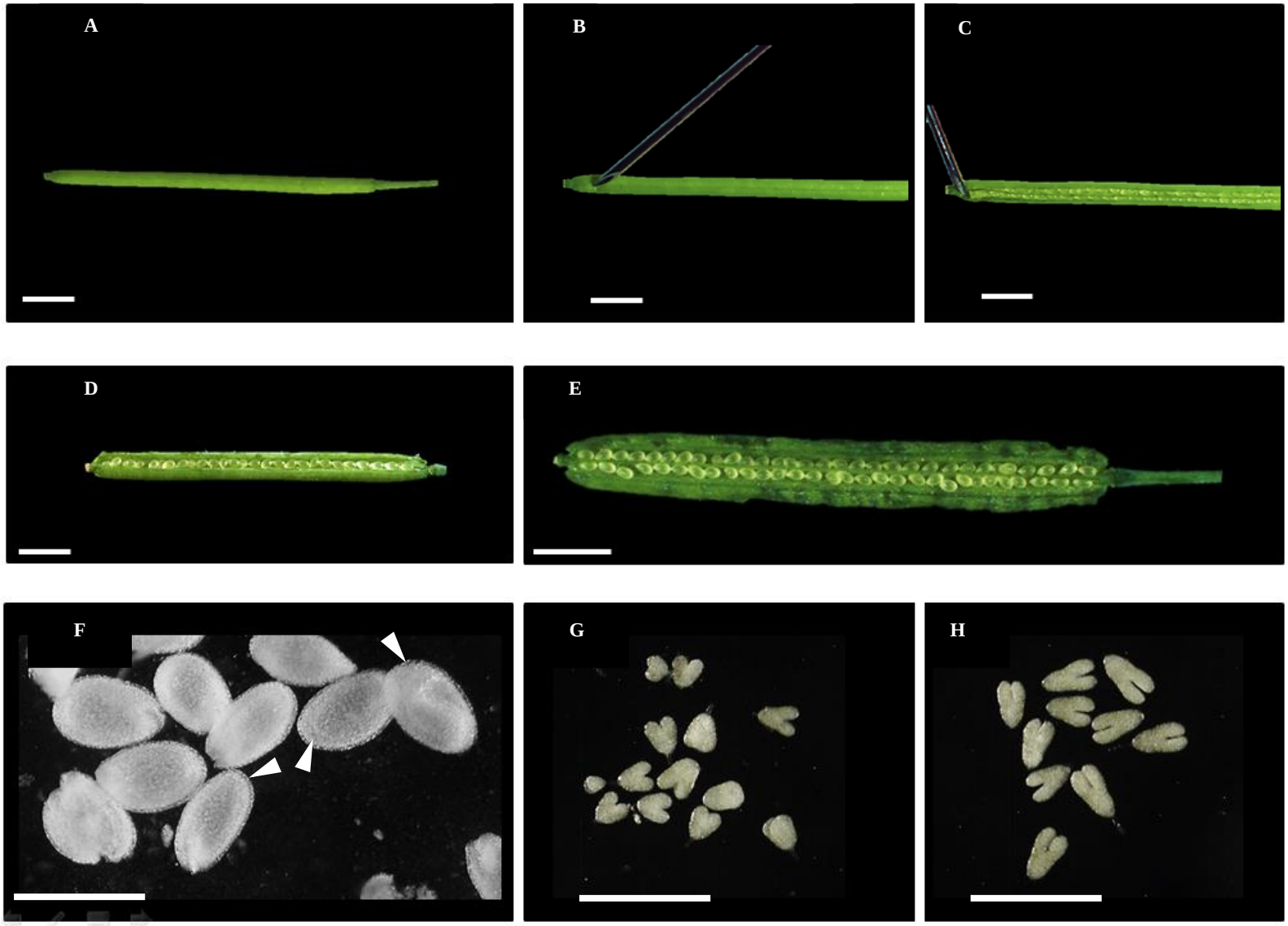
A
B
C
D
E
F
G
H

Figure 2-2. Embryo dissection procedure summary

A - E stage 17A siliques from 6-week-old, healthy adult *A. thaliana* plants. B, C- needles were used to separate the valves of the silique. D- The silique was partially opened and the developing seeds exposed. The seeds were attached the septum that runs through the middle of the silique. E- The silique was fully exposed. The carpels were peeled back to expose the developing seeds, within. One can observe the seeds attached to either side of the septum.

In F, these developing seeds were separated from the septum. They were translucent. The distal round end of the seed, that was to be cut to extract the embryo, is denoted by arrow heads. G, H – excised embryos. The younger embryos are shown in G (heart stage) and the next stage is shown in H (torpedo stage). The embryos are translucent upon dissection.

Scale bar = A-E, 3 mm; F – G, 500µm.

2.2.4 **DNA Isolation Procedure**

2.2.4.1 **Adult plant material**

Fifty microliters of extraction buffer (200 mM Tris pH 7.5, 250 mM NaCl, 25 mM EDTA, 0.5% (w/v) SDS) was added to each 1.5 ml tube, labeled with genotype and sample number. Using forceps, a leaf tissue sample (slightly smaller than the size of the inside lid of a 0.5 ml tube) was collected from each plant, and added to the tube containing the extraction buffer. The forceps were dipped in bleach, 70% ethanol, deionized water, and wiped dry with a KimWipe™ in between plant specimens to prevent cross contamination between samples.

The tissue was homogenized for about 15 seconds, using a plastic blue pestle attached to an electric drill. If the tissue tended to stay at the bottom of the tube, a yellow pipet tip was used to drag the tissue to the edge of the tube and the homogenization was repeated. An additional 300 µl of extraction buffer were added to the homogenate and the contents of the tube were mixed by vortexing for 10 seconds. The tubes were left on ice until all samples were homogenized. Next, the tubes were brought to room temperature (RT), incubated for 5 minutes, and centrifuged for 8 minutes (Eppendorf® model: 5154R, Brinkmann, Hamburg, Germany), at 13,000 x g at 4^{o}C. The tubes were carefully transferred to ice following the centrifugation and 300 µl of supernatant was removed to a fresh, chilled tube; the tube containing the pellet was discarded. The supernatant was mixed with 300 µl of chilled isopropanol by gently inverting the tube 15 times and incubated the tube for 5 minutes on ice. (It was possible to leave the sample tubes overnight at -20^{o}C at this step.) The samples were centrifuged 15 minutes at 13, 000 x g at 4^{o}C. The supernatant was poured off the pellet and 500 µl of cold 70% ethanol was added, taking care not to dislodge the pellet; the contents were mixed by inverting the tubes twice. The samples were centrifuged at 13, 000 x g for 7 min. The supernatant was discarded and the tubes were inverted

on paper towels to completely drain and air-dry the pellets. The pellets were re-suspended in 30 µl UV-sterilized water by vortexing for 3-5 seconds followed by 30-min incubation at RT. The pellets from smaller tissue samples (e.g., cotyledons) were re-suspended in lower volumes. The DNA was stored at – 20^{o}C.

2.2.4.2 **Embryos**

The embryo dissection steps were carried out using a dissecting microscope in a clean environment to minimize contamination. Fifty microliters of chilled PBS was added to a glass depression slide. On a clean microscope slide the silique to be dissected was attached with the use of double-sided sticky tape. Using fine Dumont #5 forceps the silique was gently pried open to expose the developing seeds. These were transferred to the depression slide containing the PBS solution with the use of paint brushes and fine forceps. The seeds were gently dissected (as described in the dissection protocol section) and single embryos were isolated. The embryos were washed in fresh, chilled PBS buffer to remove any maternal tissue. The cleaned embryo was transferred to the frosted part of a clean, DNA-free, conventional microscope slide. A five microliter drop of sterile Edwards' solution (200 mM Tris-HCl, pH 7.5, 250 mM NaCl, 25 mM EDTA, 0.5% (w/v) SDS in dH_2O) (Zou et al., 2002) was placed on top of the embryo. Using a fresh, sterile P10 pipette tip, the embryo was homogenized in Edwards' solution on the frosted part of the slide. The homogenate was transferred to a fresh, chilled 0.2 ml microcentrifuge tube. Another five microliters of Edwards' solution were added to the same spot on the slide where the embryo had been homogenized and pipetted up and down to collect any leftover homogenate. This was added to the microcentrifuge tube containing the homogenate, and kept at RT for 10 minutes to allow cell lysis, following which the mixture was centrifuged at 13, 000 rpm for 2 minutes at 4^{o}C (Eppendorf ® model: 5154R, Brinkmann, Hamburg, Germany). The supernatant

was carefully transferred to a new, chilled 0.2 ml microcentrifuge tube and 10 µl of 100% isopropanol was added. The tubes were incubated at RT for 2 minutes and centrifuged at 14, 000 rpm for 5 minutes at 4 ^{o}C. The isopropanol was carefully removed by inverting the tubes on a clean KimWipe™ and 50 µl of 70% ethanol was added to wash the pellet by inversion 2-3 times. The tubes were centrifuged for 5 minutes at top speed in the chilled centrifuge and ethanol was removed by careful pipetting. The pellets were allowed to air-dry for 5 minutes until all ethanol traces evaporated. The pellets were re-suspended in 10 µl of PCR grade UV-sterilized H_2O, by gentle pipetting. DNA extracts were stored at -20^{o}C until used for PCR.

2.2.5 **Genotyping of MTN-deficient mutants**

2.2.5.1 **Polymerase chain reaction (PCR)**

The isolated DNA was used for genotyping the MTN-deficient *mtn1-1mtn2-1* and *mtn1-1mtn2-5* mutants to confirm the samples used for the study. The T-DNA insertion specific left border primer (LBb1.3) was used with the reverse gene specific primer (mtn1-1 R; mtn2-1 R; mtn2-5R), along with reactions containing the two gene specific primers (mtn1-1F/R; mtn2-1F/R; mtn2-5F/R) (Ostergaard & Yanofsky, 2004), to identify the mutants homozygous, heterozygous for the insertion mutants.

Generally, PCRs were carried out in 20 µl volumes using a 19 µl master mix (PCR Buffer. four nucleotide triphosphates (dNTPs), forward and reverse primers, *Taq* polymerase, UV-sterilized water), and 1 µl of extracted DNA (Table 2-1). The PCR was performed in 0.2ml microcentrifuge tubes, using a thermocycler (Eppendorf® model: 1659, Hamburg, Germany). The reaction had an initial denaturation at 94^{o}C for 4 min. followed by 34 cycles of 94^{o}C for 30 sec, 55^{o}C for 30 sec and 72^{o}C for 1 min. a final extension period of 5 min at 72^{o}C min was added

at the end of the program. The final holding temperature was 10^{o}C until samples were removed from the machine.

The PCR genotyping of single embryos was carried out in a similar manner except the 20 µl reaction contained 2 µl of the DNA sample. The extracted DNA was allowed to thaw on ice (if frozen) and the PCR master mix was prepared as given in Table 2-1. The PCR cycle for embryo PCR was the same as for samples from adult tissue.

Table 1-1. Reagent list and final concentration of PCR mix for one reaction

Reagent	Volume / reaction (µl)	Volume / reaction for embryo PCR (µl)	Final concentration
10 x PCR Buffer (with $MgSO_4$)	2.0	2.0	1 x
dNTPs (10 mM)	0.3	0.3	150 µmol
Forward Primer (10 mM)	0.3	0.3	150 µmol
Reverse Primer (10 mM)	0.3	0.3	150 µmol
Taq polymerase (Home-made) (0.01x)	0.8	0.8	0.004 x
PCR grade H_2O	15.3	14.3	-
Final volume (no DNA)	19.0	18.0	

2.2.5.2 **Gel Electrophoresis**

Ten microliters of each reaction mix was mixed with 6X DNA loading dye (Thermo Scientific) and the mixture was separated by electrophoresis through 1% (w/v) agarose gels prepared in Tris-acetate buffer (40 mM Tris HCl, 20 mM Acetate, 1 mM EDTA, pH = 8.6). The PCR products were visualized using Safeview™ (Applied Biological Materials Inc.) which was added to the molten agarose (5 µl / 100 ml) prior to it being poured into the gel tray. Using a P10 pipette, 10 µl of each PCR sample was mixed with loading dye and added to the well. A DNA

ladder (GeneRuler DNA Ladder Mix: 100-10,000; ThermoFisher Scientific, Canada) was added to estimate fragment migration and size. The gel was electrophoresed at 90 V for 30 min at constant voltage. PCR products were visualized using the UV trans-illuminator of a BioRad gel documentation system (ChemiDoc™, BioRad, Canada).

2.2.6 **Stem cross sections**

2.2.6.1 **Obtaining the cross sections**

Healthy plants two-weeks after bolting were used for preparing stem cross sections. The main bolt was excised from the plant 1 cm above the rosette. If a side branch / cauline leaf were present at this excision point, the stem was cut 2-3 mm above it. New, sharp, double-edged razor blades, a beaker of ice cold dH_2O, a beaker with room temperature (RT) dH_2O, 6-well tissue culture plates (Sigma Aldrich), paper towels, a young fresh carrot, dissecting needle, fine paint brushes and fine #5 forceps were used.

The stem was separated from the plant using the razor blade and the cut end of the stem was immediately submerged in the RT dH_2O to prevent dehydration. Using the same razor, a 1 cm^3 cube was cut from the young carrot to provide a supporting medium for sectioning (Simon Chuong, personal communication). A hole as wide as the stem was created in the carrot using the dissecting needle, widening the hole to fit the stem piece vertically, without crushing it. One side of the carrot cube was split to allow space to insert the stem into the hole and secure it with the cut end of the stem facing upwards. The top of the carrot piece was trimmed to remove excess carrot tissue and to resemble a pyramid-like shape, leaving just enough to hold the stem in place. This allowed minimum surface area for the blade to pass through during sectioning. A new razor blade was split in half and one half was placed in the ice bath to obtain a stronger, shaper edge. A

drop of water was placed on the cut surface to maintain moisture and the chilled razor blade was used to make horizontal slices across the carrot cube encompassing the stem section (Figure 2-2). Each stem section was moved to the 6-well plate containing the water, using forceps. Once a sufficient number of sections were obtained, using the paint brush the remaining piece of stem was gently teased out of the surrounding carrot tissue.

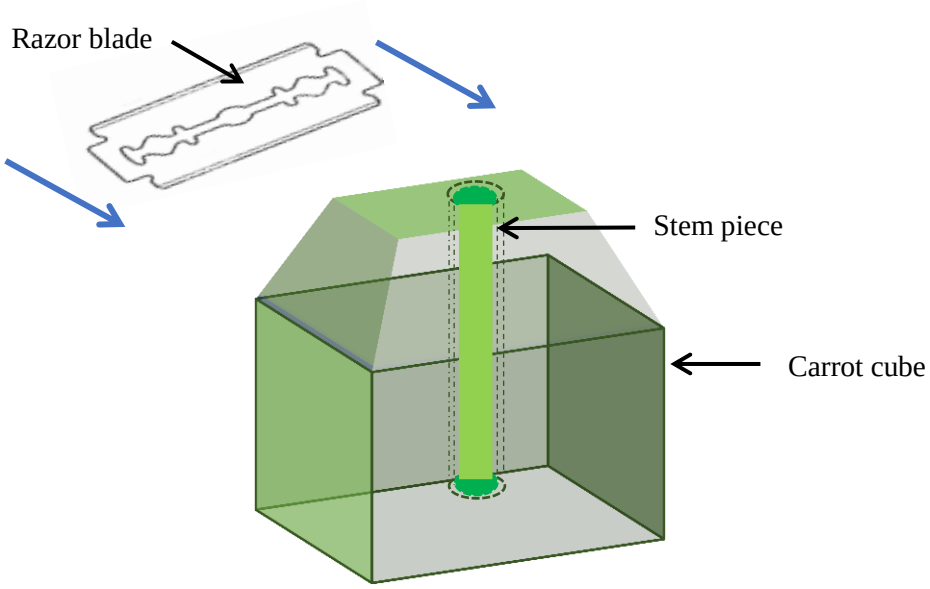

Figure 2-3. Obtaining stem cross sections

Schematic diagram of obtaining stem cross sections using a $1cm^3$ cube of carrot. The stem piece is inserted in the hole in the center of the carrot pyramid and the razor blade is gently dragged across the top horizontally.

2.2.6.2 **TBO staining of stem cross sections**

The stem cross sections were moved to a staining basket created by cutting off the tip end of a 1.5 ml microcentrifuge tube, removing the center of the lid with a heated pipet tip and closing the lid over a nylon mesh to create a basket. The sections were partially submerged in dH_2O, using the paint brush. The basket was removed from the water using forceps and the excess water was removed by dabbing the basket on a paper towel. The basket was placed in a container of 0.1% (w/v) Toluidine blue O stain (TBO) (pH 4.4) for 1 min, followed by thorough washing with distilled water until no color ran out. At this point the sections were removed using the paint brush and mounted in 25% (v/v) glycerol for microscopic observation. The refractive index (RI; the specific velocity of light traveling through a medium) of glycerol is very close to the RI of the coverslip glass. Therefore, the amount of the loss of light due to refraction is minimal, enabling better visualization of the specimen and better picture quality. Slides were rested on bench top for about 5 minutes at RT to allow the glycerol to penetrate the tissue prior to observation using a light microscope. TBO stain preparation and subsequent staining of the samples was carried out according to Peterson et al. (2008).

2.2.7 **Aniline blue staining**

To examine the germination of pollen of the *mtn1-1mtn2-1* mutant (infertile) and the effect of Spd treatment on pollen germination restoration, aniline blue staining was carried out on hand pollinated flower pistils of WT and *mtn1-1mtn2-1* mutant plants without and with Spd treatment. The sample preparation and aniline blue staining was carried out according to the methodology explained by Mori et al. (2006). Pistils from one- or two-day-old *A. thaliana* flowers, after sepals have retracted (Smyth et al., 1990), were collected and placed in a 2 ml microcentrifuge tube with enough cold fixative solution (acetic acid: 100% ethanol (EtOH)

(1:3)) to cover the sample. The tubes were placed in a vacuum chamber for about 15 minutes on ice, to facilitate infiltration of the fixative. The infiltrated samples were incubated for at least 2 hr at RT. The fixative was exchanged with 70% (v/v) EtOH and the samples were incubated for 10 min at RT. The 70% EtOH was replaced with 50% (v/v) EtOH and a 10 minute incubation at RT, followed by a 30% (v/v) EtOH treatment and finally MilliQ water.

The specimens were moved to a small petri dish containing sufficient volume of the alkaline treatment solution (ATS; 8 M NaOH) to completely cover the samples (Mori et al., 2006). The dish was covered with the lid and left overnight at RT in the dark. Following alkaline treatment, the solution was replaced with sterile distilled water, taking care not to disturb the samples. The samples were very soft at this stage and appeared transparent.

The de-colorized, water-soluble aniline blue solution (DABS; 0.1% (w/v) aniline blue in 108 mM K_3PO_4 (pH ~11)) was prepared the previous day and stored at 4^oC overnight (Mori et al., 2006). A filtration step was used for DABS the next day by filtering through a filter paper lined with active charcoal powder to remove any residual colour. Glycerol was added to the filtrate to a final concentration of 2% (v/v) to provide viscosity, better refraction index and prevent rapid dehydration of the samples. The solution was stored at 4^oC, away from light. The DABS was added to the plant samples after removing the distilled water. The samples were incubated at RT for 2 hours in the dark.

The specimens were mounted in DABS solution with added glycerol to a concentration of 4% (v/v) on microscope slides to prevent damage. The specimens were handled with fine paint brushes to avoid tissue damage. The coverslip was applied with the assistance of needles, with one edge of the cover slip touching the DABS solution on the slide and gently lowering the

coverslip over the specimen. The weight of the coverslip was adequate to gently crush the pistil and expose the inner tissue. No additional pressure was needed. Sample slides were sealed with clear nail varnish to preserve the specimen.

2.2.8 **Alexander staining for pollen viability**

In addition to aniline blue staining, Alexander stain was used to determine pollen viability. The sample collection, stain preparation and subsequent staining procedure were followed according to Peterson et al. (2010). Stage 12 flower buds (Smyth et al., 1990; see Figure 2-1) were collected from WT and *mtn1-1mtn2-1* plants rising from non Spd-treated and Spd-treated seeds. The buds were fixed in Carnoy's fixative (100% Ethanol (EtOH): chloroform: acetic acid (6:3:1)) for a period of 12 hours at room temperature. Following fixation, the buds were moved to a microscope slide using a small paintbrush. A dissecting microscope (NIKON SMZ 1500), 1 x 25 gauge insulin needle, fine #5 forceps and microscope slides were used for the dissection. The stamens were dissected out and the remaining plant debris was discarded. The fixative liquid that remained in the slide was carefully removed with the use of a KimWipe™, taking care not to let the sample dry out completely. A drop of Alexander stain solution (1 ml of 1% Malachite green + 5 ml of 1% Acid fuchsin + 0.5 ml of 1% Orange G + 4 ml glacial acetic acid + 10 ml of 95% ethanol + 25 ml of 100% glycerol + 54.5 ml of distilled H_2O) was placed on the specimen. Next the slide containing the specimen and stain was placed on a heating block at 60^oC for 5 minutes to provide gentle heating to facilitate penetration of the stain into the sample. Following the heating step, the sample was cover-slipped and gentle pressure was applied to ensure that all plant material converge to the same plane. Next the samples were sealed using clear nail varnish to prevent dehydration until visualized using light microscopy.

2.2.9 **Microscopy**

2.2.9.1 **Confocal microscopy**

The fluorescent signals of the reporter genes were detected and documented using confocal laser scanning microscopy. The Carl Zeiss LSM 510 confocal microscope (Carl Zeiss Inc. Jena, Germany), was used to observe the expression patterns of AtHB8-NUC-YFP, DR5::GFP and MP::n3GFP embryos of WT, *mtn1-1mtn2-1* and *mtn1-1mtn2-5* plants. The YFP expressing lines were excited with the argon laser set at 514 nm and the GFP expressing lines were excited by the argon laser set at 488 mm. The emissions for the YFP and GFP were detected with 505/530nm band pass filters. For both YFP and GFP, a track that included white light for bright field observation was used. Chlorophyll is excited at 488nm wavelength which interferes with the GFP signal. Therefore, an auto-fluorescent channel was added to the GFP track to detect the excitation of chlorophyll at 488 nm, and the emissions were detected with a 650 nm long pass filter. A Carl Zeiss LSM 700 confocal microscope (Carl Zeiss Inc. Jena, Germany) was used to visualize TCSn::GFP in developing WT, *mtn1-1mtn2-1* and *mtn1-1mtn2-5* root tips, and aniline blue staining of germinating pollen tubes of the mutants. The Zen 2009 blue version was used to capture and analyze the images. The Z-stack option was employed to create a 3D projection of the different layers captured. The pinhole size, master gain was set for a given magnification for all the images taken at that magnification. All files files containing confocal images were stored in the external hard drive of the Moffatt laboratory computer in a designated folder (Nimhani_Project).

2.2.9.2 **Light microscopy**

The sample collection and fixation for light microscopy was performed at the Moffatt lab. The samples were shipped to Prof. Ed Yeung, University of Alberta, for embedding, sectioning and

staining. Light microscopy analysis of the samples was carried out at the Moffatt lab, using the fixed slides sent back by Dr. Yeung. The samples were collected, fixed and partially dehydrated as outlined below prior to shipping.

Stage 17A and 17B siliques (Smyth et al., 1990), as well as healthy inflorescences, were used as samples for embedding and sectioning to observe the development of young embryos, ovules, and pollen. The mature 17B siliques were cut lengthwise in the middle and some were cut across at both ends to facilitate fixative penetration. The samples were collected directly into the freshly prepared ice-cold fixative (2.5% (v/v) glutaraldehyde, 1.6% (v/v) paraformaldehyde in 0.05 M potassium phosphate buffer (pH 7.4)) on ice. The tubes with their lids open (on ice), were placed in a desiccator under vacuum until no air bubbles rose to the surface and the tissue samples had sunk to the bottom of the tubes. The lids were closed and the tubes were incubated at 4^{o}C for 48 h in the dark to prevent browning of the tissue. After 48 h fixation the samples were washed five times with 1 ml of 0.05M potassium phosphate buffer (pH 7.4), each wash being 5 min. The tissues were dehydrated with increasing ethanol solutions (all $^{v}/_{v}$): 15%, 30% and 50% for 15 min each, under vacuum. At the 50% ethanol concentration, the samples were left at 4^{o}C for 48 h to allow de-greening, after which the 50% ethanol was replaced with fresh 50% ethanol prior to shipping.

The samples were further dehydrated in an ethanol series: 50%, 75%, 95% and 100%, by Dr. Yeung at the University of Calgary for embedding and sectioning. The dehydrated samples were embedded in plastic resin (Technovitt 7100) and 3 µm thick sections were prepared using a glass knife microtome. The sections were subsequently stained for carbohydrates and proteins. Periodic acid-Schiff's reaction for total carbohydrate (cell walls and starch granules are stained red), amido black 10B for protein, and aniline blue for callose were carried out (Smith &

McCully, 1978; Yeung, 1984). The sections were visualized using a compound light microscope (Zeiss Axiovert 200 Microscope; Carl Zeiss Inc, Toronto, Canada), and callose visualization was done using confocal microscopy.

2.2.9.3 **Differential Interference Contrast (DIC) Microscopy**

DIC microscopy was used to observe embryo development at a macro level within cleared siliques. Stage 17A siliques were selected from plants germinated in the presence or absence of Spd supplementation. The siliques were cleared using a chloral hydrate: glycerol: water (8:3:1) solution (Scarpella, 2004). The carpels were removed using hypodermic needles. Strips of Vaseline™ were applied on the slide, around the siliques to support the coverslip and prevent crushing of the developing seeds. The samples were mounted in the chloral hydrate solution and slides sealed with Vaseline to prevent dehydration. The slides were incubated in a humid box, in the dark, at 4^{o}C for 24 hr. The seeds were visualized using LSM 700 microscope (Zeiss ™) with DIC optics ‘and the images were analyzed using ZEN 2009 software. The globular, heart, torpedo and bent cotyledon stages were observed under 40X, 25x and 10X objectives, respectively.

2.2.10 **Statistical analysis**

One-way Analysis of Variance (ANOVA) was performed to determine whether Spd supplementation significantly improves seed germination rate of the G1, G2 and G3 generations of the *mtn1-1mtn2-1* mutants.

Student’s t-test performed to determine whether Spd supplementation significantly changes the vascular bundle number in the main bolt and fertile branch of the MTN-deficient mutants (*mtn1-1mtn2-1* and *mtn 1-1mtn2-5*).

2.3 **Results**

2.3.1 **Effect of exogenous feeding of Spd on fruit setting, seed setting of the *mtn1-1mtn2-1* mutants**

The *mtn1-1mtn2-1* mutants recovered from ½ MS media grown plates displayed typical growth abnormalities seen in the non-Spd-treated mutant, including infertility. The ovaries with unfertilized ovules that developed into a silique were usually shorter than WT, extending to about 3.5-4 mm in length; they did not produce any viable seeds (Figure 2-4 E, G; Figure 2-5 B). The plants of the seeds that were germinated on ½ MS media supplemented with Spd (100 µM) showed a few random branches that carried longer, fuller siliques extending to about 15 – 17 mm in length, and these siliques contained few viable seeds (Figure 2-4 F, G; Figure 2-5 C). These plants produced around 20±4 siliques per plant, whereas the WT (Figure 2-4 A, B) had over a 100 siliques/plant in general. The number of seeds in the siliques were counted and the plants arising from untreated seed (naïve) produced siliques with no seeds on average except possibly 2-5 "seed like" structures (n=20); these were non-viable. The fertile siliques on average had around 10 ±3 viable seeds (n=32), where as a WT silique (Figure 2-4 C) contained around 45-50 viable seeds. These results indicate that feeding 100µm Spd to the *mtn1-1mtn2-1* mutant leads to partial restoration of fertility (Figure 2-4).


A
B
C
D
E
F
G
*
*
*
+
+

Figure 2-4. Spermidine-mediated partial restoration of fertility in *mtn1-1mtn2-1* mutant plants

In A, a healthy 5-week-old *A. thaliana* WT plant is shown. The plant has a main bolt / stem and three side branches. A few very young secondary bolts can be seen emerging from the rosette. The main bolt is terminated in an inflorescence. A few maturing siliques are observed below the inflorescence of the main bolt. In B, a close-up of a healthy, fertile WT branch is shown. The branch terminates in an inflorescence where a few mature flowers can be observed. The siliques immediately below the inflorescence are very young, while the siliques towards the bottom of the bolt are more mature. In C, a single mature silique from a healthy, WT plant is shown. The plant shown in D, is an 8-week-old, *mtn1-1mtn2-1* homozygous double mutant plant. The rosette has a greater number of leaves and there are several numerous secondary bolts rising from the rosette, having numerous branches that appear twisted and bent. All branches end in an inflorescence.

E and F are branches of *mtn1-1mtn2-1* mutant plants that came from non-treated and Spd-treated seed, respectively. The branch in E, has short, unfilled siliques (*). The branch in F carries a few fertile siliques (+). These siliques are longer and fuller than the ones observed in E. In F, close-up images of an infertile silique from a *mtn1-1mtn2-1* plant rising from seeds not treated with Spd, and a fertile silique from restored branch of a plant that arose from Spd treated seed is shown.

Scale bars: C, G = 3 mm; A, B, E = 10 mm; D = 15 mm.

Figure 2-5. The *mtn1-1mtn2-1* mutant flower and siliques.

In A and B, *mtn1-1mtn2-1* flowers are shown. One can observe additional petals (six instead of four) in A, while the two flowers in B are fused at the stem. In C, a dissected, infertile, unfilled silique from a *mtn1-1mtn2-1* plant rising from non-Spd treated seed is shown. The carpels have been peeled back to expose the inside of the silique. Aborted ovules (arrowheads) are present on both sides of the septum. No viable seed is present. Remains of the stigmatic papillae are present at the distal end (*) of the silique. In contrast, the silique shown in D, has twelve fertilized ovules / seeds, that are present on both sides of the septum. These seeds are green in colour and appear full. However, numerous white specks, which are aborted seeds, are present as well (arrowheads). This silique was obtained from a *mtn1-1mtn2-1* plant rising from a plant germinated on Spd for 14 days.

Scale bars: A, B = 1 mm; C, D = 3 mm.

2.3.2 **Transgenerational effects of Spd supplementation *to mtn1-1mtn2-1* seeds on seed germination percentage**

The untreated seeds of the *mtn1-1mtn2-1* heterozygous mutant gave rise to naïve homozygous *mtn1-1mtn2-1* double mutants. The Spd-treated *mtn1-1mtn2-1* mutants produced few branches with randomly fertile siliques. The seeds of these fertile siliques were collected. These were designated as G1 seeds, germinated on ½ MS or ½ MS supplemented with Spd to give rise to the G1 plants and *mtn1-1mtn2-1* progeny. The G1 plants were allowed to mature and produce seeds. They did not produce as many seeds as WT, but there were approximately 40-50 seeds to follow through to the next generation. These seeds were collected and designated as G2 seeds. G2 seeds gave rise to G2 plants, from which G3 seeds were collected.

Germination of G1, G2 and G3 seeds on ½ MS media was assessed to determine the viability of seeds of descendants of Spd treated *mtn1-1mtn2-1* plants (Table 2-2). The non-treated mutants did not produce seeds. The G1 seeds (Spd), G2 seeds from plants rising from G1 seeds geminated with and without Spd as well as G3 seeds from plants rising from G2 seeds germinated with and without Spd suplementation were used. WT seeds from plants arising from seeds grown on media with and without Spd suplementation were used as controls. For each genotype / sample 150 seeds were germinated on ½ MS for 5 days following stratification.

The germination percentage values of the WT seeds collected from plants arising from seeds that were not treated and treated with Spd, had no significant difference (Table 2-2). The G1 seeds collected from *mtn1-1mtn2-1* mutant plants arising from seeds treated with Spd (G1 Spd), had the lowest germination percentage (20.57±5.07). There were no G1 ½ MS seeds to be germinated as the *mtn1-1mtn2-1* mutant plants arising from non-treated seeds, did not produce any viable seeds. Both G2 seeds obtained from *mtn1-1mtn2-1* plants arising from treated and

non-treated seeds had higher germination percentage compared to G1 Spd (36.71 ± 0.78 and 28.22 ± 1.30, respectively) however, the germination percentages were not as high as that of WT. The G2 seeds from parents of Spd treatment had significantly higher germination percentage (28.22 ± 5.07)) than G2 from ½ MS (20.57 ± 1.30), but the values were still low compared to WT. The G3 seeds from both ± Spd treated parents had significanlty higher germination than either of the G2 seeds sets (± Spd), with the G3 seeds of the Spd treated parent having the highest germination percentage of 76.46 ± 3.72.

Table 2-2. Germination percentage of WT, G1 G2 and G3 seeds on ½ MS media

Treatment (n=150)	Germination %	St. dev (±)
WT $^1/_2$ MS	98.67	1.89
WT Spd	99.33	0.94
G1 Spd	20.57	5.07
G2 $^1/_2$ MS	28.22	1.30
G2 Spd	36.71	0.78
G3 $^1/_2$ MS	61.76	3.41
G3 Spd	76.46	3.72

WT ½ MS - WT non-treated seeds; WT Spd – WT seeds supplemented with Spd; G1 Spd – G1 generation seeds supplemented with Spd; G2 ½ MS – G2 generation non-treated seeds; G2 Spd – G2 generation seeds supplemented with Spd; G3 ½ MS – G3 generation non-treated seeds; G3 Spd – G3 generation seeds supplemented with Spd

Assuming that the population variance between groups is homogenous; the dependent variable (germination) is normally distributed within each group; the observations are independent from each other, a One-way Standard Analysis of Variance (ANOVA) test was performed on seed germination percentage values. The following null hypothesis and alternate hypothesis were formulated to test if the germination percentage of the non-treated / treated generations were significantly different.

H_o: There is no significant difference between the sample means; i.e. if sample 1 mean is μ1, and sample 2 mean is μ2, then the null hypothesis can be written as:

$H_o : \mu 1 = \mu 2 = \mu 3 = \ldots = \mu k$

The alternative hypothesis was (H_A): There is a significant difference between the sample means.

The results of the one-way ANOVA (Table 2-3) indicate that there was a statistically significant difference between groups ($F_{(6,14)} = 258.76$, $p = 1.61 \text{ X } 10^{-13}$)..

Table 2-3. Summary of results of one-way ANOVA

Source	DF	Sums of Squares	Mean Square	F-Statistic	p-value
Between treatments	6	19368.645	3211.441	258.759	$1.613 \text{ x } 10^{-13}$
Within treatments	14	173.753	12.411		
Total	20	19442.398			

Mean comparisons were made using ANOVA between the group mean values of the seed germination percentages of WT ½ MS, WT Spd, G1 Spd, G2 ½ MS etc. to determine whether any of those means are statistically significantly different from each other. The results of this

comparison revealed that, the exogenous feeding of Spd partially restore fertility in the *mtn1-1mtn2-1* mutant and that this restoration of fertility is passed on to subsequent generations, increasing seed germination rate from one generation to the next.

2.3.3 **Effect of Spd supplementation on pollen and ovule development defects in MTN deficient mutants**

Ovules and pollen of *mtn1-1mtn2-1* and *mtn1-1mtn2-5* mutants and WT (control) with or without Spd supplementation were examined to assess the effect of Spd supplementation on defects in development. The WT ovules and pollen showed no major difference in morphology and development with and without the Spd treatment (Figure 2-6). The ovules had the typical developmental pattern with the normal egg apparatus in the middle, surrounded by two integument layers (Figure 2-6 A). These integuments extended all the way towards the funiculus, surrounding the embryo sac and forming the micropyle. A subtle difference from the non-treated WT ovules could be seen in the integument layers of some of the Spd-treated plant ovules. The cell files in the integuments of the Spd-treated plant ovules had some cells with bulging cell walls (arrowheads; Figure 2-6 B), thereby causing the embryo to be larger. However, as a whole, the ovule development was not hindered or affected in a deleterious way as the embryo sac remained protected and intact.

The WT pollen showed three-lobed exine with a full, intact cytoplasm in the mature grains, holding the spherical shape and no vacuoles. As shown in Figure 2-6, the pollen from the Spd-treated plants had healthy characteristics similar to pollen from untreated plants, indicating this treatment had no visible detrimental effect on pollen development.

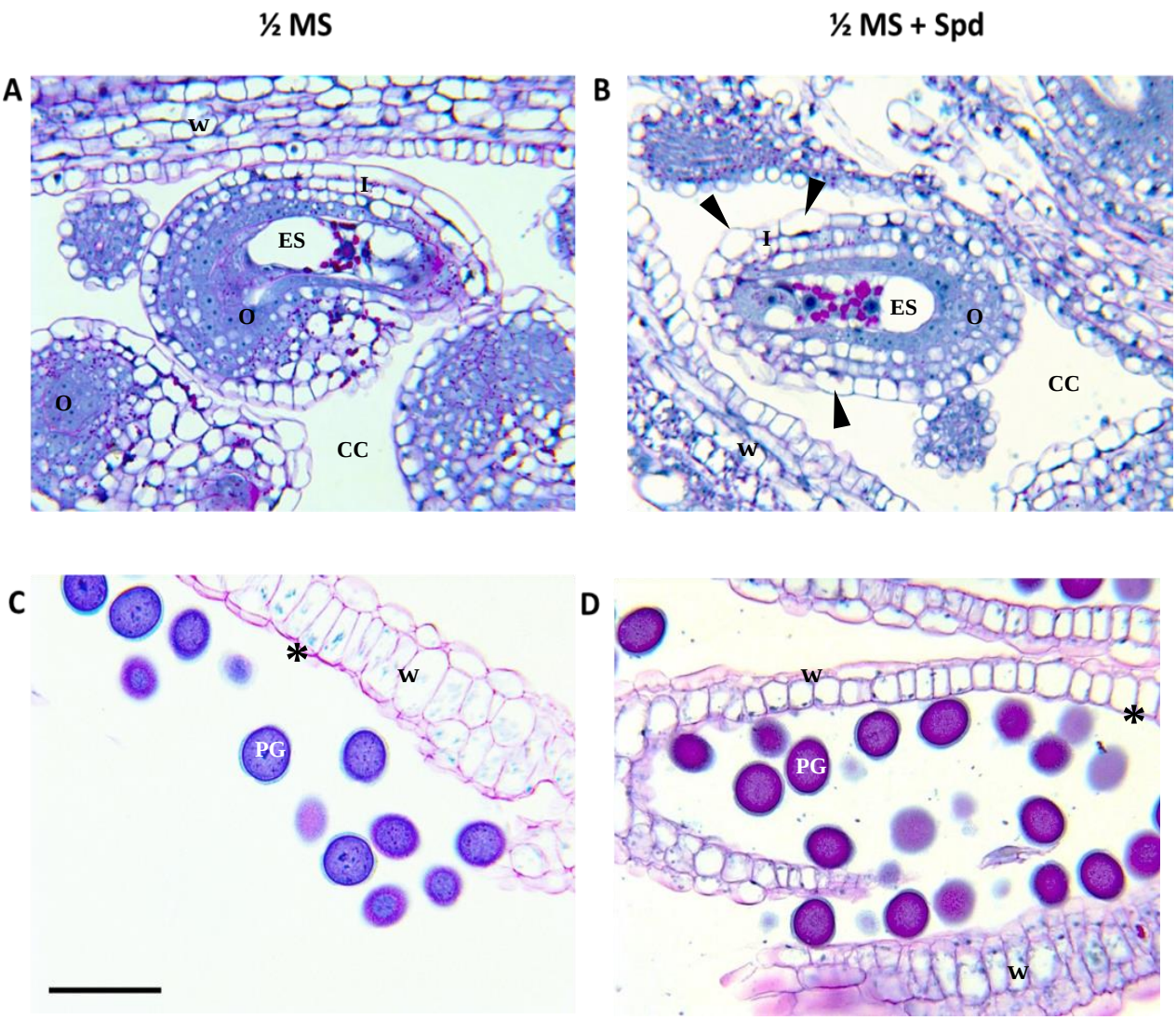
½ MS
½ MS + Spd
A
B
C
D
W
I
ES
O
CC
PG
*

Figure 2-6. WT ovules and pollen grains from *A. thaliana* plants with and without Spd supplementation

In A and B, a longitudinal section and a cross section of an ovule (O) is shown. The ovule in A is from a non-treated plant. One can see that the ovule is at full maturity, with the integuments (I) fully extended and enclosing the embryos sac (ES). The cells of the integument layers are uniform cell lines. In B, an ovule from a WT plant arising from Spd-treated seed is shown. One can observe the integument layers show some enlarged cells with bulging cell walls (arrowheads).

C and D are longitudinal sections of anthers, showing mature pollen grains (PG). The anther walls (W) show shrunken tapetum cells (*) indicating anther maturity. Pollen grains from both non-treated (C) and Spd-treated (D) plants appear phenotypically similar. The pollen grains are healthy, showing intact cytoplasm and complete 3-lobed exine. No noticeable difference can be seen between pollen grains from plants with and without treatment.

All sections were stained with TBO, Periodic Acid-Schiff's and Amido black 10B.

Scale bar = 50 μM.

The *mtn1-1mtn2-5* mutant with a 72% loss of MTN activity is fertile and thus was not expected to have defects in its reproductive tissues. The formation of the egg apparatus followed the typical developmental stages seen in the WT. However, as seen in Figure 2-7, the cells of the integument layers, particularly those of the outer integument layer, appeared to have less consistent sizes than non-treated WT (arrow heads in Figure 2-7 A and B). The Spd-treatment reduced the number of these abnormally-enlarged cells in the integument layers of *mtn1-1mtn2-5*, whereas in the WT, Spd appeared to cause them (compare Figure 2-6 A, B *vs.* Figure 2-7 A, B). Normal embryo sacs could be found in both Spd-treated and non-treated *mtn1-1mtn2-5* ovules, suggesting that the egg apparatus formation is not affected by a 72% reduction in MTN activity present in this mutant. The pollen of the non-treated *mtn1-1mtn2-5* mutants appears to have normal cytoplasmic contents, an intact exine and spherical shape. No detectable changes were observed in the pollen of Spd-treated *mtn1-1mtn2-5* plants (Figure 2-7 C and D).

The most MTN-deficient (86% loss of MTN activity) mutant *mtn1-1mtn2-1* showed many defects in reproductive organ development. No normal looking ovules were observed in the sections prepared from untreated mutant inflorescences (n=32). Instead, the sections contained evidence of aborted and shriveled up ovules inside the ovary, which were so abnormal that they were unlikely to be fertilized. In some cases (n= 15) the ovary contained an immature, developing ovule in which the embryo sac appeared to be developing, but the integument layers were not properly formed to provide protection. The developing ovules that did have an embryo sac did not show typical cell arrangement. In addition, the ovules as a whole had an atypical shape (compare Figure 2-8 B, C *vs*. Figure 2-6 A). None of the mutant silique sections from non-Spd-treated plants showed any evidence of embryo development (n=44). No egg apparatus was observed in the mature ovules, indicating the egg apparatus was aborted very early.

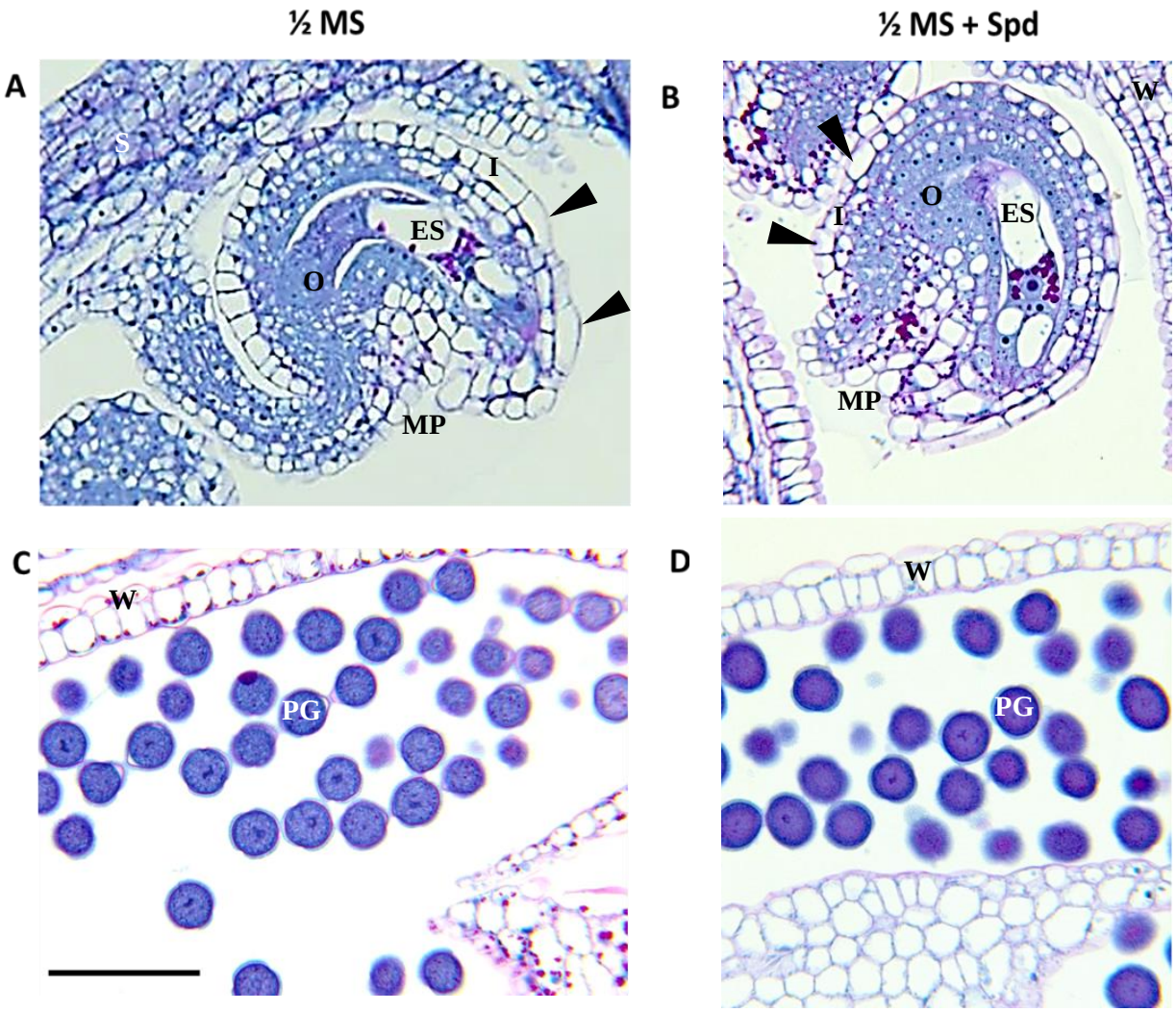
½ MS
½ MS + Spd
A
B
C
D
S
I
ES
O
MP
W
PG

Figure 2-7. The *mtn1-1mtn2-5* mutant ovules and pollen grains from plants treated with and without Spd supplementation.

In A and B, longitudinal sections of ovules (O) and in C and D, longitudinal sections of anthers are shown. In A, an ovule from a non-treated plant can be seen. The integument (I) of the ovule in A, has enlarged cells (arrowheads). The integuments have extended to enclose the embryo sac (ES), and form a micropyle (MP). The Spd treated plant ovule in B, has a few bulging cells in the integument. The embryo sac in both A and B appear normal. In C and D, mature pollen grains (PG) can be seen within the anther. The pollen in both non-treated and Spd-treated (C and D respectively) plants appear normal with intact cytoplasmic contents, and well-formed exine.

All sections were stained with TBO, Periodic Acid-Schiff's and Amido black 10B.

Scale bar = 50 µM.

The sections from the Spd treated *mtn1-1mtn2-1* mutant (which is the more severe mutant of the two, having a loss of 86% MTN activity) plants showed some evidence of a more normal ovule development. There were larger ovules present and early embryos (globular, *) were evident in a few of them (n = 5/54). The integument layers extended almost all the way towards the funiculus and form the micropyle. The development of the embryo sac was evident, but there were still minor changes present; lack of proper polarity of the embryo sac, no clear distinction of synergid cells, and cloudy cytoplasm of the central cell (Figure 2-8 C and D). Most large ovules appeared be fertilized as evidenced by enlargement of the ovule and development of integument layers, but since there were only a few embryos to be found per silique, it is possible that early abortion had taken place.

The sections of untreated *mtn1-1mtn2-1* mutant contained many pollen abnormalities: residual material was present in between the pollen grains; large vacuoles at early development stages; detached cytoplasm; degenerating cytoplasm; improper exine formation (lacking furrows). Moreover, the overall shape of the pollen grains was deformed and most did not show a fully formed exine. The anthers from the Spd-treated plants dehisced (Figure 2-9, C) and contained less sticky material within them (Figure 2-8 B *vs* C). There appeared to be a few pollen grains that had intact cytoplasm and no vacuoles with the Spd treatment; overall these particular grains could be categorized as “healthy” (Figure 2-8 F).

In addition to examining the reproductive structures of G0 and G1 plants, reproductive structures of G2 and G3 generation plants grown on media with and without Spd were investigated as well. These samples showed further improvements to integument layer arrangement and improved pollen health (Appendix VII, Figures 2-29 and 2-30).

	½ MS	½ MS + Spd
Mature silique	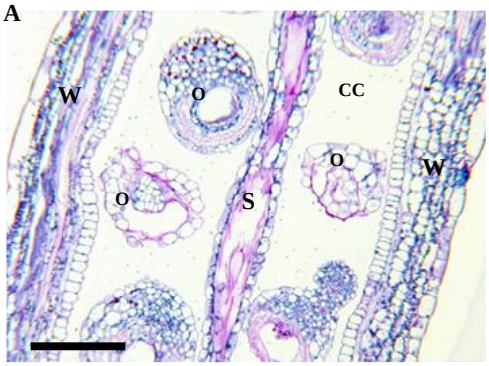	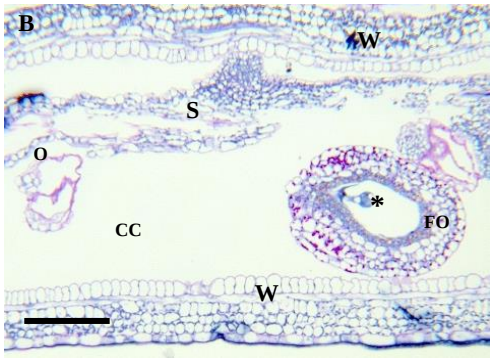
Developing ovule	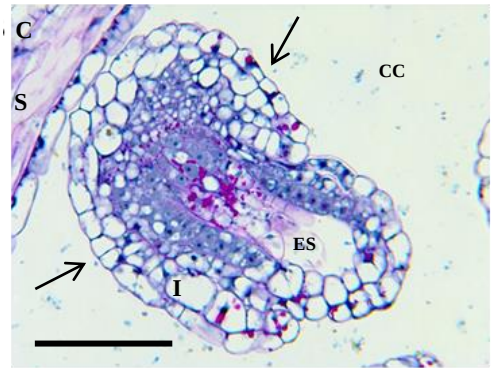	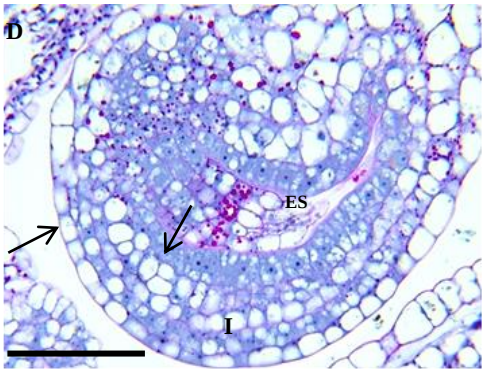
Mature anther	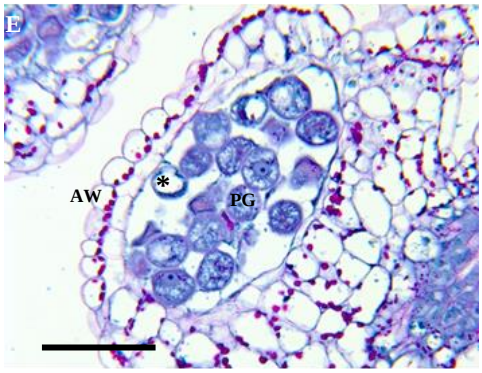	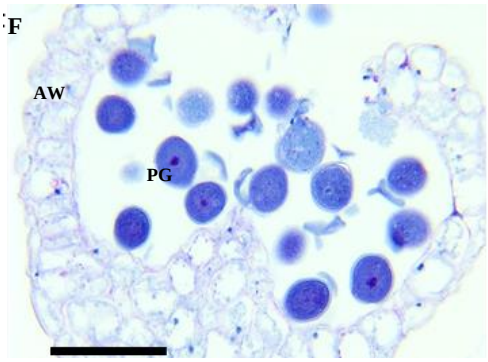

Figure 2-8. Ovules and pollen from *mtn1-1mtn2-1* plants grown on media supplemented with and without Spd

Longitudinal sections (A-D) and cross sections (E and F) of the reproductive organs of non-treated ($^1/_2$ MS) and Spd-treated ($^1/_2$ MS + 100µM Spd) *mtn1-1mtn2-1* plants.

In A and B, portions of mature carpels delimited by two walls (W) is seen. In the center of the ovary, one can observe the septum (S) on which several ovules (O) are attached. Whereas all the ovules are aborted in A, the ovule seen in B is fertilized (FO) and carries an embryo (*).

In C and D, developing ovules found in immature siliques is shown. In the non-treated plant (C) the integument extension is arrested. That is, the two integuments (I) are difficult to distinguish and the cell layers are not uniform with different cell size (*), because the two layers did not differentiate (see arrows). The embryo sac (ES) is exposed to the chamber (CC). In the Spd-treated plant (D), the integument layers (I) have fully extended and are entirely protecting the embryo sac (ES). Note that in the treated plant the cell layers are distinct and more uniform.

In E and F the anther delimited by the anther wall (W) contains several pollen grains (PG). In the non-treated plant (E), the pollen grains have disintegrating cytoplasm and large vacuole (*). Some debris, that may be callose are observed surrounding the pollen grains. In the treated plant (F) the anther chamber is seen with pollen grains with intact cytoplasm, however one (*) has aborted and display disintegrated cytoplasm.

All sections were stained with TBO, Periodic Acid-Schiff's and Amido black 10B. The outer cell wall of the anther is characterized by amyloplasts lining the inner cell wall.

Scale bar = 50 µM.

2.3.4 **Response of pollen tube growth of the *mtn1-1mtn2-1* mutants and of daughter generations to Spd supplementation**

The *mtn1-1mtn2-1* mutants have defective reproductive organ development causing infertility (Waduwara-Jayabahu et al., 2012). In the study presented in this thesis, the reproductive organs showed problems in anther dehiscence (Figure 2-9 B), incomplete breakdown of callose tissue within the anthers during pollen maturation (data not shown), problematic ovule and embryo sac development and poor pollen tube growth. The stigmas of the *mtn1-1mtn2-1* flowers have malformed or bent stigmatic papillae. The low yield of seeds from the Spd-treated plants may be due to the low pollen germination rate on the stigma of the flowers and possible reduction of pollen tube growth towards the ovules.

Aniline blue staining of stigmas of *mtn1-1mtn2-1* mutant flowers from plants grown on ½ MS and ½ MS supplemented with Spd, hand-pollinated using pollen of *mtn1-1mtn2-1* flowers grown on ½ MS and ½ MS supplemented with Spd, were collected to evaluate which organs (stigma or pollen) were more strongly affected by the MTN-deficiency and the effect of Spd on any defects. As a control for healthy pollen and stigmas of, non-treated WT flowers were used.

In the control samples of WT pollen tube growth on the WT stigmas of plants treated with Spd supplementation was indistinguishable from WT pollen tube growth on WT plants germinated in the absence of Spd. The WT stigma of both +/- Spd was very receptive to the pollen, as seen by the large number of pollen grains sticking to it (Figure 2-10 A, B). The pollen tubes extended towards the ovules within the ovary, through the style (arrowheads). There was no difference observed between the non-treated and treated plants regarding pollen receptivity, or germination (Figure 2-10, A and B).

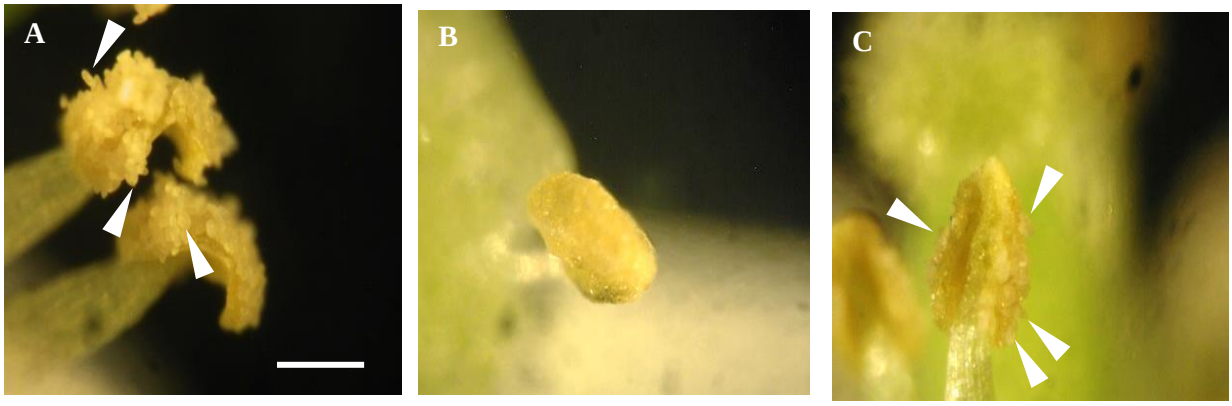

Figure 2-9. Anther dehiscence in stage 14 flowers of *A. thaliana* WT and *mtn1-1mtn2-1* mutant plants

A-C mature anthers of stage 14 flowers are shown. In A, a dehisced anther of a WT plant is presented (n=15). One can observe the mature pollen grains dispersing from the anther (arrowheads). In B, a mature anther from a non-Spd-treated *mtn1-1mtn2-1* plant is shown (n=25). The anther has not dehisced and the pollen grains are not released. The anther shown in C, is from a Spd-treated *mtn1-1mtn2-1* plant (n=30). The anther has dehisced and one can observe the pollen grains released from the anther sac (arrowheads). The pollen grains in A appear very loose and detached from each other, however the pollen grains in C appear to be more "sticky" than the pollen in A.

Scale bar = 1 mm.

Pollen from a Spd-non-treated *mtn1-1mtn2-1* plants, did not readily attach when applied to receptive stigma of Spd-non-treated WT plants (Figure 2-10, C). There were only a few grains released from the partially dehisced anther and the few grains that did attach showed very short to no pollen tube growth after 16 hours. Pollen from Spd-treated *mtn1-1mtn2-1* plants adhered better when applied to stigma of non-treated WT plants, and germinated pollen tubes extended further than the tubes from the Spd-non-treated *mtn1-1mtn2-1* plants (Figure 2-10, I). The stigmas of selfed Spd-treated *mtn1-1mtn2-1*mutant plants showed increased pollen adherence and germination than the stigmas of selfed non-treated mutants (compare Figure 2-10 D and E). However, the pollen tube germination and migration through the style did not appear to be guided towards the ovules. The pollen tubes were growing in multiple directions before finally making their way to the ovaries below. Lack of guidance may indicate an abnormal female gametophyte (Pagnussat et al., 2005; Yadegari and Drews, 2004).

To test the receptivity of the stigma of the *mtn1-1mtn2-1*, WT pollen from non-treated plants was placed on ½ MS and Spd-treated *mtn1-1mtn2-1* stigmas by hand pollination. The WT pollen on the non-treated *mtn1-1mtn2-1* stigma showed low adherence but the pollen germination was present (Figure 2-10, G). Pollen extension through the style was observed with aniline blue staining. The WT pollen on Spd-treated mutant stigma had better adherence as well as better pollen germination (compare Figure 2-10, G and H).

Alexander staining of pollen grains from WT and *mtn1-1mtn2-1* plants with and without Spd treatment was performed to test viability (data not shown due to poor image quality). Pollen form WT plants without and with Spd-treatment had 100% viability while pollen form non-treated *mtn1-1mtn2-1* plants had no viability. A few pollen grains in the anthers from Spd-treated *mtn1-1mtn2-1* plants were viable, but the majority of pollen grains of these mutants were non-viable.

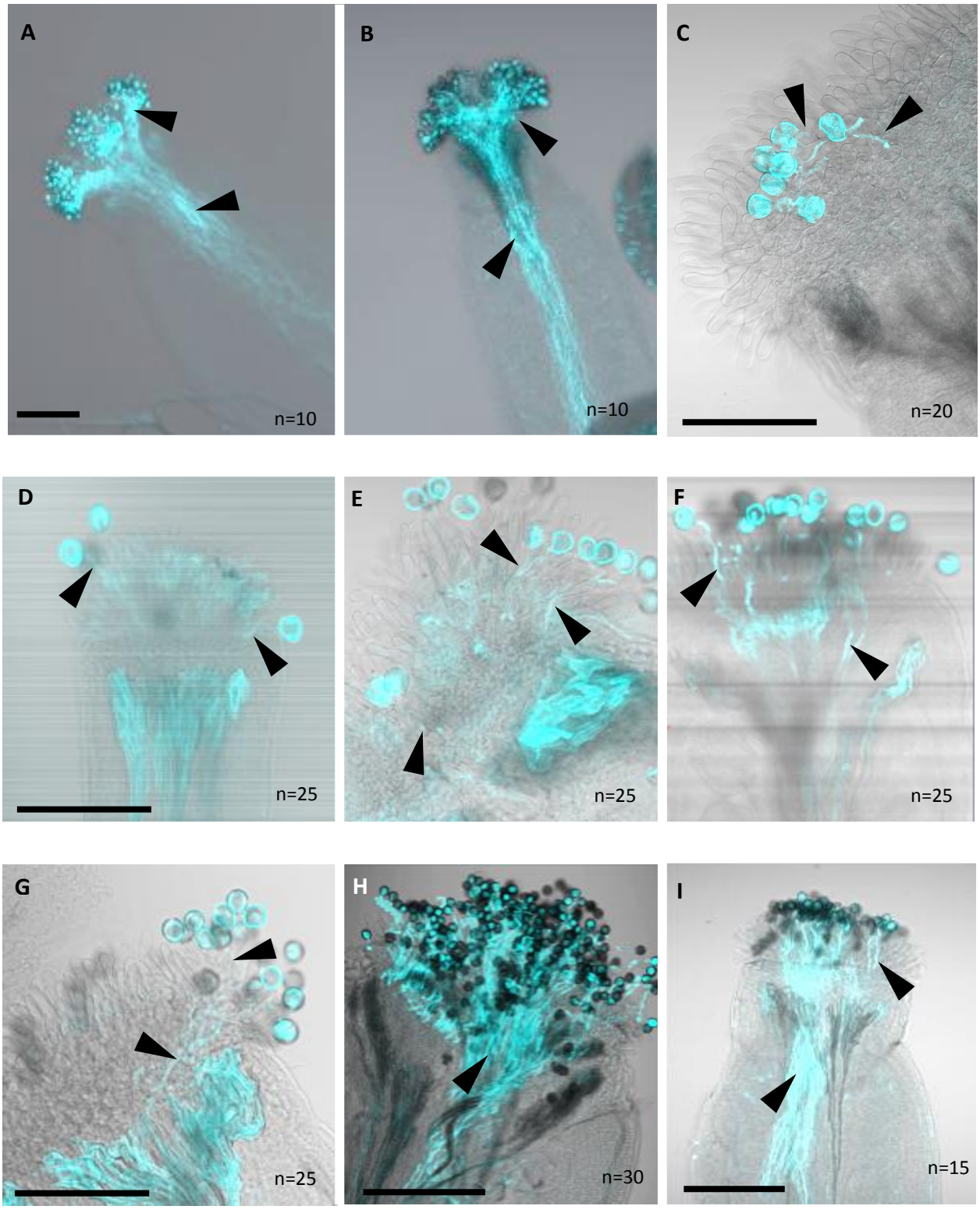
A
n=10
B
n=10
C
n=20
D
n=25
E
n=25
F
n=25
G
n=25
H
n=30
I
n=15

Figure 2-10. Aniline blue images of *mtn1-1mtn2-1* and WT pollen germination on *A. thaliana* WT and *mtn1-1mtn2-1* stigma with and without Spd

The plates A-C and I, show WT stigmas; plates D-H show *mtn1-1mtn2-1* stigmas. In A, a selfed WT stigma is presented. The stigma is covered with an abundance of WT pollen, and pollen germination is confirmed by the presence of pollen tubes (arrowheads) growing through the style. In B, a selfed, Spd-treated WT stigma is shown. This stigma too, carries a large amount of pollen that covers almost the whole stigma surface. Pollen germination is observed and pollen tubes can be seen extending through the style (arrowheads). The stigma shown in C, is a WT stigma from a non-Spd-treated plant which was hand pollinated with pollen from a non-treated *mtn1-1mtn2-1* plant. There are very few pollen grains sticking to the stigmatic surface. Pollen tube growth can be observed (arrowheads). The *mtn1-1mtn2-1* stigmas of D and G are from non-Spd treated mutant plants, while the stigmas in E, F and H are from Spd-treated *mtn1-1mtn2-1* mutants. In D, the stigma is selfed with non-treated *mtn1-1mtn2-1* pollen and in G the stigma is pollinated with WT pollen. Only three pollen grains can be seen adhered to the stigma in D, and only a very few WT pollen grains have germinated on G. In both D and G, pollen tubes have emerged, but have not entered the style. In E and H, the stigma was hand pollinated with Spd-treated mutant pollen and WT pollen respectively. One can see a larger number of pollen grains on the stigma than in D. A few pollen tubes have emerged and can be seen entering the style in E. on the other hand, a larger number of WT has germinated on the Spd-treated mutant plant stigma. The stigma in F is a Spd-treated mutant plant stigma that was hand pollinated with Spd-treated mutant pollen. Similar to E, there are several pollen grains that have adhered and extension of pollen tubes is observed (arrowheads). H is a WT stigma, pollinated with Spd-treated *mtn1-1mtn2-1* mutant pollen. The stigmatic surface is covered with germinating pollen and the pollen tubes can be observed extending through the style (arrowheads). The WT stigma in I, is also from a non-treated plant, hand pollinated with pollen from a Spd-treated *mtn1-1mtn2-1* mutant plant. There is a higher number of pollen grains adhered to the stigma and pollen tube extension can be observed through the style (arrowheads).

Each set of images show the fluorescent and white light overlay.

Scale bar = 200 ɯm

Spd supplementation to *mtn1-1mtn2-1* mutant seeds partially restored seed germination percentage (Table 2-2), and passed the restoration of germination percentage on to subsequent generations. This resulted in the G3 (out of G1, G2 and G3 generations) plants of Spd-treated *mtn1-1mtn2-1* mutants producing seeds with highest germination rate. Furthermore, the plants arisen from Spd treated *mtn1-1mtn2-1* mutant seeds produced flowers that exhibited normal ovule development and had stigmas with few healthy pollen grains which showed multidirectional growth upon germination, before making their way to the ovule suggesting lack of guidance.

In order to test whether the Spd treatment restored guided pollen tube growth in the flowers of G3 generation producing viable seeds, hand pollination of Spd non-treated and Spd-treated G3 stigmas using non-Spd-treated G3 flower pollen was carried out (Figure 2-11 A and B respectively). The stigmas of both Spd-treated and non-treated G3 plant stigmas had an abundance of germinated pollen and well guided pollen tube growth towards the ovules through the style (Figure 2-11).

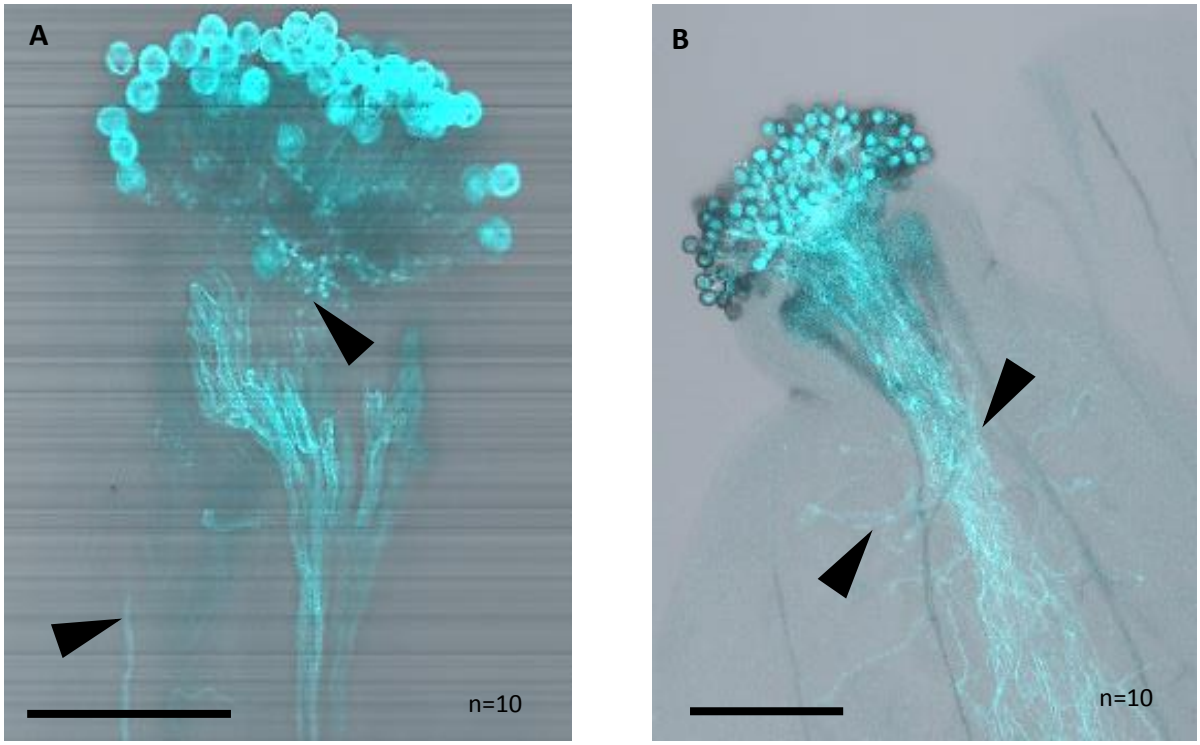

Figure 2-11. Aniline blue images of stigmas of *mtn1-1mtn2-1* G3 plants not treated with and treated with Spd.

The plates A and B show G3 stigmas. In A, a pollinated G3 stigma from seed not germinated on Spd is presented. The stigma is covered with an abundance of G3 pollen, applied by hand pollination using non-Spd –treated G3 plant pollen. The pollen germination is confirmed by the presence of pollen tubes (arrowheads) growing through the style. In B, a hand pollinated, Spd-treated G3 stigma is shown. The pollen from a non-Spd-treated G3 plant covers almost the whole stigma surface and pollen tube germination through the style can be observed (arrowheads).

Each set of images show the fluorescent and white light overlay.

Scale bar = 200 µm

2.3.5 **Effect of Spd supplementation of vascular bundle number and arrangement of the MTN-deficient mutants**

As reported previously, plants arising from the Spd-fed *mtn1-1mtn2-1* mutant seeds are partially fertile. Waduwara-Jayabahu (2012) reported that the *mtn1-1mtn2-1* mutant displays a pleiotropic phenotype which includes an increased number of vascular bundles and an irregular vascular bundle arrangement in the stems. The next stage of this research focused on whether the vasculature of the MTN-deficient mutants responds to the Spd treatment. The mutant genotypes *mtn1-1mtn2-1* and *mtn1-1mtn2-5* were used for this experiment, with WT as the control.

The TBO-stained WT stem cross-sections showed a regular arrangement of vascular bundles with an average number of 6±2 bundles (Figure 2-13 A; n=30). The WT stem cross sections from plants arising from WT seeds treated with Spd (Figure 2-13 B; n=30) showed a small increase in the vascular bundle number (7±2). Student's t-test was performed to determine the statistical significance of Spd supplementation on the number of vascular bundles in the stems. There was no significant difference in the bundle number between treatments (+/- Spd) for WT ($p \geq 0.05$).

The untreated *mtn1-1mtn2-5* mutant plants grew slightly larger in stature than the WT. (Figure 2-12 A and B). The mutants exhibited a wider stem diameter (Figure 2-14 C; n= 25) than WT. The cross sections were larger and more elliptical compared the circular cross sections of the WT. The *mtn1-1mtn2-5* stems had a higher number of vascular bundles (Figure 2-14 C; 10±2) than the untreated WT plants. The vascular bundles of the WT plants were pyramid shaped with the tip extending towards the pith and the wider bottom broadening at a compacted phloem cap. The Spd treated *mtn1-1mtn2-5* mutant seeds resulted in plants that were larger in size compared to the non-treated mutants and WT (Figure 2-12 C), having taller stems, larger rosette and larger

stem diameter (Figure 2-12, B). The stem cross sections showed increased stem diameter and a more distorted stem outline (Figure 2-14 D; n = 20). The number of vascular bundles in the *mtn1-1mtn2-5* stem was reduced with the Spd treatment (7±2) than the non-treated *mtn1-1mtn2-5* mutants. Each vascular bundle was larger compared to the non-treated *mtn1-1mtn2*-5 mutant, with increased xylem and phloem cells (Figure 2-13 C and D). The student's t-test result ($p \geq 0.05$) showed there was a statistically significant decrease in the number of bundle with the Spd treatment in the *mtn1-1mtn2-5* mutant.

The *mtn1-1mtn2-1* mutant plants with no Spd treatment (n=30) had a smaller stem diameter than the non-treated *mtn1-1mtn2-5* mutant and WT and the number of vascular bundles (14±3) was significantly ($p<0.05$) higher than that of WT or of the *mtn1-1mtn2-5* mutant ($p \geq 0.05$). The arrangement of the vascular bundles of the non-treated *mtn1-1mtn2-1* mutant was irregular, and many of the bundles had two or three xylem pyramids per bundle, as opposed to the single xylem pyramid with only one phloem stack (compare Figure 2-13 B with Figure 2-14 E). Stems of Spd-treated plants (Figure 2-14 F; n=21) had a slightly more a cylindrical shape and a close to regular placement of the vascular bundles, even though the number of bundles (13±2) was still greater than WT (Figure 2-14 A and F).

Stem cross sections were also made from the fertile and infertile branches of the *mtn1-1mtn2-1* mutant treated with Spd, to show the difference of bundle arrangement within the same plant (Figure2-14 F and G). The fertile branch was more cylindrical than the non-fertile branch (n=16) and had a lesser number of bundles with two or three xylem pyramids (3±2) compared to the infertile branch. All these findings suggest that the Spd feeding helps in reducing the vascular bundle number and irregular vascular arrangement in fertile branches of *mtn1-1mtn2-1*mutants.


A
B
C
D
E
F

Figure 2-12. Five-week-old *A. thaliana* WT and *mtn1-1mtn2-5* mutant plants with and without Spd supplementation

In A-F, 5-week-old, WT and *mtn1-1mtn2-5* plants are shown. In A, a non-Spd treated WT plant is presented. The plant has one main bolt with three branches and one secondary bolt. The rosette of the WT plant is shown in D. In B, a non-treated, 5-week-old *mtn1-1mtn2-5* mutant plant is shown. The *mtn1-1mt2-5* plant is slightly larger than the WT (A). One can observe a main bolt with five branches and two secondary bolts. The rosette of the non-treated *mtn1-1mtn2-5* plant is shown in E. A Spd treated, 5-week-old *mtn1-1mtn2-5* mutant plant is presented in C. this plant is larger than the WT and the non-treated *mtn1-1mtn2-5* mutant. The rosette of this plant is shown in F. Both the non-treated and Spd-treated mutant plant rosettes are larger than the WT rosette. However, the treated mutant rosette has the largest leaves than the other two plants shown here.

Scale bar = 10 mm

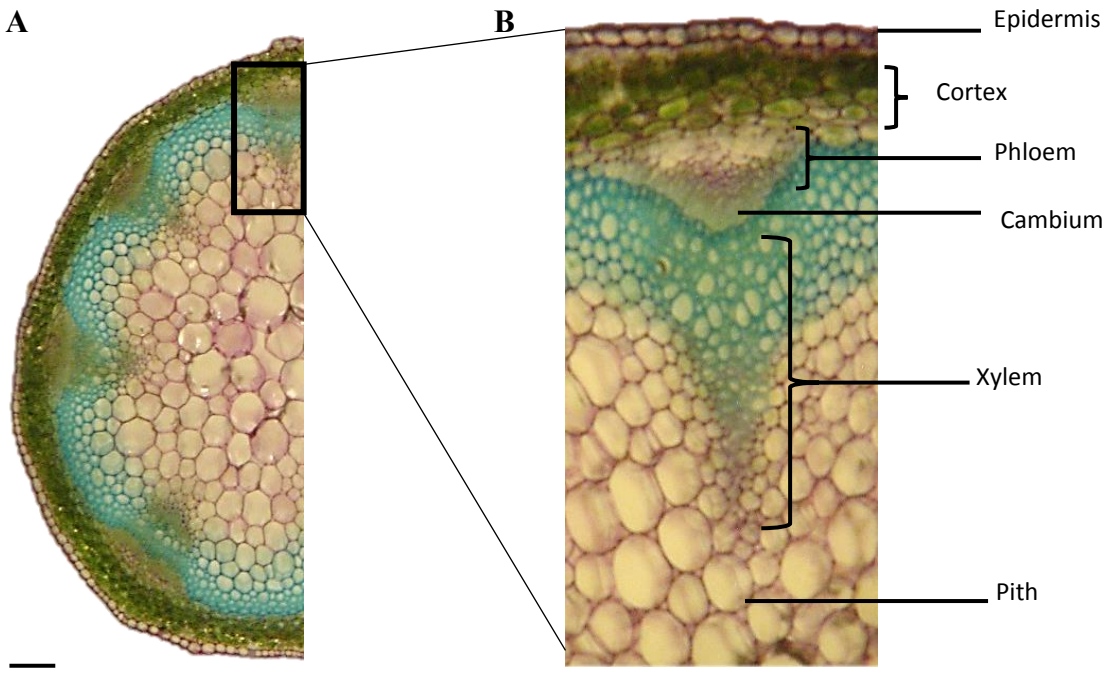

Figure 2-13. Representative image of stem cross section of a WT *A. thaliana* main bolt

(A) Stem cross section of a main bolt of non-treated 4 week-old WT plant, stained with 0.1% TBO (pH=4.4)

(B) Enlarged view of one vascular bundle. The image shows epidermis, cortex, vascular tissue (xylem, phloem, and cambium) and pith.

Scale bar = 0.1 mm

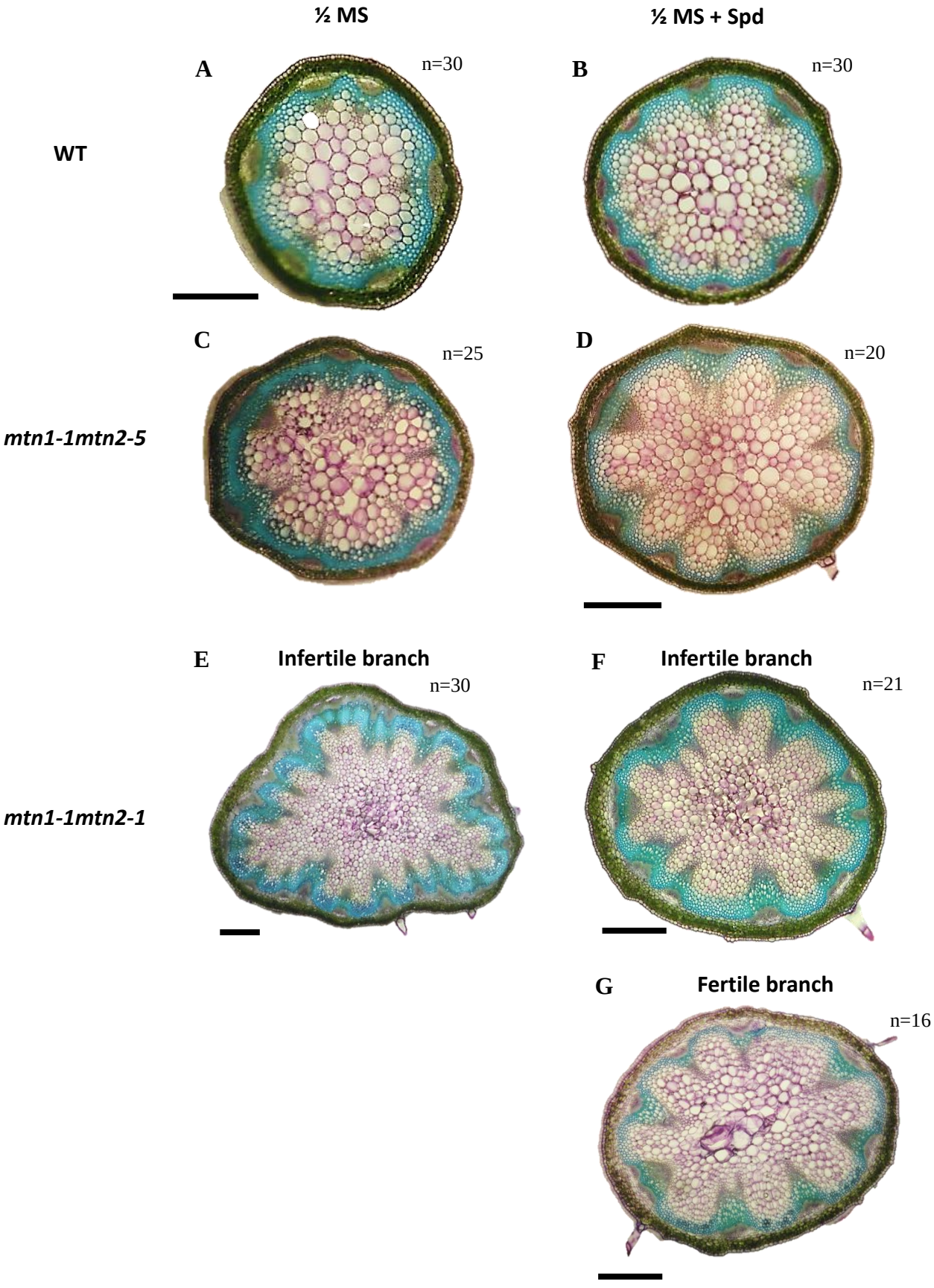
½ MS
½ MS + Spd
WT
A
n=30
B
n=30
mtn1-1mtn2-5
C
n=25
D
n=20
mtn1-1mtn2-1
E
Infertile branch
n=30
F
Infertile branch
n=21
G
Fertile branch
n=16

Figure 2-14. Cross sections of the main bolt of *A. thaliana* WT, *mtn1-1mtn2-5* and *mtn1-1mtn2-1* mutant plants with and without Spd supplementation

Plants were treated with Spd for 14 days after germination. In A, the WT stem section with no treatment ($^1/_2$ MS) has typical bundle arrangement and 6 vascular bundles. The Spd treated WT stem in B, shows an increase in bundle number. The MTN-deficient mutant stems (C - G) have increased bundle number, irregular arrangement and non-cylindrical stem shape. In C and D, the stem cross section from Spd non--treated and Spd-treated *mtn1-1mtn2-5* mutant plants are shown, respectively. Both stem sections have a higher number of vascular bundles than the WT. In E, an infertile stem from a non-Spd-treated *mtn1-1mtn2-1* plant is shown. The multiple vascular bundles arranged asymmetrically cross section infertile stem form Sections are stained with 0.1% TBO (pH 4.4).

Scale bar = 2 mm.

2.3.6 **Effect of Spd supplementation to *mtn1-1mtn2-1* parent seeds on vascular bundle number and arrangement in three daughter generations**

mtn1-1mtn2-1 mutant plants rising from Spd-treated seed were designated as G1. The G1 seeds produced by these plants as well as the daughter 2nd and 3rd generation (G2 and G3 respectively) seeds were germinated on ½ MS media to examine whether the effect of Spd supplementation of the 1st generation carried down the lineage. All the G1, G2, G3 plants were genotypically *mtn1-1mtn2-1*. The stem cross-sections were examined for vascular bundle number and the vascular bundle arrangement. Out of the three generations, the 3rd generation plants post-Spd treatment (G3) showed the most improved phenotype including fertility, erect bolts, less twisting of branches and fewer curled rosette leaves, compared to the 1st generation plants (G1).

The cross-sections of the G2 plant stems (n=15) showed an increased number of vascular bundles (12±2) compared to WT (6±2) (Figure 2-15, A *vs* C), including fused bundles with two or three xylem pyramids (Figure 2-15 C, *). However, the number of vascular bundles were less than the G1 *mtn1-1mtn2-1* plants (n=21) (Figure 2-15, B *). The stem cross sections of G2 plants also had a slightly improved symmetrical outline although it was not completely restored to WT shape (13±2, Figure 2-15, C). In contrast, the cross sections of the G3 stems (n=22) had a lower number of vascular bundles (10±3) than G1 and G2 stems. The G3 cross sections showed a symmetrical outline of the stem, which was much closer to the WT. The vascular bundle arrangement of the G3 stem cross sections showed the highest improvement, with more symmetrical arrangement within the stem. The G3 vascular bundles had fewer instances with fused bundles with multiple xylem peaks (compare * in Figure 2-15 B and C with D), however, the complete restoration of WT phenotype was not observed (Figure 2-15, A and D).

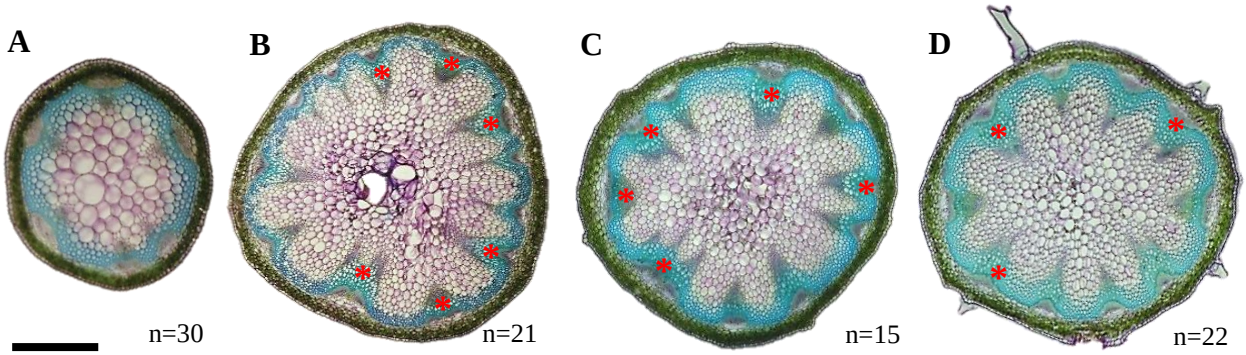

Figure 2-15. Stem cross sections of WT and *mtn1-1mtn2-1* G1, G2 and G3 plants.

The stem cross-sections were obtained from G1, G2 and G3 plants 2 weeks after bolting, 1 cm above the rosette. In A, a stem cross section from a non-Spd-treated WT plant is shown. The cross section is symmetrical with six vascular bundle arranged along the periphery. There are no fused bundles. The WT stem cross section is smaller in diameter than the *mtn1-1mtn2-1* G1, G2 and G3 cross sections. In B, a stem cross section from a Spd-treated G1 *mtn1-1mtn2-1* plant is presented. One can observe multiple vascular bundles arranged asymmetrically within the stem. Some vascular bundles appear to be fused together and have two or three xylem peaks extending towards the pith (arrowheads). In C, a stem cross section from a G2 generation plant is shown. This stem cross section contains four fused vascular bundles having two or three xylem peaks (arrowheads) among the regular-shaped vascular bundles that are arranged asymmetrically within the stem. The stem cross section shown in D is from a G3 plant. It is evident that this cross section shows a more circular outline of the stem and the vascular bundles are arranged more symmetrically. There are only two fused vascular bundles and both of them have only two peaks (*).

All sections have been stained with 0.1% TBO (pH=4.4).

Scale bar = 2 mm.

2.3.7 **PCR identification of *mtn1-1mtn2-1* mutant embryos**

Short-term Spd treatment (14 DAG) to seed of *mtn1-1mtn2-1* mutants resulted in partial restoration of fertility (Figure 2-4, F). Tissue sections of reproductive organs also showed improvements in development with Spd treatment (Figure 2- 8, D and F). Considering these outcomes, it was decided to examine the effect of Spd treatment on a more sensitive developmental stage, the embryo of MTN-deficient mutants. At the time this research was started, *mtn1-1mtn2-1* embryos had only briefly been examined for developmental defects by Shuningbo Ye (2013), for final year research project at Moffatt lab. The study reported in this thesis focused on homozygous *mtn1-1mtn2-1* embryos recovered from heterozygous *mtn1-1mtn2-1* plants grown in the presence or absence of Spd.

The dissected embryos were grouped into three major classes, based on their size. Working under the assumption that *mtn1-1mtn2-1*embryos developed more slowly than the WT, similar to the relative growth of the mature plants, it was hypothesized that the group containing the smallest embryos were the homozygous *mtn1-1mtn2-1*embryos, while the larger embryos were either heterozygous or WT at the segregating *MTN* locus. The validity of this hypothesis was tested by genotyping individual embryos in each group by PCR. The PCR results confirmed that only the smaller, developmentally delayed embryos were homozygous for the *MTN1* mutation while the intermediate and larger embryos were heterozygous or WT for the *MTN1* mutation (Figure 2-16). The embryo PCR test was performed for embryos from both Spd-treated and untreated plants and the results were same: the smaller embryos were double mutants. Based on these results, the selection of the *mtn1-1mtn2-1* embryos for the analysis of auxin distribution and procambial cell activation was performed by grouping the excised *mtn1-1mtn2-1* embryos into phenotypically distinct groups. This was not done for homozygous WT and *mtn1-1mtn2-5*.

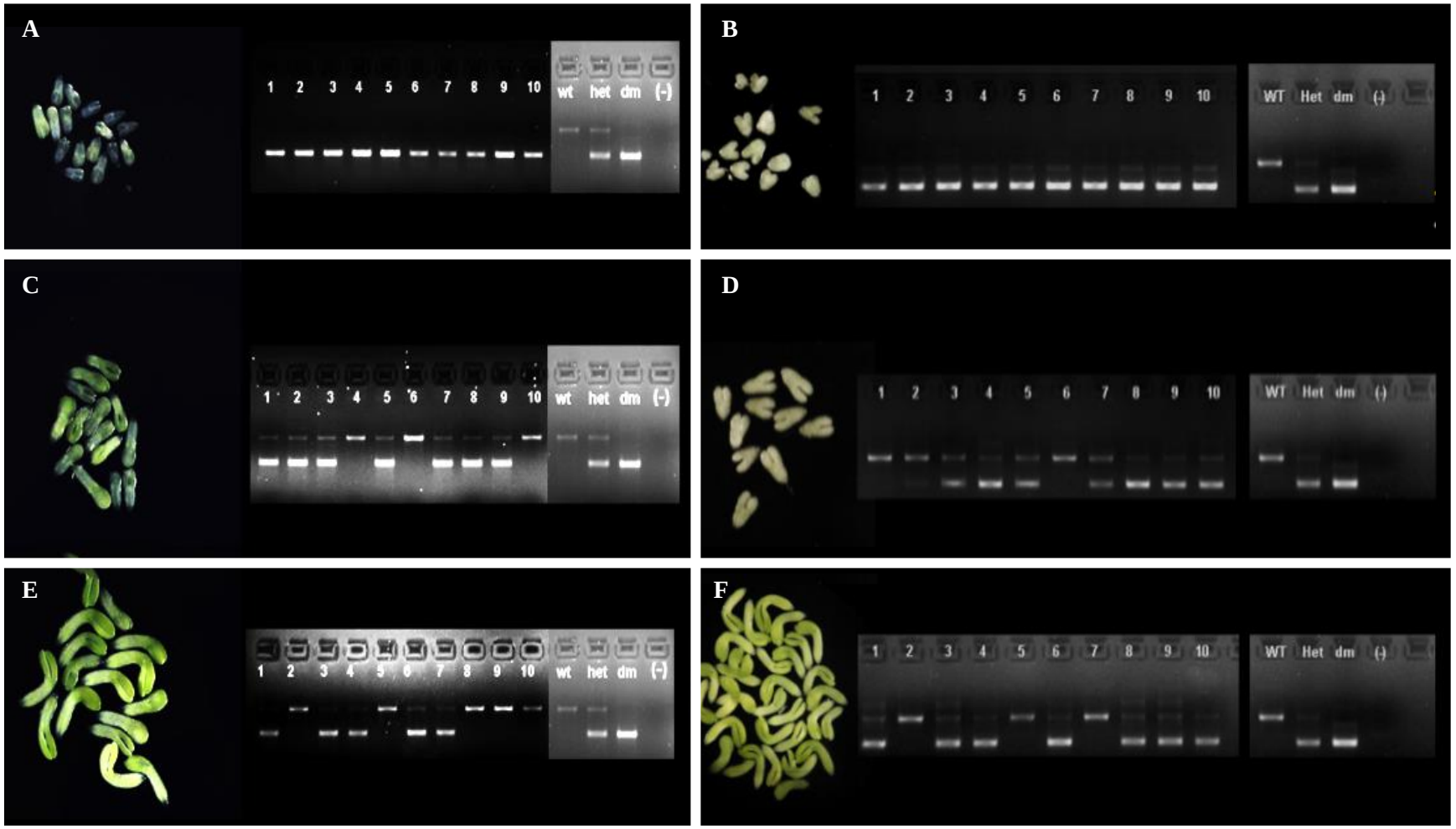
A
1 2 3 4 5 6 7 8 9 10
wt het dm (-)
B
1 2 3 4 5 6 7 8 9 10
WT Het dm (-)
C
1 2 3 4 5 6 7 8 9 10
wt het dm (-)
D
1 2 3 4 5 6 7 8 9 10
WT Het dm (-)
E
1 2 3 4 5 6 7 8 9 10
wt het dm (-)
F
1 2 3 4 5 6 7 8 9 10
WT Het dm (-)

Figure 2-16. Agarose gel electrophoresis result of single embryo PCR for the identification of the *mtn1-1mtn2-1* mutants

A-F show the phenotypically distinct groups of embryos coming from developmentally similar stage 17A siliques (A, C, E – non-Spd-treated plants; B, D, F – Spd-treated plants) from *A. thaliana* heterozygous *mtn1-1mtn2-1* mutants. The numbers 1-10 in A-F represent the sample identity given to the extracted embryo DNA (i.e. in A, PCR products of ten embryo DNA samples from non-treated plants were electrophoresed and in B, PCR products of ten embryo DNA samples from Spd-treated plants were electrophoresed etc.). The bands denoted by the letters wt, het and dm stand for the wild-type, heterozygous *mtn1-1mtn2-1* mutant and homozygous *mtn1-1mtn2-1* double mutant controls, respectively. The primers used for the PCR amplify the endogenous *MTN1* gene (WT) producing a larger fragment. The *mtn1-1* mutation specific primers amplify the T-DNA insertion region which is a smaller fragment (dm). The PCR result presented in the above gels is from a multiplex PCR involving all the above primers. Therefore, the heterozygous mutant will have two bands; one for the endogenous gene and one for the mutation. The WT only has the larger band and the double mutant will only have the smaller fragment. In A and B, the smallest group of embryos have only the banding pattern for the mutation, which is the banding pattern of the homozygous double mutant. a faint non-specific band can be observed in B, but this band is of smaller size than the WT band. In C-F, the samples show a mixture of both heterozygous and WT banding pattern.

2.3.8 **Effect of Spd supplementation on auxin distribution in embryos**

The synthetic auxin response reporter DR5*rev*::GFP leads to GFP fluorescence when auxin is sufficiently present for transcription activation of sensitive promoters. The DR5*rev*::GFP reporter expression level is a qualitative indication of the auxin distribution and does not reflect the actual auxin concentration in a given tissue (Liao et al., 2015). WT plants carrying the reporter were used as a control for comparison of DR5*rev*::GFP expression pattern in *mtn1-1mtn2-1* and *mtn1-1mtn2-5* mutants in this study. The DR5*rev*::GFP was introduced to the mutant background in *mtn1-1mtn2-1* and *mtn1-1mtn2-5* mutants by Waduwara-Jayabahu et al., (2012).

The typical pattern for the DR5 reporter in developing heart and torpedo stage embryos was very strong at the hypophysis, the future root apical meristem and the future cotyledon tips (Figure 1-11, A). Earlier embryo stages (globular and transition) and later embryo stages (bent cotyledon) are not presented, as only the heart and torpedo stages were observed for changes in the auxin response reporter expression pattern, due to time constraints. The heart stage embryo is discussed in this thesis. The changes in the expression patterns in the torpedo stage embryos +/- Spd were comparable to the heart shaped embryo: lesser or sometimes lacking DR5*rev*::GFP expression in the *mtn1-1mtn2-1* mutant cotyledon tips and diffuse expression pattern in the hypophysis region in embryos excised from Spd-non-treated plants; improved expression pattern of the reporter at cotyledon tips in some embryos and less diffuse expression in the hypophysis region of embryos excised form Spd-treated plants. The expression pattern of the DR5*rev*::GFP reporter in the embryos showed variation, although most embryos had a common pattern. Therefore, the embryos were grouped according to the expression pattern similarities, and a representative image from the most prevalent group for each genotype per treatment is presented under the

results of this thesis. The distribution of the various expression patterns is shown in Appendix IV (Figure 2-22).

The expression pattern for the non-treated and Spd-treated WT embryos (n=25 and n=30 respectively), was typical of the expected auxin distribution, with fluorescence at the cotyledon tips, hypophysis and future root apical meristem. The expression pattern for WT showed no notable change with the Spd supplementation (Figure 2-17, A and B).

The WT results were used as the baseline for the analysis of the DR5*rev*::GFP expression pattern for the two MTN-deficient mutants, *mtn1-1mtn2-1* and *mtn1-1mtn2-5*. The *mtn1-1mtn2-5* mutant embryos excised from plants with no Spd-treatment (n=20) showed strong expression at the hypophysis region, however, the expression at the cotyledon tips was variable. In some samples, one of the cotyledon tips showed a stronger fluorescence than the other (Figure 2-17, C), while in some the expression was almost equal in both tips (data not shown). The embryos from the Spd-supplemented plants (n=30) had a comparatively reduced expression at the cotyledon tips, but maintained expression at the hypophysis region (Figure 2- 17, D). In some instances the suspensor was excised along with the embryo, and the expression of the DR5*rev*::GFP reporter was observed in embryos excised from both Spd-treated and non-treated plants (Figure 2-17 A, D and F).

The *mtn1-1mtn2-1* mutant embryos obtained from heterozygous *mtn1-1mtn2-1* plants not supplemented with Spd (n=25), had very low fluorescence at the cotyledon tips and the future root tip. The expression of the reporter at the cotyledon tips was barely visible while the expression pattern at the root tip appeared weaker and more diffuse than WT (Figure 2-17, E). In some instances, when there was faint expression present in the cotyledon tips, asymmetry of

expression could be observed. However, expression of the DR5rev::GFP reporter was not always present in the cotyledon tips of the embryos. There was a strong increase in DR5*rev*::GFP expression in the *mtn1-1mtn2-1* embryos, with the Spd-treatment of the parent plant. The expression was higher at the cotyledon tips and a more defined, less diffuse expression was observed at the future root apical meristem (Figure 2-17, F).

Heart stage

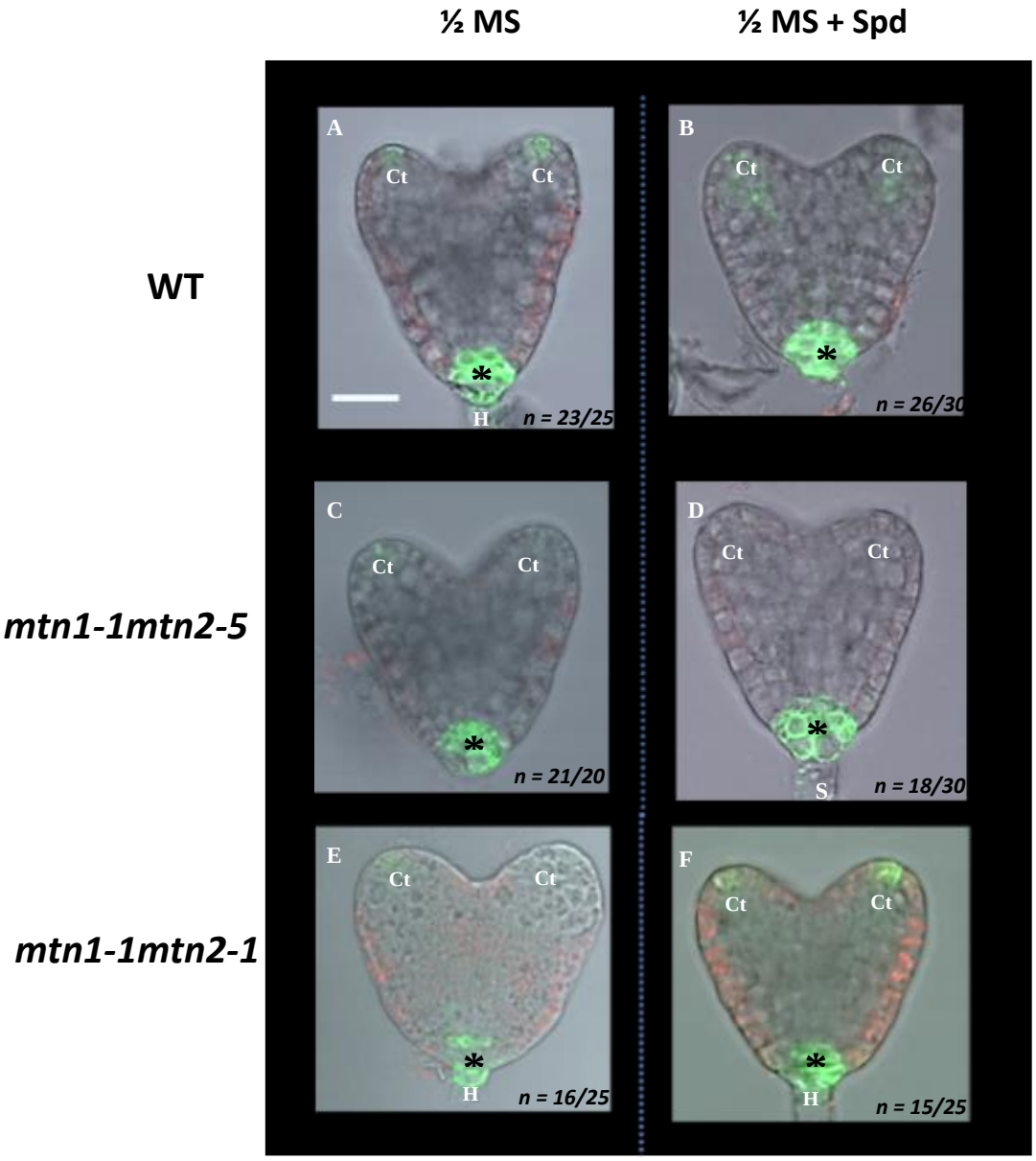
½ MS
½ MS + Spd
WT
mtn1-1mtn2-5
mtn1-1mtn2-1
A
Ct
Ct
H
n = 23/25
B
Ct
Ct
n = 26/30
C
Ct
Ct
n = 21/20
D
Ct
Ct
S
n = 18/30
E
Ct
Ct
H
n = 16/25
F
Ct
Ct
H
n = 15/25

Figure 2-17. The DR5*rev*::GFP expression pattern in WT, *mtn1-1mtn2-5* and *mtn1-1mtn2-1* heart stage embryos from plants without and with Spd supplementation.

Confocal images of embryos dissected from stage 17A siliques from genotypically identified, healthy adult plants which have been treated (B, D, F) and not treated (A, C, E) with Spd. In the WT (A, B) independent of the treatment, the expression of the reporter was as expected; it is seen in the tip of the cotyledons (Ct) and the location of the future root tip (*). The embryo is positioned with the suspensor (S – seen in D) connected via the hypophysis cell (H). In the mutant *mtn1-1mtn2-5* there is a difference when comparing treated (C) and non-treated (D) plant embryos. In C, the GFP reporter expression is faint in the cotyledons whereas it is strongly expressed in the future root tip. In contrast, the embryo from plant (D) does not display expression in the cotyledons, but exhibit in the root tip. In the mutant *mtn1-1mtn2-1* the opposite is observed. In the non-treated plant (E), expression is seen at the bottom of the embryo and faint expression can be observed in the Cts. However, the expression appears diffused. In the treated plant (F), faint expression is seen at the cotyledons and the expression at the future root tip is less diffuse (*). Images are fluorescent and bright-field overlay images. The embryos were not stained and remained live during microscopy.

Scale bar = 200 μM.

2.3.9 **Monopteros reporter expression in MTN-deficient embryos of Spd supplemented plants**

MTN mutant lines *mtn1-1mtn2-1* and *mtn1-1mtn2-5* and a WT control carrying the MP::n3GFP reporter construct were used to validate the results obtained using DR5*rev*::GFP. The heart stage and torpedo stage embryos (not shown) were dissected and examined for reporter expression.

The WT embryos showed MP::n3GFP reporter expression pattern in the entire embryo (n=25). The 3D z-stacked image appears as a complete embryo covered in fluorescent signal. The reporter is nuclear localized, therefore the expression in individual cells was observed as fluorescent spots occurring all over the embryo (Figure 2-18, A). This is the expected expression pattern for MP in a normal embryo (Hamann et al., 2002). The Spd treatment of the WT did not detectably affect the expression pattern of the *MP* reporter (Figure 2-18, B; n=25). The expression pattern in the *mtn1-1mtn2-5* mutant embryos from the non-treated plants (n=30) was a reflection parallel that of the DR5*rev*::GFP expression pattern. The MP expression was not present at the cotyledon tips, but localized to the middle region of the embryo (Figure 2-18, C), suggesting that the level of auxin in the cotyledon tips is insufficient to activate the MP gene, resulting in no fluorescence signature. The results from the Spd supplementation showed restored MP::n3GFP expression at the cotyledons with both lobes of the *mtn1-1mtn2-5* embryos displaying fluorescence (Figure 2-18, D).

The *mtn1-1mtn2-1* mutant embryos excised from plants not supplemented with Spd (n=25), had a severely decreased MP::n3GFP expression pattern compared to that observed in WT and the *mtn1-1mtn2-5* mutant embryos (compare Figure 2-18 A and C with E). The expression of the MP::n3GFP reporter was in the central region of the embryo while the expression in the cells in cotyledon region as well as at the future root tip was not detected (Figure 2-18, E). The embryos

from the Spd- supplemented *mtn1-1mtn2-1* plants (n-=30) showed an improved expression in the cotyledon tips and future root tip (Figure 2-18, F). However, it was not completely restored to the WT pattern. The overall number of cells expressing the MP::n3GFP reporter in the embryos appeared to be increased with the Spd supplementation to the parent plants.

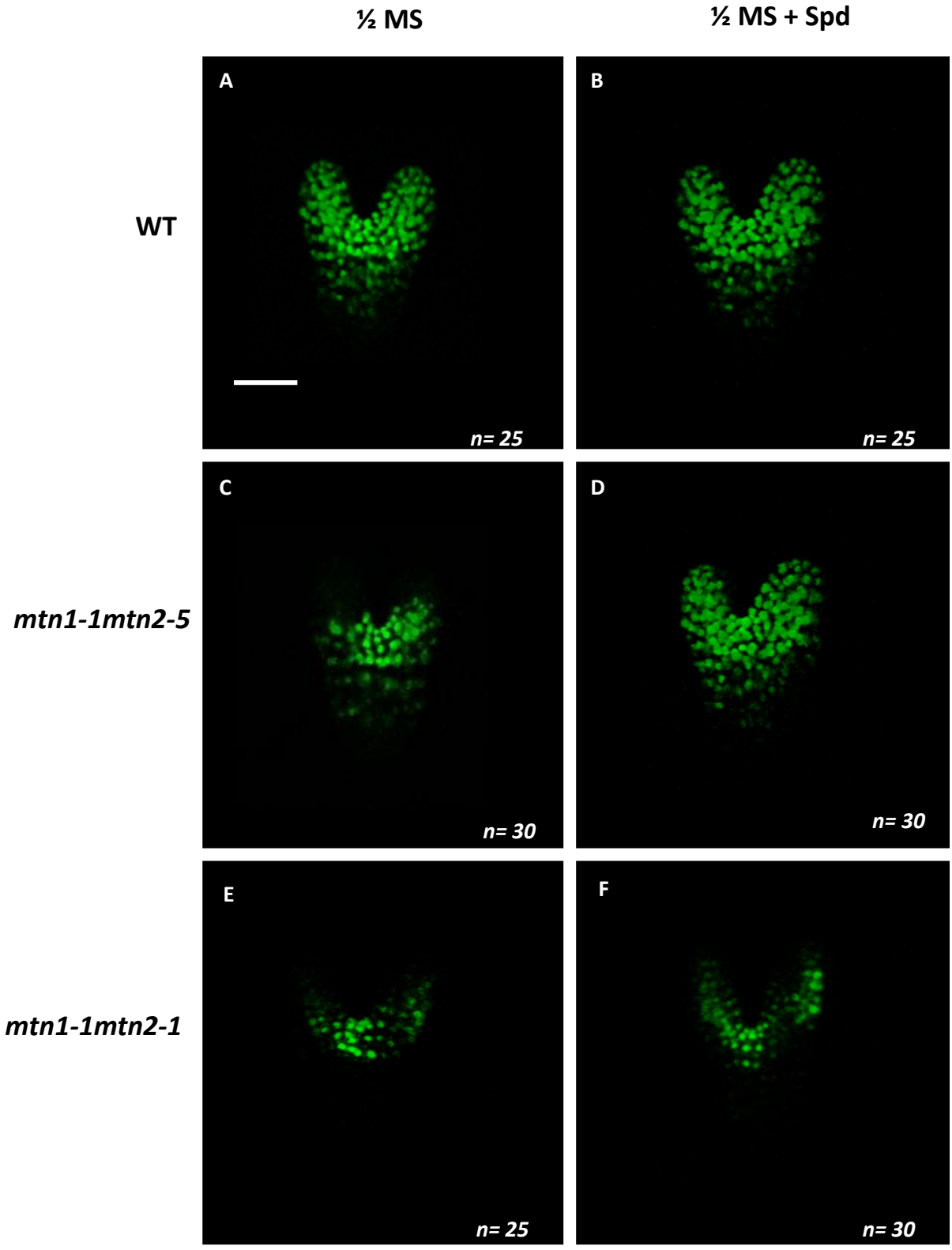
½ MS
½ MS + Spd
WT
mtn1-1mtn2-5
mtn1-1mtn2-1
A
B
C
D
E
F
n= 25
n= 25
n= 30
n= 30
n= 25
n= 30

Figure 2-18. MP::n3GFP expression of WT, *mtn1-1mtn2-5* and *mtn1-1mtn2-1* mutant embryos from plants treated without and with Spd.

In A and B, WT embryos are presented. Both embryos show reporter expression in all regions and the expression pattern shows no difference with Spd supplementation In C and D, the *mtn1-1mtn2-5* embryos from plants without treatment and with Spd-treatment are presented, respectively. The embryo shown in C has less number of cells expressing MP::n3GFP, mainly at the root and cotyledon tips. The embryos from the Spd-treated plants D, displays improved reporter expression in the cotyledons and the root tip with a higher number of cells expressing the MP reporter. E and F are embryos obtained from *mtn1-1mtn2-1* mutants without and with Spd-treatment. The embryo E has a much lower number of cells expressing MP::n3GFP, with cells missing expression at the cotyledon and hypophysis region. The expression is mainly localized to the central region of the embryo. The embryos from *mtn1-1mtn2-1* plants treated with Spd (F) show an improvement in the expression pattern of the reporter, with increased number of cells activated towards the cotyledon tips and towards the future root tip.

Scale bar = 200 µM.

2.3.10 **Response of procambial cell activation in embryos of MTN-deficient mutants to Spd supplementation**

mtn1-1mtn2-1 mutant plants have vascular abnormalities, as evidenced from the stem cross section data (Figure 2-14). The foundation for vascular development is laid down during the embryogenesis (Baima et al., 2001; Jürgens, 2001). To observe the vascular development at embryo stages, a fluorescent marker specific for provascular cells (AtHB8-NUC::YFP) was used.

The WT embryos excised from plants with no Spd treatment, showed typical "Y shaped", AtHB8-NUC::YFP reporter expression pattern in both the heart and torpedo stage (data not shown) embryos (Figure 2-19 A). The AtHB8-NUC::YFP reporter expression did not show any discernable difference in the WT embryos obtained from plants supplemented with Spd (Figure 2-19, A & B).

The AtHB8-NUC::YFP reporter expression pattern in the MTN-deficient mutants was atypical, with fewer procambial cells showing YFP expression towards the cotyledon tips. The *mtn1-1mtn2-5* mutant had a moderate expression change (Figure 2-19, C) relative to *mtn1-1mtn2-1* mutant. The number of cells expressing YFP in the cotyledon tips was intermediate between the WT and *mtn1-1mtn2-1* embryos. In most *mtn1-1mtn2-1* embryos, the central column of activated cells appeared wider and there were only a very few (1-3) cells activated towards the tips. The branches of the typical "Y" shape of the activated cell pattern appeared bent or distorted in these embryos (Figure 2-19 E).

The embryos obtained from MTN-deficient mutant plants of seeds supplemented with Spd, showed an increased number of cells expressing the AtHB8-NUC::YFP gene (Figure 2-19 D and F). The expression pattern of the reporter was modified in the *mtn1-1mtn2-1* embryos from plants of Spd-treated seeds (Figure 2-19, F) with more cells extending towards the cotyledon tips displaying fluorescence and increased fluorescence signal in the central column. The *mtn1-1mtn2-5* mutant embryos from plants of seeds exogenously supplemented with Spd also showed a modified expression pattern in the AtHB8-NUC::YFP gene expression pattern, with expression present at the central column of cell in the embryos and the cell files extending towards the cotyledon tips, creating the expected "Y shaped" pattern .

The expression pattern of both DR5*rev*::GFP and AtHB8-NUC::YFP reporters in the embryos of WT, *mtn1-1mtn2-1* and *mtn1-1mtn2-5* plants treated with and without Spd supplementation, showed minor variations among samples. The observations were grouped based on the similarity of the expression pattern. The group with the highest number of samples was considered as being representative of the treatment. The image representing this group is presented in this thesis.

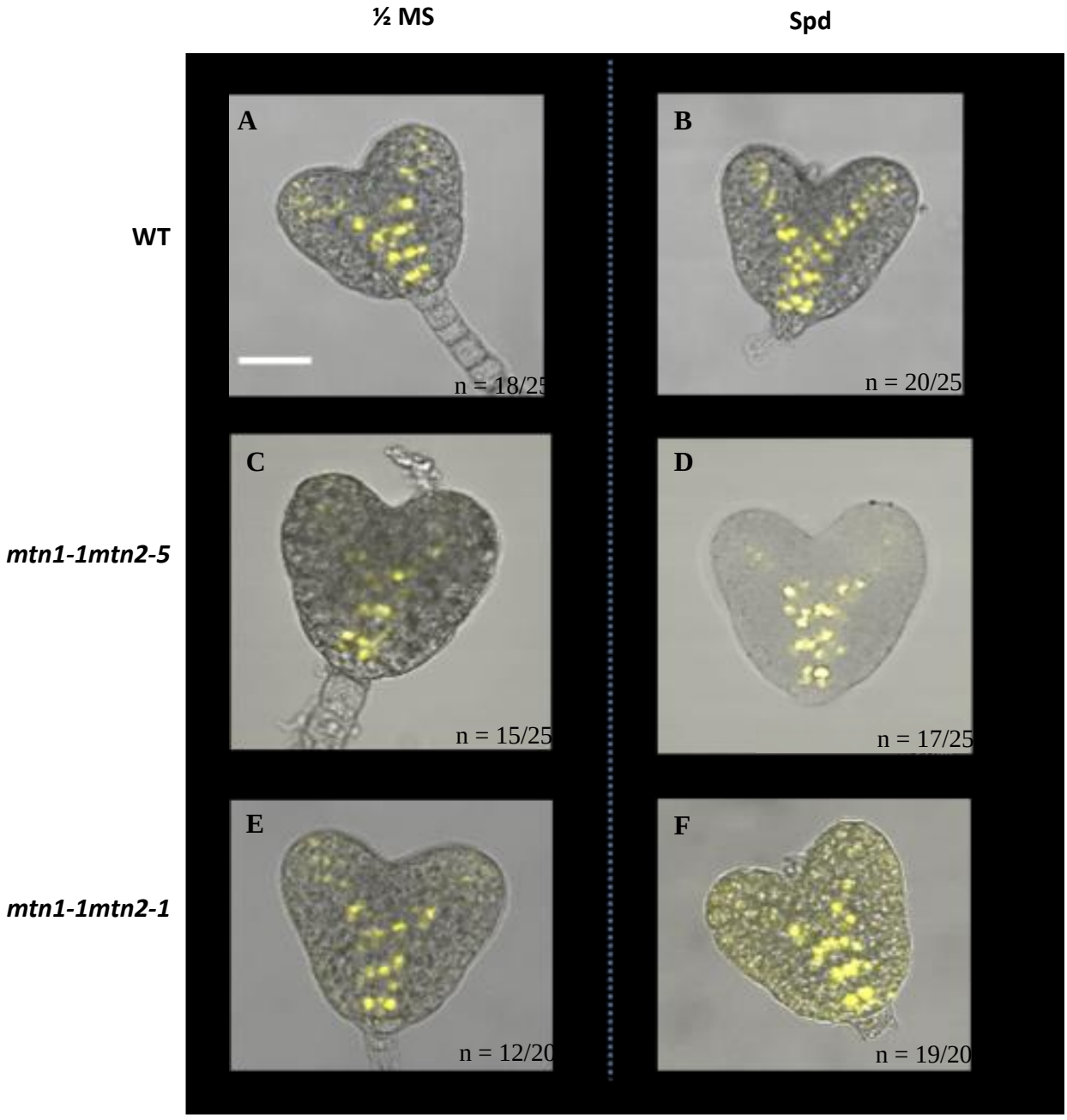
½ MS
Spd
WT
mtn1-1mtn2-5
mtn1-1mtn2-1
A
B
C
D
E
F
n = 18/25
n = 20/25
n = 15/25
n = 17/25
n = 12/20
n = 19/20

Figure 2-19. The AtHB8-NUC::YFP reporter expression in heart stage embryos from WT, *mtn1-1mtn2-5* and *mtn1-1mtn2-1* plants treated with and without Spd

The WT embryos from both non-treated and Spd-treated plants (A and B respectively) show typical AtHB8 reporter expression patterns, with the signature "Y" shape, due to central cell columns extending towards the cotyledon tips. In C, the *mtn1-1mtn2-5* mutant embryos from non-Spd-treated plant show lower expression at the tips and the *mtn1-1mtn2-1* embryos from non-Spd –treated plants (E) have even fewer activated cells. The Spd treatment resulted in no difference from the WT embryo expression pattern, however, the *mtn1-1mtn2-5* and *mtn1-1mtn2-1* embryos show a greater number of activated cells and a more "WT-like" expression pattern (D and F respectively).

Scale bar = 200 μM.

2.4 **Discussion**

2.4.1 **Effect of Spd-supplementation on MTN-deficient mutant reproduction**

2.4.1.1 **Exogenous feeding of Spd partially restores fertility of *mtn1-1mtn2-1* mutants**

The observed increase in the number of branches that carried longer, fuller siliques containing viable seeds 14 days-post-germination in plants treated with Spd, suggests a beneficial effect of Spd supplementation on fertility in MTN-deficient mutants. Waduwara-Jayabahu et al., (2012) reported that the infertile mutants showed fruit setting, following exposure of the floral meristem to Spd droplet over a period of time. A pilot experiment on germinating seeds on Spd supplemented media resulted in partial fertility in adult *mtn1-1mtn2-1* mutant plants (Waduwara-Jayabahu, 2011). Our experiment did not expose the floral meristem to Spd, instead germinated the seeds of MTN mutants in Spd supplemented medium. However, the beneficial effect of Spd supplementation on fertility became evident. Restoration of fertility did not follow an identifiable pattern; the number of restored siliques per branch, branch type (main bolt, 2^{o} branch or 3^{o} branch), while the position of the restored siliques on the branch all appear to be random. Partial restoration of silique numbers and seed numbers per silique through Spd supplementation could have been attributed to inadequacy of the concentration of Spd used for supplementation or the stage or duration of Spd supplementation. The Spd concentration used in this research was 100 µM and feeding was performed for 14 days post germination. Future research using different Spd concentrations, different growth stages as well as varying durations of treatment would help in determining whether a higher level, different stage of growth or reproduction or different duration of supplementation would bring greater beneficial effects in restoring the silique

numbers and seed setting, and thereby help in determining the optimum Spd concentration, stage of application and duration to be used in supplementation.

Spd is a key factor in eIF5A activation (Schuller et al., 2017, Hauber et al.,2010) which plays a critical role in plant growth and development (Feng et al. 2007). Knock-out mutants of eIF5A have shown to have severe developmental defects such as dwarf phenotype and infertility (Feng et al., 2007). The involvement of eIF5A in fertility and development (Feng et al., 2007; Li et al., 2014; Belda-Palazon et al., 2016), and importance of Spd in activating eIF5a, could be a way of explaining the restoration of the phenotypic issues in the *mtn1-1mtn2-1* mutant. The exogenously supplied Spd could be activating inactive forms of EiF5A in the *mtn1-1mtn2-1* mutant; thereby partially restoring fertility in random branches via eIF5A. *A. thaliana* has several PA conjugates that are effective in stress response (Alcázar et al., 2011). It is possible that the exogenously supplied Spd is conjugated within the plant and released later during reproductive development. The release of extra Spd might activate inactive forms of eIF5A thus restoring fertility.

Fertile siliques contained viable seeds that had higher germination percentages. Plants derived from these seeds produced viable seeds, although the number of seeds per plant (G1) was lower than the WT. Examination of the location of fertilized ovules / seed within the siliques did not provide any insight to a possible link between the positioning of the seed on the silique and the position of the silique on the branch. Restoration of fertility in response to Spd supplementation did not reveal any clear correlations. Thus it appears that the restoration of fruit set in the branches in response to Spd supplementation was completely random as was the position of the seed within the silique and the position of the silique on the branch.

2.4.1.2 **Spd restores pollen and ovule development**

The *mtn1-1mtn2-1* mutants show severe developmental defects in ovule and pollen development. Ovule development is arrested at very early stages where the integument layers are not fully extended to protect the developing embryo sac. There are a large number of different sized cells in the integument layers that are disorganized (Figure 2-8, C). Unlike a typical developing WT ovule which has layers of inner and outer integuments that can be distinguished, the mutant ovules have overlapping and sometimes missing layers of cells in the integuments (Figure 2-10). This suggests an uncoupling of cell division and cell expansion rates. This occurs when cell cycle clock is disturbed, leading to abnormal divisions (Neufield et al., 1998; Hemerly et al., 1995). The cyclin-dependent kinases (Cdks) are the major regulators of the cell cycle. Dominant Cdk mutants in *A. thaliana* have shown increased cell size (Hemerly et al., 1995). However, Hemerly et al. (1995) reported that cell development controls (e.g. cyclin-dependent kinase; CDC2) in plants can act independently from cell division rates. The appearance of large bulging cells amongst smaller compacted cells in *mtn1-1mtn2-1* and *mtn1-1mtn2-5* (Figure 2-9 and 2-10) in this study is consistent with the presence of a differential rate of cell division across the integument layers (Chevalier et al., 2011; Mattsson et al., 1999). This differential cell division rate in the developing ovule is an indication of incorrect cell-to-cell communication, where intercell-layer signaling might be impaired (Chevalier et al., 2011). The Spd-supplementation may have caused increased or misdirected cell signals leading to rapid cell expansion in some but not in all cells in the integument layers. Embedded sections of ovaries of stage 14 flowers (ready for pollination) of *mtn1-1mtn2-1* mutants show aborted and shrunken

ovules. The embryo sac itself was not functionally developed with a proper polarization and separation of the different cells of the egg apparatus. The central cell appeared very cloudy and the synergid and antipodal cells cannot be properly distinguished. This is another indication of cell-cell miscommunication. Cell-cell communication occurs via plasmodesmata (Ding et al., 1999). If the plasmodesmata of the *mtn1-1mtn2-1* mutant are non-functional, then cell-cell communication will be impaired. The *mtn1-1mtn2-1* mutant is known to have abnormal callose deposition (Waduwara-Jayabahu 2011). It is possible that abnormal callose depositions around the plasmodesmata neck (Strome et al., 2014) could be blocking the plasmodesmata, impairing its function. Due to the improper integument development and embryo sac malformation, *mtn1-1mtn2-1* ovules may abort at very early development stages.

Pollen health of the *mtn11mtn2-1* mutant was poor. The immature pollen contained large vacuoles and maturing pollen showed degenerating cytoplasm. Mature pollen lacked proper exine and no proper furrows. This unhealthy pollen (Fan et al., 2001) remains in anthers even at full maturity of the flowers, due to improper anther dehiscence. During the hand pollination experiment to determine pollen germination, anthers of the mutant had to be manually opened using fine needles and forceps to access the pollen.

Spd treatment of the *mtn1-1mtn2-1* mutant improved integument health and the ovules appeared to develop further than the non-Spd- treated plant ovule. This improvement was not restored to WT level; however, the integument layers had extended to surround the embryo sac. It is possible that the exogenous Spd is increasing the cell expansion rate of the integument cells slightly or irregularly. The abnormal shape of the ovules appeared to be mainly due to the

improper development of the integuments. The embryo sac also showed improvement achieving a somewhat regular shape, although the individual cells of the egg apparatus were not very clear. However, a few embryos were observed and the plants did produce viable seeds although at a very low frequency. This suggests an improvement in reproductive organ development (ovules and pollen) in the MTN-deficient mutant plant due to the Spd supplementation. The low fertilization of the ovules may be related to the pollen development defects in the mutant. Pollen health is slightly improved with a few grains across the embedded sections appearing with full intact cytoplasm and a greatly improved exine. These grains could be called "healthy" and would contribute towards fertilizing an improved ovule.

The *mtn1-1mtn2-5* mutant on the other hand is fertile without any treatment and normal ovules and pollen were expected. However, when examining the developing ovules, the integument layers of the mutant contained bulging large cells among smaller compacted cells. The layers of the integuments were not as disorganized as the *mtn1-1mtn2-1* but they still indicated differential cell division rate possibly attributed to cell-cell communication issues (Chevalier et al., 2011; Hove et al., 2015). The Spd treatment reduced the occurrence of these large bulging cells and the layers were more organized and regular. Pollen health was not a problem in this mutant and both non-treated and treated pollen grains looked similar to WT.

The WT ovules showed an onset of large bulging cells in the integument layers with the supplementation of Spd. The embryo sac was not affected and pollen health was not altered. The appearance of larger cells in the regular integument layers after Spd exposure indicated that the cell division rate of WT integument layers is affected. This suggests influence of Spd on cell-cell

communication thereby disrupting the balance leading to mis-communication of signals, in the WT. However, in MTN-deficient mutants (*mtn1-1mtn2-1* and *mtn1-1mtn2-5*) Spd supplementation improved cell-cell communication compared to non-supplemented mutants, suggesting that the exogenously supplied Spd had improved cell-cell communication to regulate cell division and expansion rates.

Adult *mtn1-1mtn2-5* plants are robust and larger than WT. with Spd-supplementation the *mtn1-1mtn2-5* plants display a much larger phenotype. Given the level of residual MTN activity (~28%), the expected phenotype for the *mtn1-1mtn2-5* mutant was of an intermediate between the WT and the more severe *mtn1-1mtn2-1* mutant. However, the growth phenotype and the response of the the *mtn1-1mtn2-5* to Spd was not of an intermediate mutant. This mutant appeared to be better at growth with Spd supplementation than the WT. On the other hand, the more severe *mtn1-1mtn2-1* mutant is delayed in development and is only slightly improved by the treatment. The only genetic difference between the two mutants is the position of the T-DNA insertion. Further experiments need to be conducted to examine the possibility of the positional effect of the mutation on how the two different mutants respond.

Taken together, the above findings support the hypothesis that Spd affects cell-cell communication creating cross talk between previous blocked elements. Further examination of Spd effects on cell communication should be carried out in future using plasmodesmata mutants (eg; Callose biosynthesis mutant: *Cals3*; Sevilem et al., 2013), cell-signaling mutants (Cyclin-dependent kinase 2 mutant: *Cdc2*; Chevalier et al., 2011).

2.4.1.3 **Pollen tube growth is improved by Spd supplementation of the *mtn1-1mtn2-1* mutants**

The *mtn1-1mtn2-1* stigma is not as receptive to pollen, as evidenced by very little pollen adherence as compared to WT stigmas following hand pollination in the research reported in this thesis. In selfed *mtn1-1mtn2-1* flowers pollen adhesion is compromised. This maybe not only due to stigmatic properties, but also attributed to pollen properties as well (Edlund et al., 2004). When WT pollen was applied to the mutant stigma, the pollen did adhere better, but still some empty areas were observed. It is possible that these bare areas were non-receptive to pollen, suggesting that the *MTN* mutant stigma has pollen receptivity issues. The stigmatic papillae were bent and deformed when observed through the microscope which leads to low receptivity to pollen (data not shown).

Pollen germination on the stigma occurs in three steps (Edlund et al, 2004; Wang et al., 2010). The initial step is hydration, where the pollen grain adsorbs water molecules from the papillae, the next step is cell-cell communication between the pollen grain and stigmatic papillae, and the final step is pollen tube germination. If the hydration or cell-cell communication does not occur properly, the pollen tube germination does not take place (Edlund et al., 2004; Wang et al., 2010). The adherence of WT pollen to the mutant papillae shows that the primary problem does not lie with the stigma, but with the pollen grains of the mutant. However, the *mtn1-1mtn2-1* mutant stigmas are stubby and have twisted and bent stigmatic papillae, indicating that stigmatic properties are problematic as well. Spd treatment of the *mtn1-1mtn2-1* mutant show improved stigma with improved pollen germination. Better stigmatic papillae was observed through

microscopic observation, however, this improvement was not universal, as many stigmas with mis-shaped and bent stigmatic papillae could also be observed. Mutant pollen (*mtn1-1mtn2-1*) applied on WT stigma did not adhere properly and did not germinate well, indicating that mutant pollen are abnormal. Spd-treated *mtn1-1mtn2-1* plant pollen showed significant improvement in adherence and germination on both selfed and WT stigmas. Embedded sections of Spd-treated *mtn1-1mtn2-1* plant anthers showed improved pollen health. This is evidence that the Spd does improve pollen and stigma properties, both during development of the reproductive tissue as well as during cell-cell communication. The G3 pollen from both Spd-treated plants and non-treated plants applied to G3 stigmas had good adherence. Aniline blue stating showed guided pollen tube growth towards the ovules. These results suggest transgenerational improvement of pollen viability in response to Spd supplementation.

2.4.2 **Effect of Spd on abnormal vascular arrangement of MTN-deficient mutants**

2.4.2.1 **Spd restores the arrangement of the vascular bundles of the MTN-deficient mutants**

In response to Spd supplementation, a significant ($p<0.05$) reduction in the number of vascular bundles in the *mtn1-1mtn2-5* mutant (10±2 versus 7±2) and the *mtn1-1mtn2-1* mutant and slight improvement in the irregular arrangement of the vascular bundles of the *mtn1-1mtn2-1* mutant were detected in stems (Figure 2-14). However, the recovery of the vascular pattern was still not as close to WT as expected. Recycling of MTA by MTN is essential for normal vascular development in *A. thaliana*. The MTN-deficient double mutants (*mtn1-1mtn2-1*) retain only about 14% of MTN enzyme activity (Waduwara-Jayabahu et al., 2012). The inadequate recovery of the vascular pattern observed in this study suggests that the concentration of 100 µM of Spd

was not sufficient to completely overcome the effects of MTN-deficiency. The plant vascular system is established at embryonic developmental stages (Foster et al., 1952). Vascular patterning (apical/basal in stems and root; reticulate in leaves) is governed by a tightly controlled hormonal balance between auxin and cytokinin (Turner and Sieburth, 2003). The determination of cell fate during the differentiation of primary cells to tissue specific cell types is facilitated by PAT and CAT (Bennett et al., 2016). Signals brought over by PAT are communicated to the surrounding cell via CAT (Bennett et al., 2016). Cell-to-cell communication is important during determination of cell fate, as early as embryonic development, as the primary meristem tissues are established at the early embryo stage (Hove et al., 2015). Disrupted or mis-regulated hormone homeostasis during early embryonic development may lead to mis-identity of cells in the meristematic tissue, which will lead to developmental defects at later growth (Chevalier et al., 2011; Hove et al., 2015). The abnormal vascular patterning (asymmetrical arrangement and higher number of vascular bundles) of the naïve *mtn1-1mtn2-1* mutant might be attributed to problems related to cell-cell communication (Notaguchi & Okamoto, 2015) and problematic hormone homeostasis (Hove et al., 2015). Thus, the observed reduction in the number of vascular bundles and arrangement in Spd supplemented developing seedlings suggests possible improvement in cell-cell communication, cross talk between PAT and CAT and hormonal balance attributed to Spd supplementation.

The restoration of fertility to random branches in the G1 plants did not appear to follow any discernable pattern. However, this randomness maybe explained by comparing available literature on *A. thaliana BRANCHED1* mutants (*BRC1*) (Aguilar-Martínez, et al., 2007). The

BRC1 is expressed in axillary buds. The expression of *BRC1* inhibits the axillary buds from growing. Studies have shown that *BRC1* acts within the buds to control bud development signals and is mediated by auxin induced apical dominance (Aguilar-Martínez, et al., 2007). If the impaired auxin transport of the *mtn1-1mtn2-1* mutant is at least partially rescued by Spd, then certain axillary buds might break free from the apical dominance, thus grow out and bear fruits. However, since the mutants have many underlying problems as well, this alone would not be sufficient for a full recovery of fertility. Therefore, the restoration for fertility in the G1 is partial and completely random. Spd is the precursor of two other polyamines, Spm and Tspm. Furthermore, documented evidence indicates that the Tspm synthase gene *ACL5* is required for proper xylem formation is induced by auxin (Hanzawa et al., 1997). The *ACL5* mutant *tkv* and the *bud2* mutant both have altered vascular development and have stunted growth (Carlsbecker et al., 2010; Cui et al., 2010; Baima et al., 2014). The slight recovery of the vascular bundle arrangement as well as the reduction of the vascular bundle number may be at least in part attributed to Tspm synthase activity by Spd supplementation. This is only a speculation because Tspm activity was not measured during this research.

One of the key functions of Spd is the activation of the eukaryotic translation initiation factor 5A (eIF5A). Under Spd-limiting conditions, activation of eIF5A takes place in an availability-dependent manner (Chattopadhyay et al., 2003; Chattopadhyay et al., 2008; Kang and Hershey, 1994; Nishimura et al., 2005). Eukaryotic translation initiation factor 5A is reported to play a role in protoxylem development in *A. thaliana* (Ren et al., 2013). The involvement of Spd in eIF5A activation and the observed improvement in vascular development cannot be excluded. As suggested earlier in the discussion, exogenously supplemented Spd could be conjugated (Alcázar

et al., 2011) and later released within the plant during maturity. The release of conjugated Spd might not be properly controlled in the *mtn1-1mtn2-1* mutant due to problems related to cell signaling. Future research could be carried out using Spd-conjugate mutants and eIF5A mutants in the MTN-deficient backgrounds (*mtn1-1mtn2-1* and *mtn1-1mtn2-5*) to examine how Spd feeding during early development could affect fertility restoration in random branches upon maturity.

2.4.2.2 **Response of plant growth to Spd-supplementation**

The *mtn1-1mtn2-5*mutant is always larger than WT, with a greater stem diameter (4±1 mm *vs* 2.5±1 mm). In response to the Spd treatment, the *mtn1-1mtn2-5* mutant plants became even larger in size and taller and more robust compared WT (Figure 2-12). The *mtn1-1mtn2-5* mutant plants were expected to have an intermediate growth between the WT and the severe *mtn1-1mtn2-1* mutant, because the *mtn1-1mtn2-5* mutant has ~28% residual MTN activity; higher than *mtn1-1mtn2-1* (~14% residual MTN activity. The larger size of *mtn1-1mtn2-5* plants in response to Spd cannot be directly explained, but if linked to fertility, it could be connected with eIF5A. Spd is required for eIF5A activation (Chattopadhyay et al., 2008), and eIF5A overexpression mutants have increased fertility and larger sizes such as taller plants and broader leaves (Liu et al., 2008). Tassoni et al. (2000), reports a 30% increase in leaf mass in the adult plant, when *A. thaliana* seeds were grown on solid media supplemented with 0.5 mM Spd. Preliminary experiments were conducted to assess the levels of active and inactive eIF5a isoforms in crude protein extracts of 10-day-old seedlings +/- Spd. The results of these experiments were inconclusive, with issues related to instability of the extracted eIF5a isoforms and inconsistencies

in the western blots (personal communication with Maye Saechao). Although the Spd-treated *mtn1-1mtn2-1* plants did not become larger compared to the non-treated plants, improved fertility is a very significant effect that can be related to eIF5A. It is possible that sampling whole seedlings that were 10-days-old were not ideal. Total protein extract from whole seedlings will not produce tissue specific expression values, but rather an overall value. The fertility restoration occurs in the reproductive tissue of the mature plants. In the pilot experiment by Waduwara-Jayabahu (2011), PA droplets were applied to the floral meristem of the *mtn1-1mtn2-1* mutants. Examination of eiF5A levels in floral buds could be the next step to further investigate whether the Spd mediated fertility restoration is mediated through eIF5A. Measuring eIF5A levels in the mutants, with and without Spd treatment as well as measuring eIF5A levels in both restored and non-restored branches could be a starting point.

2.4.2.3 **Spd-mediated restoration of vascular bundle arrangement is transgenerational**

The subsequent generations of the Spd-treated *mtn1-1mtn2-1* mutant (G2, G3 etc) were phenotypically similar to WT as compared to non-treated *mtn1-1mtn2-1*. However, the G2 and G3 still displayed some of the abnormalities of the non-treated *mtn1-1mtn2-1* parent (i.e., fasciation in the stems / branches, twisted rosette leaves, delayed reproductive transition). To test the hypothesis of transgenerational effect of Spd-mediated improvement of vascular bundle arrangement, stem cross sections of G2 and G3 plants were examined. It was clear that the effect of Spd on vasculature is transgenerational; i.e. the transgenerational improvement was cumulative as fertility improved. The vascular bundle arrangement in the G3 was greatly

improved compared to G1 plants, but G2, the immediate progeny of the G1 plants were not as restored as G3.

The Spd effect on the G1 plants is reflected on the G2 and G3 generations suggesting an epigenetic basis for this effect. This can be simply explained as, the parent is exposed to intrinsic or extrinsic factors that affect metabolic and hormonal regulatory processes (Hauser et al., 2011). The seeds develop in the maternal environment and are subjected to maternal hormonal imbalances and this may play a role in the development of the offspring. Induction of epigenetic genes and the inheritance of increased genetic variability are observed in organisms with reduced genome stability. Such inheritance and inductions occur as a response to environmental variables (Lamke and Baurle, 2017). Plants utilize this phenomenon, for adaptation to altered, adverse conditions (Rakyan et al., 2003; Hauser et al., 2011). Epigenetic regulation of chromatin architecture modification to promote expression of specific genes and stress memory facilitates plant to combat and overcome stress exposure (Banerjee and Roychoudhury, 2017). Conventional thinking assumes that a phenotype of an organism is primarily determined by its genetic inheritance and specific environmental factors (Rakyan et al., 2003). However, this thinking is challenged simply by the presence of many examples where incomplete penetrance and variable expressivity cannot be explained by simple genetic inheritance and environmental heterogeneity (Rakyan et al., 2003; Hauser et al., 2011).

The pleotropic phenotype of the MTN-deficient mutants is attributed to the over-accumulation of MTA within the plant due to the MTN mutations (Waduwara-Jayabahu et al., 2012). The Met recycling pathway and other related pathways (PA, NA and ethylene biosynthesis) is affected by

the over-accumulation of MTA, due to lack of MTN activity and the feedback inhibition of synthase enzymes by MTA (Burstenbinder et al., 2010; Waduwara-Jayabahu et al., 2012). Because of the impaired Met recycling in the MTN-deficient plant due to the *MTN* gene mutations and accumulation of MTA, it is possible that the Met requirement for methylation reactions in the plant is not fulfilled completely. To our understanding DNA methylation and histone modification controls the epigenetic state of genes. During plant development, these epigenetic pathways are perturbed and produce developmental phenotypes (Feng et al., 2010). In the *mtn1-1mtn2-1* mutant background, when the G_0 parent (naïve *mtn1-1mtn2-1*) is exposed to Spd during its initial growth, the whole plant is affected and at maturity, the maternal environment is different from that of a non-treated plant. The G1 generation develops in this altered maternal environment. When the G1 plants reach maturity and produce seeds, the maternal environment is different from the G_0 conditions as the parent was exposed to the exogenous Spd. Although all these subsequent generations are genotypically identical to the initial untreated parent (*mtn1-1mtn2-1*), these later generations show incremental improvements reflecting an altered epigenetic status due to the exposure to exogenous supply of Spd. Plants are experts at adapting to unfavorable environmental conditions. The Spd treated *mtn1-1mtn2-1* mutant and its later generations could be an example of when plants try to fix an intrinsic problem with environmental factors. The MTN-deficient mutant had developmental problems. Upon exposure to an abundance of Spd, a polyamine that was not produced properly due to the mutation, the plant tried to correct itself. Once successful, these new alterations that were made were carried forward to the next generation epigenetically, to ensure better growth and survival.

2.4.1 **Effect of Spd on auxin distribution and cell fate determination**

2.4.1.1 **Spd supplementation to MTN-deficient parent plants improves auxin distribution in the embryos**

Auxin moves from the shoot apical meristem through the plant via active polar auxin transport. This mobility produces a gradient of available auxin in tissues which triggers specific gene expression and biological processes that respond to auxin (Spicer et al, 2013; Michniewicz et al, 2007). The auxin flow through the procambial cells in the embryo is responsible for activating these cells to differentiate into xylem cells via AtHB8 expression (Baima et al., 2001). Problems in the auxin flow may produce an abnormal gradient, resulting in improper activation of procambial cells (Baima et al., 2001, 2004). Thus examining the auxin flow within the embryos was carried out as the next step of the research.

The synthetic auxin response reporter DR5::GFP was introduced to the mutant backgrounds *mtn1-1mtn2-1* and *mtn1-1mtn2-5* (Waduwara-Jayabahu, 2011). This reporter leads to GFP fluorescence when auxin is present. A preliminary examination of the AtHB8 expression in the embryos from a heterozygous MTN-deficient mutant (*MTN1-1mtn1-1mtn2-1mtn2-1*) was carried out at the Moffatt lab by Shuningbo Ye (2013). The embryos were excised from a mutant line carrying the *AtHB8*::GUS reporter. The excised embryos had disrupted procambial cell activation of varying degree. The embryos were not genotypically identified therefore the results were inconclusive (Shuningbo Ye, 2013). The DR5*rev*::GFP reporter expression level is a qualitative indication of the auxin distribution and does not reflect the actual auxin concentration in a given tissue. WT plants carrying the reporter were used as a control in our study for

comparison of DR5*rev*::GFP expression pattern. The typical pattern for the DR5 reporter in developing heart and torpedo stage embryos was very strong at the hypophysis, the future root apical meristem and the future cotyledon tips (Figure 2-16). The central column of cells, leading to the cotyledon tips appear fluorescent, as the auxin is mobilized towards the root end of the embryo, through the central column of cells from the cotyledon tips.

The expression pattern of the DR5*rev*::GFP reporter is dependent on the available auxin of the tissue (Ulmasov et al., 1997; Zhou et al., 2014). The embryos having a normal auxin distribution will show typical DR5 expression pattern as observed in the WT embryos with and without Spd treatment. The low intensity of fluorescence at the cotyledon tips of the mtn1-1mtn2-5 mutant is an indication of low auxin in these regions of the embryo.

The barely visible expression at the cotyledon tips of the more severe *mtn1-1mtn2-1* indicates that this mutant has very low auxin flow to the cotyledon tips, than to the *mtn1-1mtn2-5* mutant. Further, this mutant has a dispersed fluorescent pattern at the future root tip region, where additional cells show reporter expression, suggesting that the auxin is not being distributed normally. The Spd treatment improves the expression pattern of both mutants, indicating the possibility of Spd rectifying the auxin mobilization issue in the mutant. This result is supported by the increased expression level at the cotyledons in both mutant types as well as the more restricted and WT-like expression at the root tip region of the *mtn1-1mtn2-1* mutant embryos (Figure 2-16).

The auxin mobility model proposed by Dengler et al. (2006) explains auxin movement and re-distribution within the plant in association with PIN proteins and the SAM. The auxin produced

by the SAM, is mobilized by the PIN proteins. The PINs re-distribute to align in a fashion to connect the cells forming the procambium (Dengler et al., 2006). It is possible that the Spd is affecting PIN mobility in the mutant allowing better auxin mobility. Further experiments need to be carried out to examine PIN protein positioning and PIN gene activation in the MTN-deficient mutant backgrounds with Spd supplementation.

2.4.1.2 **Monopteros reporter expression confirms the improvement of auxin distribution in embryos of Spd supplemented plants**

Auxin is involved in regulating many genes in growth and development; the activation of the *AtHB8* gene is preceded by the activation of *MP*. The transcription of the *MP* gene is activated by the auxin gradient in the cells; the production of MP in-turn activates *AtHB8* gene expression in the procambial cells to produce xylem vessels (Hardtke et al., 1998; Schlereth et al., 2010). Since activation of *MP* is dependent on the available auxin gradient, the reporter expression can be seen in all cells in which auxin is present at the given time. The result of the *MP* reporter confirmed the auxin changes indicated by the DR5 and *AtHB8* reporter expression.

The supplementation of 100 µM of Spd for 14 days after germination shows a marked improvement in auxin distribution patterns and subsequent activation of auxin dependent genes. The *mtn1-1mtn2-5* mutant showed greater improvement in MP;:n3GFP reporter expression with the Spd supplementation, possibly due to less problems in auxin distribution than *mtn1-1mtn2-1*. The *mtn1-1mtn2-1* mutant had more problematic auxin flow and vascular patterning related issues, which were only partially recovered by the treatment. One reason for this could be the interlinking of most hormone dependent pathways with other regulatory pathways. The Spd

supplementation may recover the auxin distribution to a certain extent but auxin movement alone is dependent on many other factors, such as PIN localization (Galweiler et al., 1998; Dengler et al., 2006), feedback of MP activation, environmental factors, maternal factors etc.

2.4.1.3 **Procambial cell activation in the MTN-deficient mutant embryos is improved by Spd supplementation to the parent**

The activation of the procambial cells is dependent on the auxin gradient within the embryo (Baima et al., 1995; Baima et al., 2001). The mis-activation of the procambial cells can be caused by improper auxin flow producing an unbalanced auxin gradient. The expression pattern of the *AtHB8*-NUC::YFP reporter in the MTN-deficient mutants showed that the procambial cell activation was not normal. In the mutant embryo certain regions (near the future cotyledons) where YFP reporter expression was expected failed to show anticipated expression. For example, the number of procambial cells that were activated towards the cotyledon tips, was low and in some embryos there were none to be seen.. These evidences indicate that procambial cells have not been properly activated. Waduwara-Jayabahu et al. (2012) demonstrated auxin transport issues in the adult plant. This suggests that the *mtn1-1mtn2-1* mutants have auxin mobility problems even at the embryonic stage. The Spd treatment showed an improvement of YFP reporter expression pattern in both MTN-deficient mutants (*mtn1-1mtn2-1* and *mtn1-1mtn2*-5) consistent with an improvement in auxin distribution. The *mtn1-1mtn2-5* mutant which is the closest to WT in *AtHB8* expression in procambial cells had an increased number of cells activated with the Spd treatment. The improvements found in vascular tissue with respect to the bundle arrangement and number related to auxin mobility, are further confirmed by this embryo vascular pattern improvement (Scarpella et al., 2004, 2006).

The AtHB8-NUC::YFP reporter expression is seen in procambial cells that are activated by auxin flow (Baima et al., 2001). Therefore, to explain the improved expression of the YFP reporter (i.e., the activation of procambial cells) auxin response reporters were examined in this research. Determination of future vascular tissue arrangement is laid down at embryo development, as early as heart stage (Ohashi-Ito & Fukuda, 2010; Hove et al., 2015). The mis-activation or non-activation of vascular precursors at these early stages of the mutant could be what is reflected in the vascular arrangement in the maturing plants. The adult mutant is known to have auxin mobility related problems (Waduwara-Jayabahu, 2011), and vascular tissue determination is one of the many aspects of auxin.

2.5 **Future directions**

2.5.1 **Abnormal fertility of decapitated branches of Spd-treated *mtn1-1mtn2-1* mutants**

A fascinating observation was made by Dr. Barbara Moffatt, when examining decapitated branches of Spd-treated *mtn1-1mtn2-1* mutant plants (G1). These plants were grown to collect floral buds for RNA-seq analysis. Once the buds were collected from the *mtn1-1mtn2-1* (G1) plants, the plants were allowed to continue growing in order to collect tissue for further experiments. The decapitated branches of both non-treated (½ MS) and Spd-treated plants showed fertile, expanded filled in siliques (Appendix II; Figure 2-20).

When an angiosperm is decapitated, lateral bud activation and shoot branching occur due to the removal of apical dominance that is maintained by the auxin flow from the SAM (Dun et al., 2006). In *A. thaliana*, the growth and elongation of the axillary buds at rosette nodes is restricted by floral transition of the plant (Dun et al., 2006).

There are several hypotheses proposed to explain apical dominance over branching / axillary bud development. The majority of evidence from apical dominance studies supports the classical hypothesis of auxin control over axillary bud growth (Li et al., 1995; Dun et al., 2006). The classical hypothesis suggests that the decapitation of the apical portion of the plant increases CK release to axillary buds (Turnbull et al., 1997). The other hypothesis is the auxin transport hypothesis (Dun et al., 2006). In this hypothesis, a more qualitative rather than quantitative effect of auxin on the axillary bud activation is assumed. The auxin is proposed to be mobilized in a stream from the apical tip, basipetally via PAT (Dun et al., 2006). When the apical meristem is present, this mobility stream is thought to be "fully loaded" thereby limiting the auxin to axillary buds, establishing apical dominance. The removal of the apical meristem, would hypothetically remove apical dominance in this scenario. The third hypothesis that is widely tested is the bud transition hypothesis. The assumptions of this hypothesis are that the buds can remain in one of three stages; the buds have a dormant period, the buds move to a stage of transition or the buds enter a sustained growth stage (Napoli et al., 1999; Beveridge, 2006). Feedback regulation is also proposed as a way of explaining apical dominance and axillary bud initiation. Hormonal homeostasis in plants is tightly regulated by feedback signals (Beveridge, 2006; Dunet al., 2006). Studies in *A. thaliana* shoot branching mutant *MAX1* (Stirnberg et al., 2002) flavonoid levels

suggest associations of flavonoids with auxin transport. It has been reported that some flavonoids reduce auxin transport in Zuccini (Jacobs and Rubery, 1988).

It is possible that a similar phenomenon has occurred in these decapitated plants (Appendix II, Figure 2-20). The removal of floral bud from the tip of the branch would have removed the apical dominance via one of the proposed mechanisms, allowing auxin synthesis and mobility from lower lateral nodes. This would have facilitated the improvement of cell-to-cell communication and thus, transport thereby creating fertile siliques below the decapitation line. The improvement of cell-cell communication could be attributed to the Spd supplementation as the Spd treated plants had larger and fuller siliques compared to the non-treated plants.

2.5.2 **Anomalous callose degradation in *mtn1-1mtn2-1* anthers**

Upon examination of reproductive organs of the *mtn1-1mtn2-1* mutant, residual callose deposits were seen in mature anthers and in unexpected anther cell layers (Appendix III, Figure 2-21). During microspore development, callose is generated by the microspore mother cell. Upon pollen maturity, callase enzyme is secreted by the tapetum to breakdown the callose surrounding the pollen grains, to facilitate pollen release (Winiarczyk et al., 2012; McCormick, 2004). Preliminary observations of aniline blue stained sections of embedded *mtn1-1mtn2-1* anthers show callose deposition during initial microspore development (Appendix III, Figure 2-21). However, the degeneration of callose at the end of pollen maturity did not occur properly. Close examination of the sectioned anthers revealed that the tapetum of the *mtn1-1mtn2-1* mutant becomes abnormal with maturity, having highly vacuolated cells. This is detrimental to pollen health. The aniline stained sections show that the callose deposition in the anther chamber is also

unusual. The callose is only supposed to be present in the anther chamber, surrounding the pollen grains, however, in some extreme cases, the callose was seen on the anther wall, next to the tapetum, which is highly unusual.

Phytohormones auxin and JA as well as flavonoids are associated with root and shoot growth, seed and pollen development as well as anther dehiscence (Thompson et al., 2010). The inability of the *mtn1-1mtn2-1* mutant anther to dehisce, the possible tapetum issues related to callose breakdown and abnormal callose deposition within the anthers could be explained by the impaired auxin mobility and high JA levels (Waduwara Jayabahu et al., 2012) in the mutant. Testing of JA levels with Spd supplementation as well as detailed examination of callose deposition and breakdown in the *mtn1-1mtn2-1* mutant should be carried out in future research.

2.5.3 **Response of CK to Spd supplementation**

In addition to examining the embryo stages, as a pilot experiment, the root tips of seven-day-old seedlings (WT, *mtn1-1mtn2-1* and *mtn1-1mtn2-5*) grown on Spd supplemented media were examined to assess CK responsive expression in root meristems in the presence of Spd. The CK reporter TCSn::GFP (Zürcher et al., 2013) was used in this preliminary experiment.

The TCSn::GFP reporter expression in developing roots show increased levels in the presence of Spd overall. The WT and *mtn1-1mtn2-5* mutant (n = 5 each) had higher TCSn::GFP expression compared to the *mtn1-1mtn2-1* mutant with no treatment (n= 6), but the levels of expression in the *mtn1-1mtn2-5* mutant roots was less than WT. Variation of the intensity levels was observed in all roots with and without Spd-treatment. The expression level of the TSCn::GFP reporter in

the Spd-treated *mtn1-1mtn2-1* mutant roots (n=6) was less than the non-Spd-treated *mtn1-1mtn2-1* mutant roots (n=7), which was the opposite of WT and *mtn1-1mtn2-5* expression pattern in the roots. (Appendix VII, Figure 2-28). This was different from what was expected. However the expression pattern was similar to the publication by Liu and Muller (2017), with lower fluorescence intensity at the root tip and the vascular column. This observation was fascinating and presented more questions regarding the behavior of the *mtn1-1mtn2*-5 mutant. The findings presented earlier in this thesis indicated that even though the expected response of the *mtn1-1mtn2-5* to treatment was and intermediate between WT and the severe *mtn1-1mtn2-1* mutant, the *mtn1-1mtn2-5* does not always behave as such. Further investigations in to how the positional effect of the mutation in the *mtn1-1mtn2-5* mutant affects the plants' response to treatment should be carried out. However, the finding of this pilot study is preliminary and insufficient to draw any significant conclusions. A larger sample size needs to be analyzed to obtain a baseline of the TCSn::GFP expression intensity for future experiments.

References

Adams, D. O., & Yang, S. F. (1979). Ethylene biosynthesis: Identification of 1-aminocyclopropane-1-carboxylic acid as an intermediate in the conversion of methionine to ethylene. *Proceedings of the National Academy of Sciences of the United States of America*, *76*(1), 170–174. Retrieved from https://www.ncbi.nlm.nih.gov/pmc/articles/PMC382898/

Aguilar-Martínez, J. A., Poza-Carrión, C., & Cubas, P. (2007). Arabidopsis BRANCHED1 Acts as an Integrator of Branching Signals within Axillary Buds. *The Plant Cell*, *19*(2), 458–472. https://doi.org/10.1105/tpc.106.048934

Albers, E. (2009). Metabolic characteristics and importance of the universal methionine salvage pathway recycling methionine from 5′-methylthioadenosine. *IUBMB Life, 61*(12), 1132-1142. doi: 10.1002/iub.278

Alcázar, R., & Tiburcio, A. F. (2014). Plant polyamines in stress and development: an emerging area of research in plant sciences. *Frontiers in Plant Science, 5*. https://doi.org/10.3389/fpls.2014.00319

Alcázar, R., Bitrián, M., Bartels, D., Koncz, C., Altabella, T., & Tiburcio, A. F. (2011). Polyamine metabolic canalization in response to drought stress in Arabidopsis and the resurrection plant Craterostigma plantagineum. *Plant Signaling & Behavior*, *6*(2), 243–250. https://doi.org/10.4161/psb.6.2.14317

Alonso-Blanco, C., Andrade, J., Becker, C., Bemm, F., Bergelson, J., Borgwardt, K. M., . . . Zhou, X. (2016). 1,135 Genomes Reveal the Global Pattern of Polymorphism in Arabidopsis thaliana. *Cell, 166*(2), 481-491. doi: 10.1016/j.cell.2016.05.063

Al-Shehbaz, I. A., & O'Kane, S. L. (2002). Taxonomy and Phylogeny of Arabidopsis (Brassicaceae). *The Arabidopsis Book / American Society of Plant Biologists*, *1*. https://doi.org/10.1199/tab.0001

Amijima, M., Iwata, Y., Koizumi, N., & Mishiba, K.I. (2014). The polar auxin transport inhibitor TIBA inhibits endoreduplication in dark grown spinach hypocotyls. *Plant Science: An International Journal of Experimental Plant Biology*, *225*, 45–51. https://doi.org/10.1016/j.plantsci.2014.05.007

Amir, R., Hacham, Y., & Galili, G. (2002). Cystathionine γ-synthase and threonine synthase operate in concert to regulate carbon flow towards methionine in plants. *Trends in Plant Science*, *7*(4), 153–156. https://doi.org/10.1016/S1360-1385(02)02227-6

Armengot, L., Marquès-Bueno, M. M., & Jaillais, Y. (2016). Regulation of polar auxin transport by protein and lipid kinases. *Journal of Experimental Botany*, *67*(14), 4015–4037. https://doi.org/10.1093/jxb/erw216

Bagni, N., & Serafini-Fracassini, D. (1985). Involvement of polyamines in the mechanism of break of dormancy in Helianthus tuberosus. *Bulletin de La Société Botanique de France. Actualités Botaniques*, *132*(1), 119–125. https://doi.org/10.1080/01811789.1985.10826718

Baima, S., Forte, V., Possenti, M., Peñalosa, A., Leoni, G., Salvi, S., … Morelli, G. (2014). Negative Feedback Regulation of Auxin Signaling by ATHB8/ACL5–BUD2 Transcription Module. *Molecular Plant*, *7*(6), 1006–1025. https://doi.org/10.1093/mp/ssu051

Baima, S., Nobili, F., Sessa, G., Lucchetti, S., Ruberti, I., & Morelli, G. (1995). The expression of the Athb-8 homeobox gene is restricted to provascular cells in Arabidopsis

thaliana. *Development*, *121*(12), 4171–4182. Retrieved from http://dev.biologists.org/content/121/12/4171

Baima, S., Possenti, M., Matteucci, A., Wisman, E., Altamura, M. M., Ruberti, I., & Morelli, G. (2001). The Arabidopsis ATHB-8 HD-zip protein acts as a differentiation-promoting transcription factor of the vascular meristems. *Plant Physiol*, *126*(2), 643-655. doi: 10.1104/pp.126.2.643

Banerjee, A., & Roychoudhury, A. (2017). Epigenetic regulation during salinity and drought stress in plants: Histone modifications and DNA methylation. *Plant Gene*, *11*, 199–204. https://doi.org/10.1016/j.plgene.2017.05.011

Bedford, M. T., & Clarke, S. G. (2009). Protein Arginine Methylation in Mammals: Who, What, and Why. *Mol Cell*, *33*(1), 1-13. doi: 10.1016/j.molcel.2008.12.013

Belda-Palazón, B., Almendáriz, C., Martí, E., Carbonell, J., & Ferrando, A. (2016). Relevance of the Axis Spermidine/eIF5A for Plant Growth and Development. *Frontiers in Plant Science*, *7*. https://doi.org/10.3389/fpls.2016.00245

Benjamins, R., Quint, A., Weijers, D., Hooykaas, P., & Offringa, R. (2001). The PINOID protein kinase regulates organ development in Arabidopsis by enhancing polar auxin transport. *Development*, *128*(20), 4057–4067. Retrieved from http://dev.biologists.org/content/128/20/4057

Bennett, T., Hines, G., van Rongen, M., Waldie, T., Sawchuk, M. G., Scarpella, E., . . . Leyser, O. (2016). Connective Auxin Transport in the Shoot Facilitates Communication between Shoot Apices. *PLoS Biol*, *14*(4), e1002446. doi: 10.1371/journal.pbio.1002446

Berkel, K. van, Boer, R. J. de, Scheres, B., & Tusscher, K. ten. (2013). Polar auxin transport: models and mechanisms. *Development*, *140*(11), 2253–2268. https://doi.org/10.1242/dev.079111

Berleth, T., & Jurgens, G. (1993). The role of the monopteros gene in organising the basal body region of the Arabidopsis embryo. *Development*, *118*(2), 575–587. Retrieved from http://dev.biologists.org/content/118/2/575

Beveridge, C. A. (2006). Axillary bud outgrowth: sending a message. *Current Opinion in Plant Biology*, *9*(1), 35–40. https://doi.org/10.1016/j.pbi.2005.11.006

Boyes, D. C., Zayed, A. M., Ascenzi, R., McCaskill, A. J., Hoffman, N. E., Davis, K. R., & Görlach, J. (2001). Growth stage-based phenotypic analysis of Arabidopsis: a model for high throughput functional genomics in plants. *The Plant Cell*, *13*(7), 1499–1510.

Breuninger, H., Rikirsch, E., Hermann, M., Ueda, M., & Laux, T. (2008). Differential Expression of WOX Genes Mediates Apical-Basal Axis Formation in the Arabidopsis Embryo. *Developmental Cell*, *14*(6), 867–876. https://doi.org/10.1016/j.devcel.2008.03.008

Brunoud, G., Wells, D. M., Oliva, M., Larrieu, A., Mirabet, V., Burrow, A. H., … Vernoux, T. (2012). A novel sensor to map auxin response and distribution at high spatio-temporal resolution. *Nature*, *482*(7383), 103–106. https://doi.org/10.1038/nature10791

Burstenbinder, K., Rzewuski, G., Wirtz, M., Hell, R., & Sauter, M. (2007). The role of methionine recycling for ethylene synthesis in Arabidopsis. *The Plant Journal: For Cell and Molecular Biology*, *49*(2), 238–249. https://doi.org/10.1111/j.1365-313X.2006.02942.x

Burstenbinder, K., Waduwara, I., Schoor, S., Moffatt, B. A., Wirtz, M., Minocha, S. C., . . . Sauter, M. (2010). Inhibition of 5'-methylthioadenosine metabolism in the Yang cycle alters polyamine

levels, and impairs seedling growth and reproduction in Arabidopsis. *Plant J*, *62*(6), 977-988. doi: 10.1111/j.1365-313X.2010.04211.x

Carland, F. M., & McHale, N. A. (1996). LOP1: a gene involved in auxin transport and vascular patterning in Arabidopsis. *Development (Cambridge, England)*, *122*(6), 1811–1819.

Carlsbecker, A., Lee, J.-Y., Roberts, C. J., Dettmer, J., Lehesranta, S., Zhou, J., … Benfey, P. N. (2010). Cell signalling by microRNA165/6 directs gene dose-dependent root cell fate. *Nature*, *465*(7296), 316–321. https://doi.org/10.1038/nature08977

Chattopadhyay, M. K., Park, M. H., & Tabor, H. (2008). Hypusine modification for growth is the major function of spermidine in Saccharomyces cerevisiae polyamine auxotrophs grown in limiting spermidine. *Proceedings of the National Academy of Sciences of the United States of America*, *105*(18), 6554–6559. https://doi.org/10.1073/pnas.0710970105

Chattopadhyay, M. K., Tabor, C. W., & Tabor, H. (2003). Spermidine but not spermine is essential for hypusine biosynthesis and growth in Saccharomyces cerevisiae: Spermine is converted to spermidine in vivo by the FMS1-amine oxidase. *Proc Natl Acad Sci U S A*, *100*(24), 13869-13874.

Chevalier, É., Loubert- Hudon, A., Zimmerman, E. L., & Matton, D. P. (2011). Cell–cell communication and signalling pathways within the ovule: from its inception to fertilization. *New Phytologist*, *192*(1), 13–28. https://doi.org/10.1111/j.1469-8137.2011.03836.x

Chou, H. Y., Lin, Y. H., Shiu, G. L., Tang, H. Y., Cheng, M. L., Shiao, M. S., & Pai, L. M. (2014). ADI1, a methionine salvage pathway enzyme, is required for Drosophila fecundity. *Journal of Biomedical Science*, 21, 64. https://doi.org/10.1186/s12929-014-0064-4

Clay, N. K., & Nelson, T. (2005). Arabidopsis thickvein Mutation Affects Vein Thickness and Organ Vascularization, and Resides in a Provascular Cell-Specific Spermine Synthase Involved in Vein Definition and in Polar Auxin Transport. *Plant Physiology*, *138*(2), 767–777. https://doi.org/10.1104/pp.104.055756

Cnops, G., Wang, X., Linstead, P., Montagu, M. V., Lijsebettens, M. V., & Dolan, L. (2000). Tornado1 and tornado2 are required for the specification of radial and circumferential pattern in the Arabidopsis root. *Development*, *127*(15), 3385–3394. Retrieved from http://dev.biologists.org/content/127/15/3385

Costanzo, E., Trehin, C., & Vandenbussche, M. (2014). The role of WOX genes in flower development. *Annals of Botany*, *114*(7), 1545–1553. https://doi.org/10.1093/aob/mcu123

Cui, X., Ge, C., Wang, R., Wang, H., Chen, W., Fu, Z., … Wang, Y. (2010). The BUD2 mutation affects plant architecture through altering cytokinin and auxin responses in Arabidopsis. *Cell Research*, *20*(5), 576–586. https://doi.org/10.1038/cr.2010.51

Danchin, A. (2016). Coping with inevitable accidents in metabolism. *Microbial Biotechnology*, *10*(1), 57–72. https://doi.org/10.1111/1751-7915.12461

De Rybel, B., Mähönen, A. P., Helariutta, Y., & Weijers, D. (2016). Plant vascular development: from early specification to differentiation. *Nature Reviews Molecular Cell Biology*, *17*(1), 30–40. https://doi.org/10.1038/nrm.2015.6

Dello Ioio, R., Linhares, F. S., Scacchi, E., Casamitjana-Martinez, E., Heidstra, R., Costantino, P., & Sabatini, S. (2007). Cytokinins determine Arabidopsis root-meristem size by controlling cell

differentiation. *Current Biology: CB*, *17*(8), 678–682. https://doi.org/10.1016/j.cub.2007.02.047

Deng, X., Gu, L., Liu, C., Lu, T., Lu, F., Lu, Z., . . . Cao, X. (2010). Arginine methylation mediated by the Arabidopsis homolog of PRMT5 is essential for proper pre-mRNA splicing. *Proc Natl Acad Sci U S A*, *107*(44), 19114-19119. doi: 10.1073/pnas.1009669107

Dengler, N. G. (2006). The shoot apical meristem and development of vascular architecture. *Canadian Journal of Botany-Revue Canadienne De Botanique*, *84*(11), 1660–1671. https://doi.org/10.1139/B06-126

Dever, T. E., & Ivanov, I. P. (2018). Roles of polyamines in translation. *Journal of Biological Chemistry*, *293*(48), 18719–18729. https://doi.org/10.1074/jbc.TM118.003338

Ding, B., Itaya, A., & Woo, Y.-M. (1999). Plasmodesmata and Cell-to-Cell Communication in Plants. In K. W. Jeon (Ed.), *International Review of Cytology* (Vol. 190, pp. 251–316). Academic Press. https://doi.org/10.1016/S0074-7696(08)62149-X

Dreyfus, C., Lemaire, D., Mari, S., Pignol, D., & Arnoux, P. (2009). Crystallographic snapshots of iterative substrate translocations during nicotianamine synthesis in Archaea. *Proc Natl Acad Sci U S A*, *106*(38), 16180-16184. doi: 10.1073/pnas.0904439106

Droux, M. (2004). Sulfur assimilation and the role of sulfur in plant metabolism: a survey. *Photosynthesis Research*, *79*(3), 331–348. https://doi.org/10.1023/B:PRES.0000017196.95499.11

Dun, E. A., Ferguson, B. J., & Beveridge, C. A. (2006). Apical Dominance and Shoot Branching. Divergent Opinions or Divergent Mechanisms? *Plant Physiology*, *142*(3), 812–819. https://doi.org/10.1104/pp.106.086868

Edlund, A. F., Swanson, R., & Preuss, D. (2004). Pollen and Stigma Structure and Function: The Role of Diversity in Pollination. *The Plant Cell*, *16*(suppl 1), S84–S97. https://doi.org/10.1105/tpc.015800

Eisenberg, T., Knauer, H., Schauer, A., Buttner, S., Ruckenstuhl, C., Carmona-Gutierrez, D., . . . Madeo, F. (2009). Induction of autophagy by spermidine promotes longevity. *Nat Cell Biol*, *11*(11), 1305-1314. doi: 10.1038/ncb1975

Fan, L. M., Wang, Y. F., Wang, H., & Wu, W. H. (2001). In vitro Arabidopsis pollen germination and characterization of the inward potassium currents in Arabidopsis pollen grain protoplasts. *Journal of Experimental Botany*, *52*(361), 1603–1614. https://doi.org/10.1093/jexbot/52.361.1603

Feng, H., Chen, Q., Feng, J., Zhang, J., Yang, X., & Zuo, J. (2007). Functional Characterization of the Arabidopsis Eukaryotic Translation Initiation Factor 5A-2 That Plays a Crucial Role in Plant Growth and Development by Regulating Cell Division, Cell Growth, and Cell Death. *Plant Physiology*, *144*(3), 1531-1545. doi: 10.1104/pp.107.098079

Fontecave, M., Atta, M., & Mulliez, E. (2004). S-adenosylmethionine: nothing goes to waste. *Trends in Biochemical Sciences*, *29*(5), 243–249. https://doi.org/10.1016/j.tibs.2004.03.007

Foster, R. J., McRae, D. H., & Bonner, J. (1952). Auxin-Induced Growth Inhibition a Natural Consequence of Two-Point Attachment. *Proceedings of the National Academy of Sciences of the United States of America*, *38*(12), 1014–1022. Retrieved from https://www.ncbi.nlm.nih.gov/pmc/articles/PMC1063702/

Friml, J., Vieten, A., Sauer, M., Weijers, D., Schwarz, H., Hamann, T., … Jürgens, G. (2003). Efflux-dependent auxin gradients establish the apical–basal axis of Arabidopsis. *Nature*, *426*(6963), 147–153. https://doi.org/10.1038/nature02085

Frugier, M., Florentz, C., Hosseini, M. W., Lehn, J. M., & Giegé, R. (1994). Synthetic polyamines stimulate in vitro transcription by T7 RNA polymerase. *Nucleic Acids Res, 22*(14), 2784-2790.

Fukuda, H. (2004). Signals that control plant vascular cell differentiation. *Nature Reviews Molecular Cell Biology, 5*, 379. doi: 10.1038/nrm1364

Gallardo, K., Job, C., Groot, S. P. C., Puype, M., Demol, H., Vandekerckhove, J., & Job, D. (2002). Importance of methionine biosynthesis for Arabidopsis seed germination and seedling growth. *Physiologia Plantarum, 116*(2), 238–247

Galweiler, L., Guan, C., Müller, A., Wisman, E., Mendgen, K., Yephremov, A., & Palme, K. (1998). Regulation of Polar Auxin Transport by AtPIN1 in Arabidopsis Vascular Tissue. *Science*, *282*(5397), 2226–2230. https://doi.org/10.1126/science.282.5397.2226

Garcia-Jimenez, P., Rodrigo, M., & Robaina, R. R. (1998). Influence of plant growth regulators, polyamines and glycerol interaction on growth and morphogenesis of carposporelings of Grateloupia cultured in vitro. *Journal of Applied Phycology*, *10*(1), 95-100. doi: 10.1023/a:1008063532233

Gazzarrini, S., Tsuchiya, Y., Lumba, S., Okamoto, M., & McCourt, P. (2004). The Transcription Factor FUSCA3 Controls Developmental Timing in Arabidopsis through the Hormones Gibberellin and Abscisic Acid. *Developmental Cell*, *7*(3), 373–385. https://doi.org/10.1016/j.devcel.2004.06.017

Giglione, C., Vallon, O., & Meinnel, T. (2003). Control of protein life-span by N-terminal methionine excision. *The EMBO Journal*, *22*(1), 13–23. https://doi.org/10.1093/emboj/cdg007

Giovanelli, J., Mudd, S. H., & Datko, A. H. (1985). Quantitative Analysis of Pathways of Methionine Metabolism and Their Regulation in Lemna. *Plant Physiology, 78*(3), 555–560. https://doi.org/10.1104/pp.78.3.555

Goda, H., Sawa, S., Asami, T., Fujioka, S., Shimada, Y., & Yoshida, S. (2004). Comprehensive Comparison of Auxin-Regulated and Brassinosteroid-Regulated Genes in Arabidopsis. *Plant Physiology*, *134*(4), 1555–1573. https://doi.org/10.1104/pp.103.034736

Gray, W. M. (2004). Hormonal Regulation of Plant Growth and Development. *PLoS Biology*, *2*(9). https://doi.org/10.1371/journal.pbio.0020311

Hake, S. (1992). Unraveling the knots in plant development. *Trends in Genetics*, *8*(3), 109–114. https://doi.org/10.1016/0168-9525(92)90199-E

Hamann, T., Benkova, E., Bäurle, I., Kientz, M., & Jürgens, G. (2002). The Arabidopsis BODENLOS gene encodes an auxin response protein inhibiting MONOPTEROS-mediated embryo patterning. *Genes & Development*, *16*(13), 1610–1615. https://doi.org/10.1101/gad.229402

Hanzawa, Y., Takahashi, T., & Komeda, Y. (1997). ACL5: an Arabidopsis gene required for internodal elongation after flowering. *The Plant Journal: For Cell and Molecular Biology*, *12*(4), 863–874.

Hardtke, C. S., & Berleth, T. (1998). The Arabidopsis gene MONOPTEROS encodes a transcription factor mediating embryo axis formation and vascular development. *The EMBO Journal*, *17*(5), 1405–1411. https://doi.org/10.1093/emboj/17.5.1405

Hernando, C. E., Sanchez, S. E., Mancini, E., & Yanovsky, M. J. (2015). Genome wide comparative analysis of the effects of PRMT5 and PRMT4/CARM1 arginine methyltransferases on the Arabidopsis thaliana transcriptome. *BMC Genomics, 16*, 192. doi: 10.1186/s12864-015-1399-2

Hesse, H., Kreft, O., Maimann, S., Zeh, M., & Hoefgen, R. (2004). Current understanding of the

regulation of methionine biosynthesis in plants. *Journal of Experimental Botany*, *55*(404), 1799–1808. https://doi.org/10.1093/jxb/erh139

Higuchi, K., Suzuki, K., Nakanishi, H., Yamaguchi, H., Nishizawa, N. K., & Mori, S. (1999). Cloning of nicotianamine synthase genes, novel genes involved in the biosynthesis of phytosiderophores. *Plant Physiol*, *119*(2), 471-480.

Hove, C. A. ten, Lu, K. J., & Weijers, D. (2015). Building a plant: cell fate specification in the early Arabidopsis embryo. *Development*, *142*(3), 420–430. https://doi.org/10.1242/dev.111500

Huttly, A. (2009). Reporter genes. *Methods Mol Biol, 478*, 39-69. doi: 10.1007/978-1-59745-379-0_3

Imai, A., Matsuyama, T., Hanzawa, Y., Akiyama, T., Tamaoki, M., Saji, H., . . . Takahashi, T. (2004). Spermidine synthase genes are essential for survival of Arabidopsis. *Plant Physiol, 135*(3), 1565-1573.

Jacobs, M., & Rubery, P. H. (1988). Naturally occurring auxin transport regulators. *Science (New York, N.Y.)*, *241*(4863), 346–349. https://doi.org/10.1126/science.241.4863.346

Jansson, J. K. (2003). Marker and reporter genes: illuminating tools for environmental microbiologists. *Current Opinion in Microbiology*, *6*(3), 310–316.

Jürgens, G. (2001). Apical–basal pattern formation in Arabidopsis embryogenesis. *The EMBO Journal*, *20*(14), 3609–3616. https://doi.org/10.1093/emboj/20.14.3609

Kakehi, J., Kuwashiro, Y., Niitsu, M., & Takahashi, T. (2008). Thermospermine is required for stem elongation in Arabidopsis thaliana. *Plant & Cell Physiology*, *49*(9), 1342–1349. https://doi.org/10.1093/pcp/pcn109

Kang, H. A., & Hershey, J. W. (1994). Effect of initiation factor eIF-5A depletion on protein synthesis and proliferation of Saccharomyces cerevisiae. *Journal of Biological Chemistry*, *269*(6), 3934–3940. Retrieved from http://www.jbc.org/content/269/6/3934

Katekar, G. F., & Geissler, A. E. (1980). Auxin Transport Inhibitors. *Plant Physiology*, *66*(6), 1190–1195. Retrieved from https://www.ncbi.nlm.nih.gov/pmc/articles/PMC440814/

Kersey, P. J., Allen, J. E., Armean, I., Boddu, S., Bolt, B. J., Carvalho-Silva, D., . . . Staines, D. M. (2016). Ensembl Genomes 2016: more genomes, more complexity. *Nucleic Acids Res*, *44*(D1), D574-580. doi: 10.1093/nar/gkv1209

King, H. A., & Gerber, A. P. (2016). Translatome profiling: methods for genome-scale analysis of mRNA translation. *Briefings in Functional Genomics*, *15*(1), 22–31. https://doi.org/10.1093/bfgp/elu045

Klatte, M., Schuler, M., Wirtz, M., Fink-Straube, C., Hell, R., & Bauer, P. (2009). The Analysis of Arabidopsis Nicotianamine Synthase Mutants Reveals Functions for Nicotianamine in Seed Iron Loading and Iron Deficiency Responses. *Plant Physiology*, *150*(1), 257–271. https://doi.org/10.1104/pp.109.136374

Lamke, J., & Bäurle, I. (2017). Epigenetic and chromatin-based mechanisms in environmental stress adaptation and stress memory in plants. *Genome Biology*, *18*(1), 124. https://doi.org/10.1186/s13059-017-1263-6

Le Bris, M. (2017).Hormones in Growth and Development. *Reference Module in Life Sciences*,Elsevier,ISBN 9780128096338. https://doi.org/10.1016/B978-0-12-809633-8.05058-5

Leustek, T., & Saito, K. (1999). Sulfate Transport and Assimilation in Plants. *Plant Physiology*, *120*(3), 637–644. https://doi.org/10.1104/pp.120.3.637

Li, C. J., Guevara, E., Herrera, J., & Bangerth, F. (1995). Effect of apex excision and replacement by 1-naphthylacetic acid on cytokinin concentration and apical dominance in pea plants. *Physiologia Plantarum*. Retrieved from http://agris.fao.org/agris-search/search.do?recordID=DK19950152983

Li, W., & Lan, P. (2017). The Understanding of the Plant Iron Deficiency Responses in Strategy I Plants and the Role of Ethylene in This Process by Omic Approaches. *Frontiers in Plant Science*, *8*. https://doi.org/10.3389/fpls.2017.00040

Liao, C.Y., Smet, W., Brunoud, G., Yoshida, S., Vernoux, T., & Weijers, D. (2015). Reporters for sensitive and quantitative measurement of auxin response. *Nature Methods, 12*(3), 207-210, 202 p following 210. doi: 10.1038/nmeth.3279

Ling, H. Q., Koch, G., Bäumlein, H., & Ganal, M. W. (1999). Map-based cloning of chloronerva, a gene involved in iron uptake of higher plants encoding nicotianamine synthase. *Proceedings of the National Academy of Sciences of the United States of America*, *96*(12), 7098–7103. Retrieved from https://www.ncbi.nlm.nih.gov/pmc/articles/PMC22069/

Liu, J., & Müller, B. (2017). Imaging TCSn::GFP, a Synthetic Cytokinin Reporter, in Arabidopsis thaliana. In *Plant Hormones*(pp. 81–90). Humana Press, New York, NY. https://doi.org/10.1007/978-1-4939-6469-7_9

Liu, Y., Gu, D., Wu, W., Wen, X., & Liao, Y. (2013). The Relationship between Polyamines and Hormones in the Regulation of Wheat Grain Filling. *PLOS ONE*, *8*(10), e78196. https://doi.org/10.1371/journal.pone.0078196

Liu, Z. B., Ulmasov, T., Shi, X., Hagen, G., & Guilfoyle, T. J. (1994). Soybean GH3 promoter contains multiple auxin-inducible elements. *The Plant Cell*, *6*(5), 645–657. https://doi.org/10.1105/tpc.6.5.645

Liu, Z., Duguay, J., Ma, F., Wang, T.-W., Tshin, R., Hopkins, M. T., … Thompson, J. E. (2008). Modulation of eIF5A1 expression alters xylem abundance in Arabidopsis thaliana. *Journal of Experimental Botany*, *59*(4), 939–950. https://doi.org/10.1093/jxb/ern017

Lorenzo, O., Piqueras, R., Sánchez-Serrano, J. J., & Solano, R. (2003). ETHYLENE RESPONSE FACTOR1 Integrates Signals from Ethylene and Jasmonate Pathways in Plant Defense. *The Plant Cell*, *15*(1), 165–178. https://doi.org/10.1105/tpc.007468

Mähönen, A. P., Bonke, M., Kauppinen, L., Riikonen, M., Benfey, P. N., & Helariutta, Y. (2000). A novel two-component hybrid molecule regulates vascular morphogenesis of the Arabidopsis root. *Genes & Development*, *14*(23), 2938–2943. Retrieved from https://www.ncbi.nlm.nih.gov/pmc/articles/PMC317089/

Marjon, K., Cameron, Michael J., Quang, P., Clasquin, Michelle F., Mandley, E., Kunii, K., . . . Marks, Kevin M. (2016). *MTAP* Deletions in Cancer Create Vulnerability to Targeting of the MAT2A/PRMT5/RIOK1 Axis. *Cell Reports, 15*(3), 574-587. doi: 10.1016/j.celrep.2016.03.043

Mattsson, J., Sung, Z. R., & Berleth, T. (1999). Responses of plant vascular systems to auxin transport inhibition. *Development*, *126*(13), 2979–2991. Retrieved from http://dev.biologists.org/content/126/13/2979

Mavrakis, K. J., McDonald, E. R., 3rd, Schlabach, M. R., Billy, E., Hoffman, G. R., deWeck, A., . . . Sellers, W. R. (2016). Disordered methionine metabolism in MTAP/CDKN2A-deleted cancers leads to dependence on PRMT5. *Science, 351*(6278), 1208-1213. doi: 10.1126/science.aad5944

Mayer, Y., Torres Ruiz, R. A., Berleth, T., Misera, S., & Jurgens, G. (Institut fur G. und M. (1991). Mutations affecting body organization in the Arabidopsis embryo. *Nature (United Kingdom)*. Retrieved from http://agris.fao.org/agris-search/search.do?recordID=GB9121721

Michniewicz, M., Brewer, P. B., & Friml, J. (2007). Polar Auxin Transport and Asymmetric Auxin Distribution. *The Arabidopsis Book / American Society of Plant Biologists*, *5*. https://doi.org/10.1199/tab.0108

Minocha, R., Majumdar, R., & Minocha, S. C. (2014). Polyamines and abiotic stress in plants: a complex relationship1. *Frontiers in Plant Science*, *5*. https://doi.org/10.3389/fpls.2014.00175

Möller, B., & Weijers, D. (2009). Auxin Control of Embryo Patterning. *Cold Spring Harbor Perspectives in Biology*, *1*(5), a001545. https://doi.org/10.1101/cshperspect.a001545 Mori T., Kuroiwa H., Higashiyama, T., and Kuroiwa T. (2006). Generative Cell Specific 1 is essential for angiosperm fertilization. Nature Cell Biology 8(1): 64-71.

Mori, T., Kuroiwa, H., Higashiyama, T., & Kuroiwa, T. (2006). GENERATIVE CELL SPECIFIC 1 is essential for angiosperm fertilization. *Nature Cell Biology*, *8*(1), 64–71. https://doi.org/10.1038/ncb1345

Murashige, T., & Skoog, F. (1962). A Revised Medium for Rapid Growth and Bio Assays with Tobacco Tissue Cultures. *Physiologia Plantarum*, *15*(3), 473–497. https://doi.org/10.1111/j.1399-3054.1962.tb08052.x

Napoli, C. A., Beveridge, C. A., & Snowden, K. C. (1999). Reevaluating concepts of apical dominance and the control of axillary bud outgrowth. *Current Topics in Developmental Biology*, *44*, 127–169.

Nemhauser, J. L., Mockler, T. C., & Chory, J. (2004). Interdependency of Brassinosteroid and Auxin Signaling in Arabidopsis. *PLOS Biology*, *2*(9), e258. https://doi.org/10.1371/journal.pbio.0020258

Nemhauser, J., & Chory, J. (2002). Photomorphogenesis. *The Arabidopsis Book / American Society of Plant Biologists*, *1*. https://doi.org/10.1199/tab.0054

Nguyen, A. Q. D., Schneider, J., Reddy, G. K., & Wendisch, V. F. (2015). Fermentative Production of the Diamine Putrescine: System Metabolic Engineering of Corynebacterium Glutamicum. *Metabolites*, *5*(2), 211–231. https://doi.org/10.3390/metabo5020211

Nishimura, K., Murozumi, K., Shirahata, A., Park, Myung H., Kashiwagi, K., & Igarashi, K. (2005). Independent roles of eIF5A and polyamines in cell proliferation. *Biochemical Journal*, *385*(Pt 3), 779-785. doi: 10.1042/BJ20041477

Nobori, T., Takabayashi, K., Tran, P., Orvis, L., Batova, A., Yu, A. L., & Carson, D. A. (1996). Genomic cloning of methylthioadenosine phosphorylase: a purine metabolic enzyme deficient in multiple different cancers. *Proceedings of the National Academy of Sciences of the United States of America*, *93*(12), 6203–6208.

Notaguchi, M., & Okamoto, S. (2015). Dynamics of long-distance signaling via plant vascular tissues. *Frontiers in Plant Science*, *6*. https://doi.org/10.3389/fpls.2015.00161

Nybo, K. (2012). GFP Imaging in Fixed Cells. *BioTechniques*, *52*(6), 359–360. https://doi.org/10.2144/000113872

Ohashi-Ito, K., & Fukuda, H. (2010). Transcriptional regulation of vascular cell fates. *Current Opinion in Plant Biology*, *13*(6), 670–676. https://doi.org/10.1016/j.pbi.2010.08.011

Ostergaard, L., & Yanofsky, M. F. (2004). Establishing gene function by mutagenesis in Arabidopsis thaliana. *Plant J*, *39*(5), 682-696. doi: 10.1111/j.1365-313X.2004.02149.x

Pagnussat, G. C., Yu, H.-J., Ngo, Q. A., Rajani, S., Mayalagu, S., Johnson, C. S., … Sundaresan, V. (2005). Genetic and molecular identification of genes required for female gametophyte development and function in Arabidopsis. *Development*, *132*(3), 603–614. https://doi.org/10.1242/dev.01595

Peterson, R. L., Peterson, C. A., & Melville, L. h. (2008). *Teaching Plant Anatomy Through Creative Laboratory Exercises*. NRC Research Press. https://doi.org/10.1139/9780660197982

Peterson, R., Slovin, J. P., & Chen, C. (2010). A simplified method for differential staining of aborted and non-aborted pollen grains. *International Journal of Plant Biology*, *1*(2), e13–e13. https://doi.org/10.4081/pb.2010.e13

Pich, A., & Scholz, G. (1996). Translocation of copper and other micronutrients in tomato plants (Lycopersicon esculentum Mill.): nicotianamine-stimulated copper transport in the xylem. *Journal of Experimental Botany*, *47*(1), 41–47. https://doi.org/10.1093/jxb/47.1.41

Pommerrenig, B., Feussner, K., Zierer, W., Rabinovych, V., Klebl, F., Feussner, I., & Sauer, N. (2011). Phloem-Specific Expression of Yang Cycle Genes and Identification of Novel Yang Cycle Enzymes in Plantago and Arabidopsis[C][W]. *The Plant Cell*, *23*(5), 1904–1919. https://doi.org/10.1105/tpc.110.079657

Rademacher, E. H., Möller, B., Lokerse, A. S., Llavata-Peris, C. I., van den Berg, W., & Weijers, D. (2011). A cellular expression map of the Arabidopsis AUXIN RESPONSE FACTOR gene family. *The Plant Journal*, *68*(4), 597–606. https://doi.org/10.1111/j.1365-313X.2011.04710.x

Rakyan, V. K., Chong, S., Champ, M. E., Cuthbert, P. C., Morgan, H. D., Luu, K. V. K., & Whitelaw, E. (2003). Transgenerational inheritance of epigenetic states at the murine AxinFu allele occurs after maternal and paternal transmission. *Proceedings of the National Academy of Sciences of the United States of America*, *100*(5), 2538–2543. https://doi.org/10.1073/pnas.0436776100

Rangan, P., Subramani, R., Kumar, R., Singh, A. K., & Singh, R. (2014). Recent Advances in Polyamine Metabolism and Abiotic Stress Tolerance. *BioMed Research International*, *2014*, e239621. https://doi.org/10.1155/2014/239621

Ravanel, S., Block, M. A., Rippert, P., Jabrin, S., Curien, G., Rebeille, F., & Douce, R. (2004). Methionine metabolism in plants: chloroplasts are autonomous for de novo methionine synthesis and can import S-adenosylmethionine from the cytosol. *J Biol Chem*, *279*(21), 22548-22557. doi: 10.1074/jbc.M313250200

Ravanel, S., Gakière, B., Job, D., & Douce, R. (1998). The specific features of methionine biosynthesis and metabolism in plants. *Proceedings of the National Academy of Sciences*, *95*(13), 7805–7812. https://doi.org/10.1073/pnas.95.13.7805

Ren, B., Chen, Q., Hong, S., Zhao, W., Feng, J., Feng, H., & Zuo, J. (2013). The Arabidopsis Eukaryotic Translation Initiation Factor eIF5A-2 Regulates Root Protoxylem Development by Modulating Cytokinin Signaling. *The Plant Cell*, *25*(10), 3841–3857. https://doi.org/10.1105/tpc.113.116236

Rerie, W. G., Feldmann, K. A., & Marks, M. D. (1994). The GLABRA2 gene encodes a homeo domain protein required for normal trichome development in Arabidopsis. *Genes & Development*, *8*(12), 1388–1399.

Richter, S., Anders, N., Wolters, H., Beckmann, H., Thomann, A., Heinrich, R., … Jürgens, G. (2010). Role of the GNOM gene in Arabidopsis apical-basal patterning--From mutant phenotype to cellular mechanism of protein action. *European Journal of Cell Biology*, *89*(2–3), 138–144. https://doi.org/10.1016/j.ejcb.2009.11.020

Rubery, P. H., & Sheldrake, A. R. (1974). Carrier-mediated auxin transport. *Planta*, *118*(2), 101-121. doi: 10.1007/bf00388387

Saini, P., Eyler, D. E., Green, R., & Dever, T. E. (2009). Hypusine-containing protein eIF5A promotes translation elongation. *Nature*, *459*(7243), 118–121. https://doi.org/10.1038/nature08034

Sauter, M., Moffatt, B., Saechao, M. C., Hell, R., & Wirtz, M. (2013). Methionine salvage and S-adenosylmethionine: essential links between sulfur, ethylene and polyamine biosynthesis. *Biochemical Journal*, *451*(2), 145–154. https://doi.org/10.1042/BJ20121744

Scanlon, M. J. (2003). The Polar Auxin Transport Inhibitor N-1-Naphthylphthalamic Acid Disrupts Leaf Initiation, KNOX Protein Regulation, and Formation of Leaf Margins in Maize. *Plant Physiology*, *133*(2), 597–605. https://doi.org/10.1104/pp.103.026880

Scarpella, E., Barkoulas, M., & Tsiantis, M. (2010). Control of Leaf and Vein Development by Auxin. *Cold Spring Harbor Perspectives in Biology*, *2*(1). https://doi.org/10.1101/cshperspect.a001511

Scarpella, E., Francis, P., & Berleth, T. (2004). Stage-specific markers define early steps of procambium development in Arabidopsis leaves and correlate termination of vein formation with mesophyll differentiation. *Development*, *131*(14), 3445–3455. https://doi.org/10.1242/dev.01182

Scarpella, E., Marcos, D., Friml, J., & Berleth, T. (2006). Control of leaf vascular patterning by polar auxin transport. *Genes & Development*, *20*(8), 1015–1027. https://doi.org/10.1101/gad.1402406

Schaller, G. E., Bishopp, A., & Kieber, J. J. (2015). The Yin-Yang of Hormones: Cytokinin and Auxin Interactions in Plant Development. *The Plant Cell*, *27*(1), 44–63. https://doi.org/10.1105/tpc.114.133595

Schlereth, A., Möller, B., Liu, W., Kientz, M., Flipse, J., Rademacher, E. H., … Weijers, D. (2010). MONOPTEROS controls embryonic root initiation by regulating a mobile transcription factor. *Nature*, *464*(7290), 913–916. https://doi.org/10.1038/nature08836

Schuetz, M., Smith, R., & Ellis, B. (2013). Xylem tissue specification, patterning, and differentiation mechanisms. *Journal of Experimental Botany, 64*(1), 11-31. doi: 10.1093/jxb/ers287

Schuler, M., Rellán-Álvarez, R., Fink-Straube, C., Abadía, J., & Bauer, P. (2012). Nicotianamine functions in the Phloem-based transport of iron to sink organs, in pollen development and pollen tube growth in Arabidopsis. *The Plant Cell*, *24*(6), 2380–2400. https://doi.org/10.1105/tpc.112.099077

Sessa, G., Morelli, G., & Ruberti, I. (1993). The Athb-1 and -2 HD-Zip domains homodimerize forming complexes of different DNA binding specificities. *The EMBO Journal*, *12*(9), 3507–3517. Retrieved from http://www.ncbi.nlm.nih.gov/pmc/articles/PMC413627/

Siu, K. K., Lee, J. E., Sufrin, J. R., Moffatt, B. A., McMillan, M., Cornell, K. A., . . . Howell, P. L. (2008). Molecular determinants of substrate specificity in plant 5'-methylthioadenosine nucleosidases. *J Mol Biol, 378*(1), 112-128. doi: 10.1016/j.jmb.2008.01.088

Smith, M. M., & McCully, M. E. (1978). A critical evaluation of the specificity of aniline blue induced fluorescence. *Protoplasma*, *95*(3), 229–254. https://doi.org/10.1007/BF01294453

Smyth, D. R., Bowman, J. L., & Meyerowitz, E. M. (1990). Early flower development in Arabidopsis. *The Plant Cell*, *2*(8), 755–767. https://doi.org/10.1105/tpc.2.8.755

Spicer, R., Tisdale-Orr, T., & Talavera, C. (2013). Auxin-Responsive DR5 Promoter Coupled with Transport Assays Suggest Separate but Linked Routes of Auxin Transport during Woody Stem Development in Populus. *PLOS ONE*, *8*(8), e72499. https://doi.org/10.1371/journal.pone.0072499

Stirnberg, P., van De Sande, K., & Leyser, H. M. O. (2002). MAX1 and MAX2 control shoot lateral branching in Arabidopsis. *Development (Cambridge, England)*, *129*(5), 1131–1141.

Su, Y. H., Liu, Y. B., & Zhang, X. S. (2011). Auxin–Cytokinin Interaction Regulates Meristem Development. *Molecular Plant*, *4*(4), 616–625. https://doi.org/10.1093/mp/ssr007

Tabor, C. W., & Tabor, and H. (1984). Polyamines. *Annual Review of Biochemistry*, *53*(1), 749–790. https://doi.org/10.1146/annurev.bi.53.070184.003533

Takahashi, M., Terada, Y., Nakai, I., Nakanishi, H., Yoshimura, E., Mori, S., & Nishizawa, N. K. (2003). Role of Nicotianamine in the Intracellular Delivery of Metals and Plant Reproductive Development. *The Plant Cell*, *15*(6), 1263–1280. https://doi.org/10.1105/tpc.010256

Takahashi, T., & Kakehi, J.-I. (2010). Polyamines: ubiquitous polycations with unique roles in growth and stress responses. *Annals of Botany*, *105*(1), 1-6. doi: 10.1093/aob/mcp259

Tassoni, A., Antognoni, F., & Bagni, N. (1996). Polyamine Binding to Plasma Membrane Vesicles Isolated from Zucchini Hypocotyls. *Plant Physiology*, *110*(3), 817–824. Retrieved from https://www.ncbi.nlm.nih.gov/pmc/articles/PMC157781/

Tassoni, A., van Buuren, M., Franceschetti, M., Fornalè, S., & Bagni, N. (2000). Polyamine content and metabolism in Arabidopsis thaliana and effect of spermidine on plant development. *Plant Physiology and Biochemistry*, *38*(5), 383–393. https://doi.org/10.1016/S0981-9428(00)00757-9

The Arabidopsis Genome Initiative. "Analysis of the Genome Sequence of the Flowering Plant Arabidopsis Thaliana." *Nature* 408 (December 14, 2000): 796.

Thompson, E. P., Wilkins, C., Demidchik, V., Davies, J. M., & Glover, B. J. (2010). An Arabidopsis flavonoid transporter is required for anther dehiscence and pollen development. *Journal of Experimental Botany*, *61*(2), 439–451. https://doi.org/10.1093/jxb/erp312

Torii, K. U. (2004). Leucine-Rich Repeat Receptor Kinases in Plants: Structure, Function, and Signal Transduction Pathways. *Int Rev Cytol*, *234*, 1-46. doi: http://dx.doi.org/10.1016/S0074-7696(04)34001-5

Turnbull, C. G. N., Raymond, M. A. A., Dodd, I. C., & Morris, S. E. (1997). Rapid increases in cytokinin concentration in lateral buds of chickpea (Cicer arietinum L.) during release of apical dominance. *Planta*, *202*(3), 271–276. https://doi.org/10.1007/s004250050128

Turner, S., & Sieburth, L. E. (2003). Vascular Patterning. *The Arabidopsis Book / American Society of Plant Biologists*, *2*. https://doi.org/10.1199/tab.0073

Ulmasov, T., Murfett, J., Hagen, G., & Guilfoyle, T. J. (1997). Aux/IAA proteins repress expression of reporter genes containing natural and highly active synthetic auxin response elements. *The Plant Cell*, *9*(11), 1963–1971. https://doi.org/10.1105/tpc.9.11.1963

Vera-Sirera, F., Minguet, E. G., Singh, S. K., Ljung, K., Tuominen, H., Blázquez, M. A., & Carbonell, J.

(2010). Role of polyamines in plant vascular development. *Plant Physiology and Biochemistry: PPB*, *48*(7), 534–539. https://doi.org/10.1016/j.plaphy.2010.01.011

Waduwara-Jayabahu, I. C. (2011). Significance of methylthioadenosine to plant growth and development.*(Doctoral dissertation)*. Department of Biology, University of Waterloo, Canada.

Waduwara-Jayabahu, I., Oppermann, Y., Wirtz, M., Hull, Z. T., Schoor, S., Plotnikov, A. N., . . . Moffatt, B. A. (2012). Recycling of methylthioadenosine is essential for normal vascular development and reproduction in Arabidopsis. *Plant Physiology, 158*(4), 1728-1744. doi: 10.1104/pp.111.191072

Wang, H.J., Huang, J. C., & Jauh, G.Y. (2010). Pollen Germination and Tube Growth. In J.-C. Kader & M. Delseny (Eds.), *Advances in Botanical Research* (Vol. 54, pp. 1–52). Academic Press. https://doi.org/10.1016/S0065-2296(10)54001-1

Winiarczyk, K., Jaroszuk-Ściseł, J., & Kupisz, K. (2012). Characterization of callase (β-1,3-D-glucanase) activity during microsporogenesis in the sterile anthers of Allium sativum L. and the fertile anthers of A. atropurpureum. *Sexual Plant Reproduction*, *25*(2), 123–131. https://doi.org/10.1007/s00497-012-0184-5

Winter, D., Vinegar, B., Nahal, H., Ammar, R., Wilson, G. V., & Provart, N. J. (2007). An "Electronic Fluorescent Pictograph" browser for exploring and analyzing large-scale biological data sets. *PLoS One*, *2*(8), e718. doi: 10.1371/journal.pone.0000718

Yadegari, R., & Drews, G. N. (2004). Female Gametophyte Development. *The Plant Cell*, *16*(suppl 1), S133–S141. https://doi.org/10.1105/tpc.018192

Yang, J. H., & Wang, H. (2016). Molecular Mechanisms for Vascular Development and Secondary Cell Wall Formation. *Frontiers in Plant Science*, *7*. https://doi.org/10.3389/fpls.2016.00356

Ye, J. S. (2013). Investigating the spermidine-mediated fertility restoration of 5'-methylthioadenosine nucleosidase deficient *Arabidopsis thaliana* plants. *(Undergraduste research report)*. Department of Biology, University of Waterloo, Canada

Yeung, E. C. (1984). Histological and histochemical staining procedures. *Laboratory Procedures and Their Applications*, *1*, 689–697. https://doi.org/10.1016/b978-0-12-715001-7.50083-4

Zhao, Y. (2010). Auxin biosynthesis and its role in plant development. *Annual Review of Plant Biology*, *61*, 49–64. https://doi.org/10.1146/annurev-arplant-042809-112308

Zhou, J., Yu, F., Wang, X., Yang, Y., Yu, C., Liu, H., … Chen, J. (2014). Specific Expression of DR5 Promoter in Rice Roots Using a tCUP Derived Promoter-Reporter System. *PLoS ONE*, *9*(1). https://doi.org/10.1371/journal.pone.0087008

Zhou, Z. Y., Zhang, C. G., Wu, L., Zhang, C. G., Chai, J., Wang, M., . . . Guo, G. Q. (2011). Functional characterization of the CKRC1/TAA1 gene and dissection of hormonal actions in the Arabidopsis root. *Plant J, 66*(3), 516-527. doi: 10.1111/j.1365-313X.2011.04509.x

Ziemienowicz, A. (2001). Plant selectable markers and reporter genes. *Acta Physiologiae Plantarum, 23*(3), 363-374. doi: 10.1007/s11738-001-0045-6

Zierer, W., Hajirezaei, M. R., Eggert, K., Sauer, N., von Wirén, N., & Pommerrenig, B. (2016). Phloem-Specific Methionine Recycling Fuels Polyamine Biosynthesis in a Sulfur-Dependent Manner and Promotes Flower and Seed Development. *Plant Physiology*, *170*(2), 790–806. https://doi.org/10.1104/pp.15.00786

Zou, J. W., Sun, M.-X., & Yang, H.-Y. (2002). Single-embryo RT-PCR assay to study gene expression dynamics during embryogenesis inArabidopsis thaliana. *Plant Molecular Biology Reporter*, *20*(1), 19–26. https://doi.org/10.1007/BF02801929

Zurcher, E., Tavor-Deslex, D., Lituiev, D., Enkerli, K., Tarr, P. T., & Müller, B. (2013). A Robust and Sensitive Synthetic Sensor to Monitor the Transcriptional Output of the Cytokinin Signaling Network in Planta. *Plant Physiology*, *161*(3), 1066–1075. https://doi.org/10.1104/pp.112.211763

Appendices

Appendix I

Statistical analysis of effect of Spd on vascular bundle number of WT and MTN-deficient mutant plants

t test for WT c vs WT Spd

t-Test: Two-Sample Assuming Unequal Variances

	Variable 1	*Variable 2*
Mean	6.579	6.789
Variance	1.035	0.6199
Observations	30	30
Hypothesized Mean Difference	0	
df	58	
t Stat	-0.713	
P(T<=t) one-tail	0.240	
t Critical one-tail	1.691	
P(T<=t) two-tail	0.481	
t Critical two-tail	2.032	

t test for *mtn1-1mtn2-5* c vs *mtn1-1mtn2-5* Spd

t-Test: Two-Sample Assuming Unequal Variances

	Variable 1	*Variable 2*
Mean	10.133	7.9
Variance	2.124	0.544
Observations	25	20
Hypothesized Mean Difference	0	
df	43	
t Stat	5.044	
P(T<=t) one-tail	2.367E-05	
t Critical one-tail	1.717	
P(T<=t) two-tail	4.734E-05	
t Critical two-tail	2.074	

t test for *mtn1-1mtn2-1* c vs *mtn1-1mtn2-1* Spd fertile

t-Test: Two-Sample Assuming Unequal Variances

	Variable 1	*Variable 2*
Mean	14.428	13.091
Variance	3.187	2.491
Observations	30	21
Hypothesized Mean Difference	0	
df	49	
t Stat	1.985	
P(T<=t) one-tail	0.030	
t Critical one-tail	1.713	
P(T<=t) two-tail	0.060	
t Critical two-tail	2.069	

t test for WT c vs *mtn1-1mtn2-5 c*

t-Test: Two-Sample Assuming Unequal Variances

	Variable 1	*Variable 2*
Mean	6.55	10.133
Variance	0.998	2.124
Observations	30	25
Hypothesized Mean Difference	0	
df	53	
t Stat	-8.189	
P(T<=t) one-tail	1.432E-08	
t Critical one-tail	1.713	
P(T<=t) two-tail	2.864E-08	
t Critical two-tail	2.069	

t test for WT c vs *mtn1-1mtn2-1* c

t-Test: Two-Sample Assuming Unequal Variances

	Variable 1	*Variable 2*
Mean	6.55	14.429
Variance	0.997	3.187
Observations	30	30
Hypothesized Mean Difference	0	
df	58	
t Stat	-14.956	
P(T<=t) one-tail	2.9E-12	
t Critical one-tail	1.729	
P(T<=t) two-tail	5.8E-12	
t Critical two-tail	2.093	

Appendix II

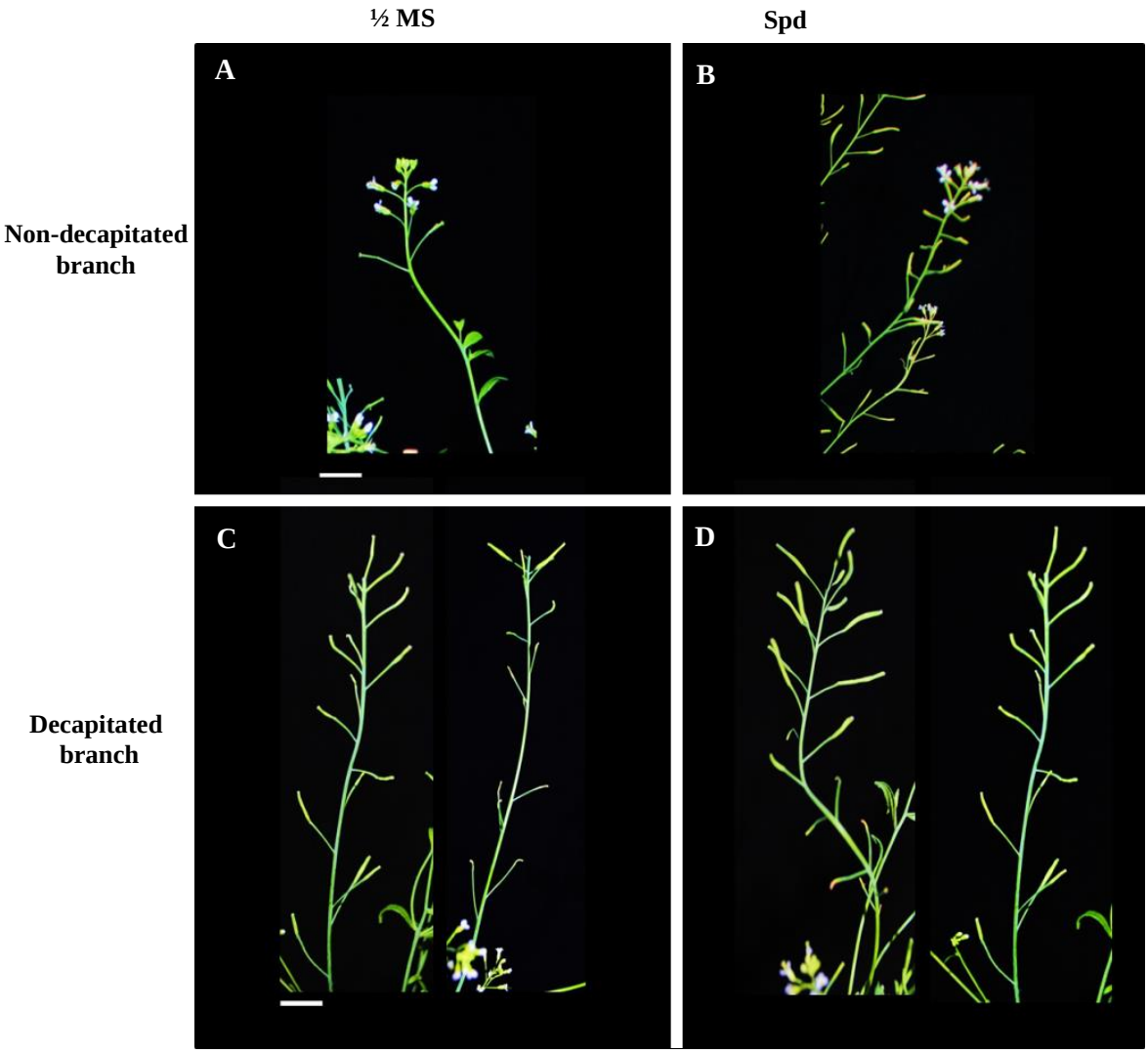

Figure 2-20. The fertility of decapitated *mtn1-1mtn2-1* G1 plants

In A, an infertile *mtn1-1mtn2-1* branch is shown. The branch has stunted, short siliques. In B, a fertile branch from a Spd treated *mtn1-1mtn2-1* plant (G1) is presented. The fertile branch has a few fertile, extended siliques. The branches shown in C are from a non-treated *mtn1-1mtn2-1* mutant. It can be seen that the terminal bud of the branch is removed. There are a a few siliques below the decapitation point that have elongated. In D, two branches from a G1 plant is shown. The terminal bud of the branch has been removed. The siliques below the decapitation point of the two branches have extended and appear similar to the fully mature, fertile siliques of normal *A. thaliana*.

Scale bar = 10 mm.

Appendix III

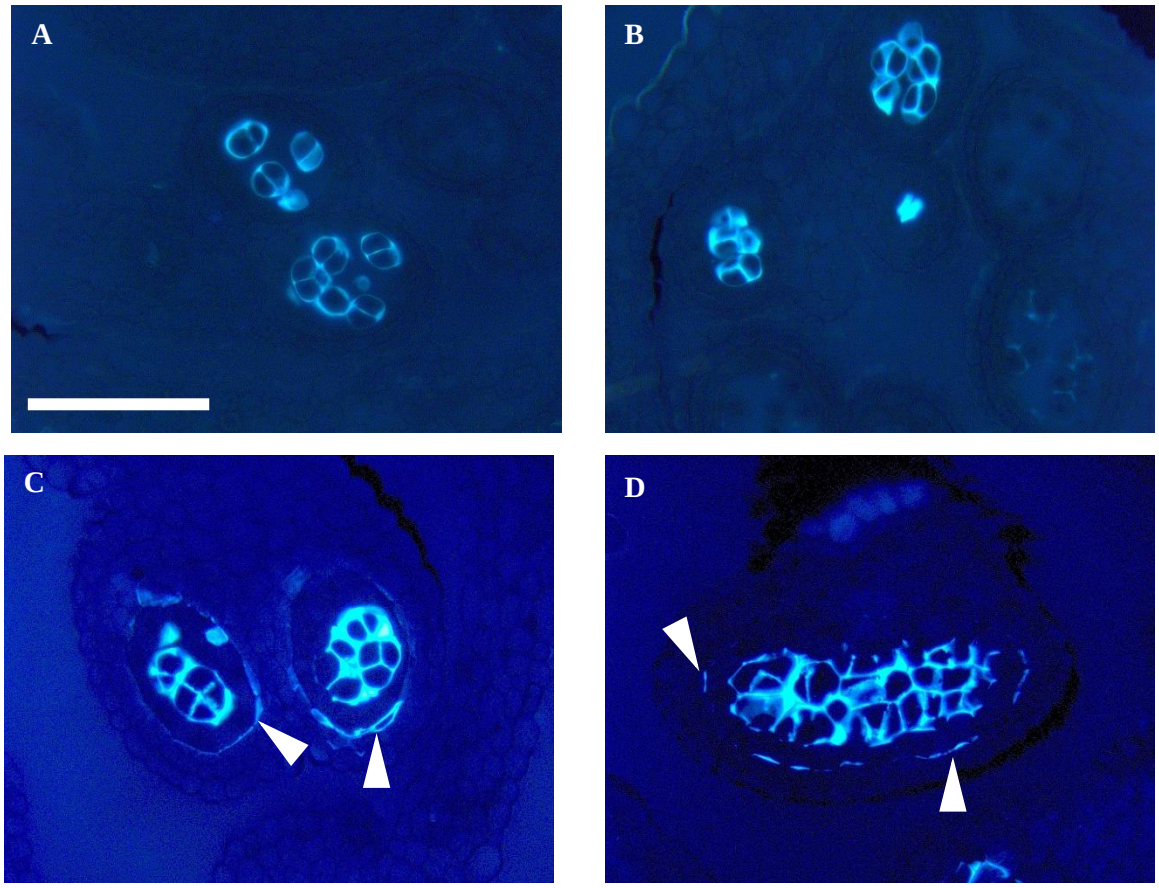

Figure 2-21. Abnormal callose deposition in anthers of *mtn1-1mtn2-1* plants

In A- D cross sections of developing anthers, with aniline blue staining is presented. The anthers in A and B are from WT plant s+/- Spd. Pollen tetrads can be seen in the anther chamber, surrounded with callose. Anthers from non-treated and Spd-treated *mtn1-1mtn2-1* plants (C and D respectively) are shown. There is excess callose deposition around the tetrads in both panels. Abnormal callose deposition is evident by callose staining is also present in the cell layer adjacent to the tapetum (arrowheads). Scale bar= 50 µM

Appendix IV

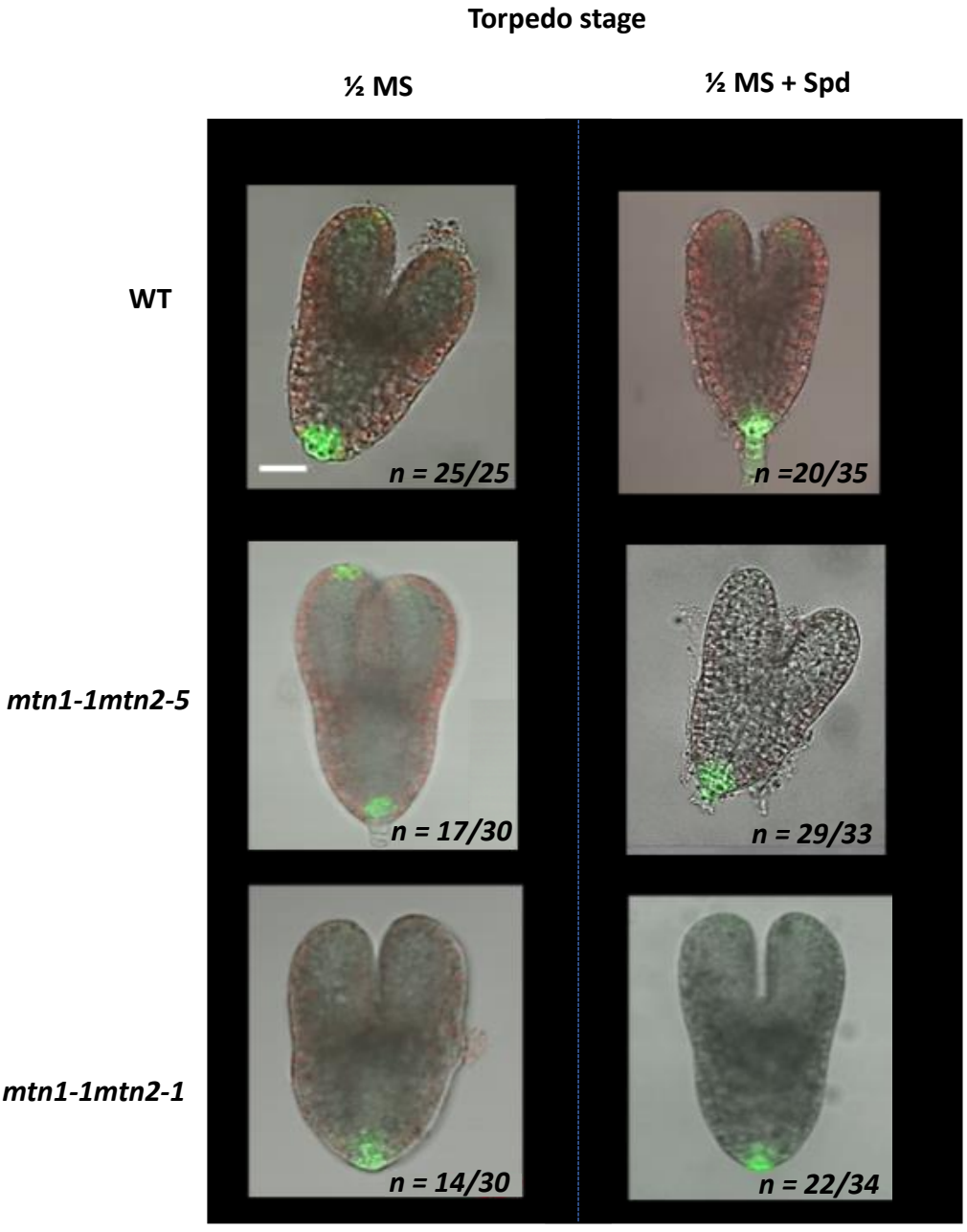
Torpedo stage
½ MS
½ MS + Spd
WT
mtn1-1mtn2-5
mtn1-1mtn2-1
n = 25/25
n =20/35
n = 17/30
n = 29/33
n = 14/30
n = 22/34

Figure 2-22. The DR5*rev*::GFP expression pattern in WT, *mtn1-1mtn2-5* and *mtn1-1mtn2-1* torpedo stage embryos from plants without and with Spd supplementation.

The GFP reporter expression is observed at the cotyledon tips, future root tip and hypophysis cells (Not present in all) of the WT embryos (A and B). The expression pattern of the *mtn1-1mtn2-5* mutant embryos with no treatment shown in C, is lower at the cotyledon and root tips, but the Spd supplementation improves the DR5*rev*::GFP reporter expression at these locations, indicating an increase in the auxin maxima (D). The *mtn1-1mtn2-1* embryos from non-Spd treated plants (E), show lower expression of the DR5*rev*::GFP reporter overall with undetectable expression levels at the cotyledon tips. The expression at the root tip appears diffused and faint. With the Spd treatment (F), however, the expression is stronger with the cotyledon tips showing fluorescence. The expression at the root tip is more restricted and defined compared to no treatment.

Scale bar = 200 μM.

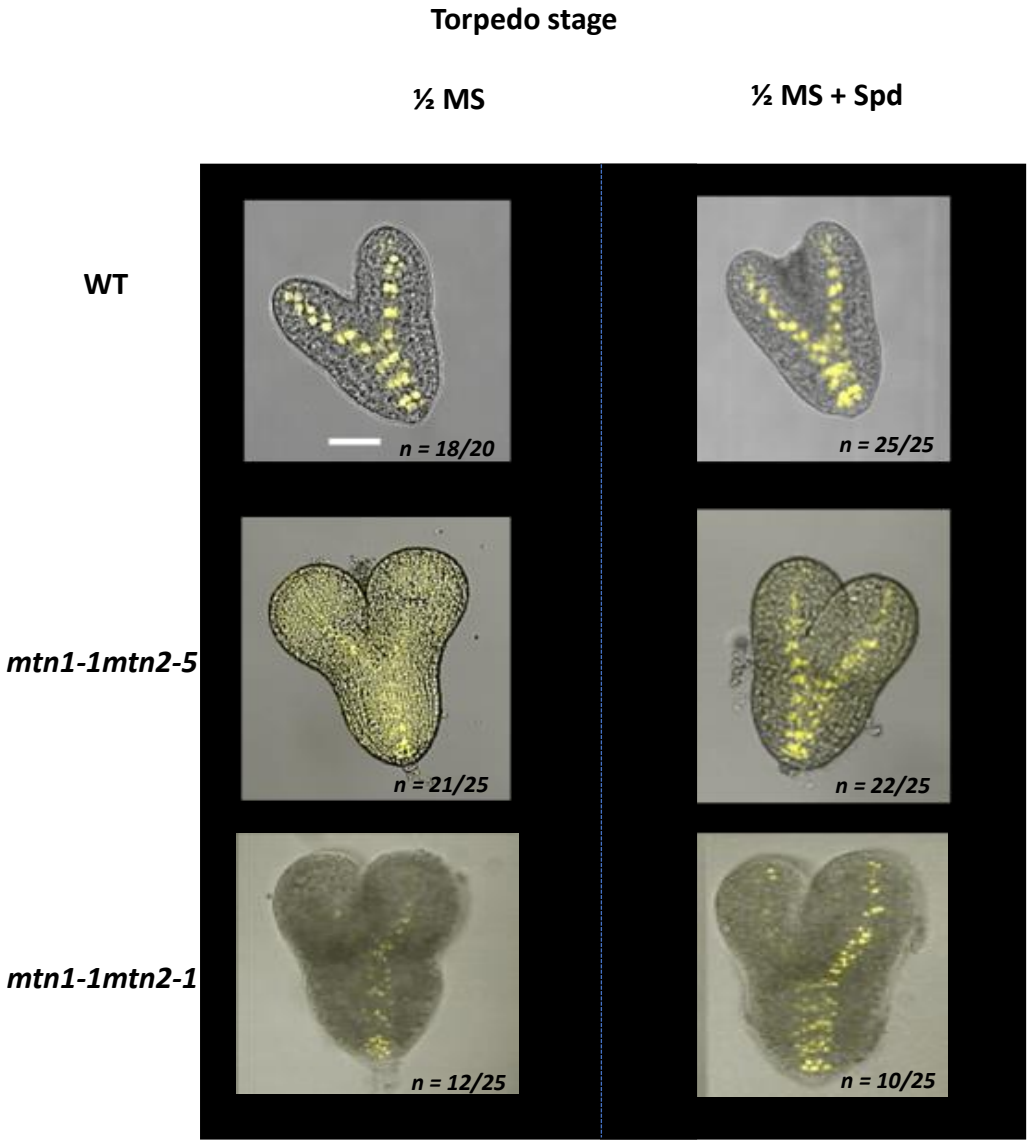
Torpedo stage
½ MS
½ MS + Spd
WT
mtn1-1mtn2-5
mtn1-1mtn2-1
n = 18/20
n = 25/25
n = 21/25
n = 22/25
n = 12/25
n = 10/25

Figure 2-23 The *AtHB8*-NUC::YFP reporter expression in torpedo stage embryos from WT, *mtn1-1mtn2-5* and *mtn1-1mtn2-1* plants treated with and without Spd.

The WT embryos (A and B) show typical *AtHB8* expression patter holding the signature "Y" shape, with the central cell columns activated and extending towards the cotyledon tips. The *mtn1-1mtn2-5* mutant embryos from non-treated plants (C), show lower activated cell number at the tips and the Spd supplementation shows improved expression of the reporter (D). The *mtn1-1mtn2-1* embryos from non-Spd treated plants (E) have even less munber of cells expressing the reporter. The embryos from Spd-treated plants (F) have increased number of YFP reporter expressing cells extending towards the future cotyledon tips.

Scale bar = 200 μM.

Appendix V

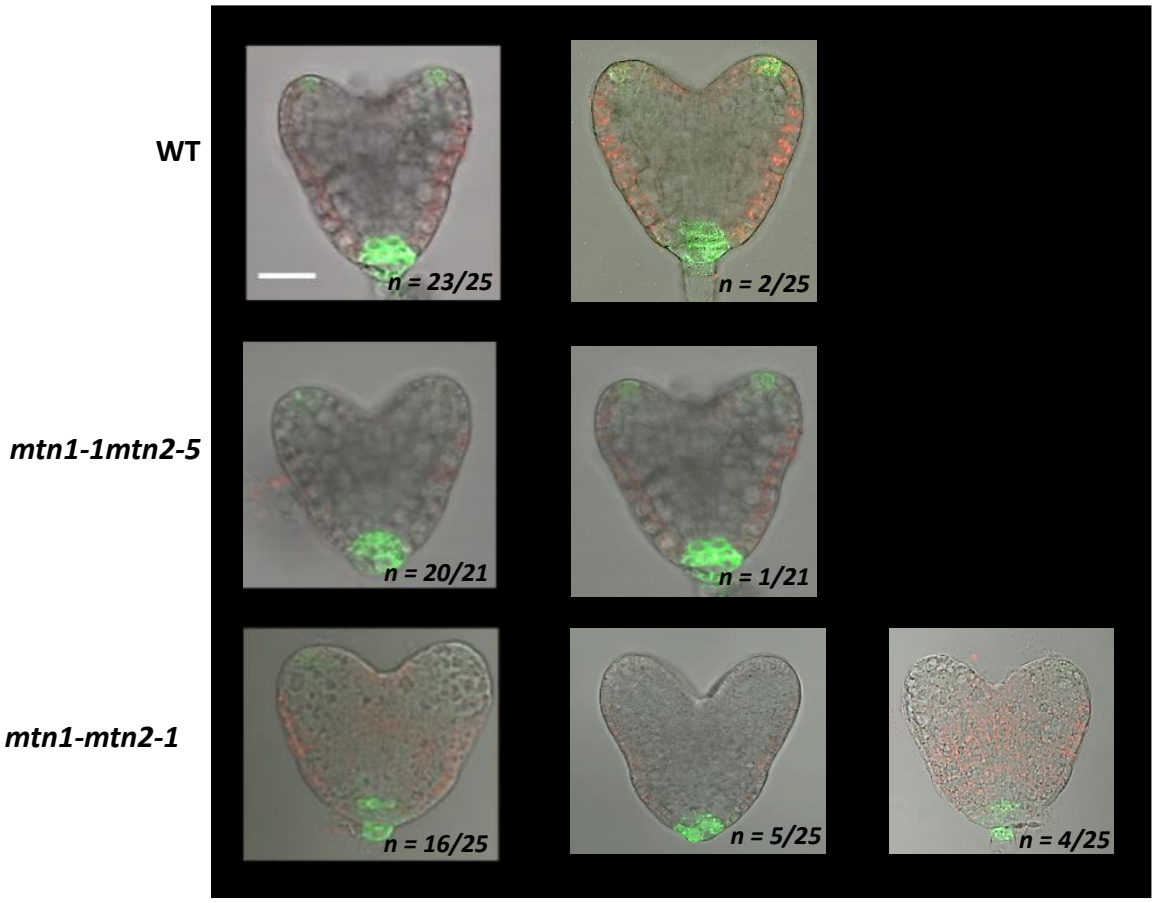

Figure 2-24. Representative images of embryo groups expressing DR5*rev*::GFP reporter.

The WT, *mtn1-1mtn2-5* and *mtn1-1mtn2-1*emrbyos excised from non-Spd-treated (½ MS) plants expressing DR5*rev*::GFP reporter. The embryos were grouped according to the variation observed in the expression pattern.

Scale bar= 200 µM

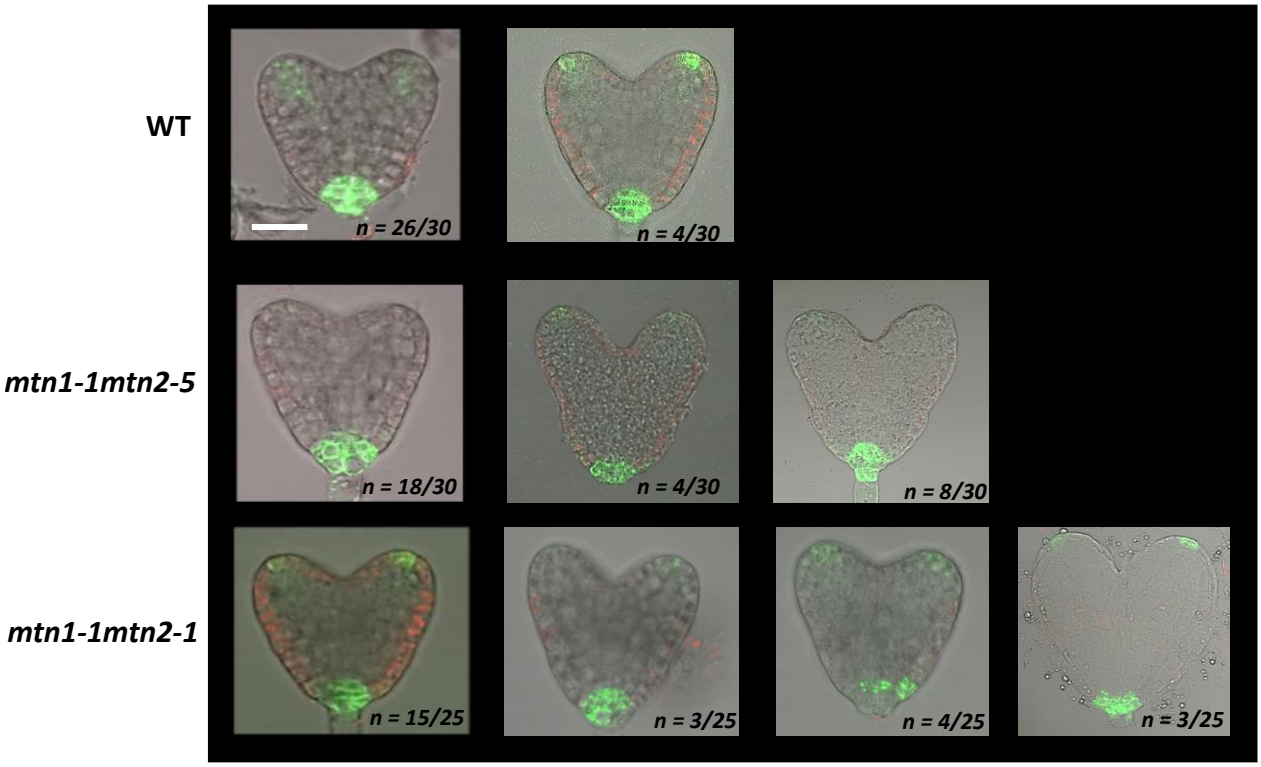

Figure 2-25. Representative images of embryo groups from plants treated with Spd, expressing DR5*rev*::GFP reporter.

The WT, *mtn1-1mtn2-5* and *mtn1-1mtn2-1*emrbyos excised from Spd-treated plants expressing DR5*rev*::GFP reporter. The embryos were grouped according to the variation observed in the expression pattern.

Scale bar= 200 µM

Appendix VI

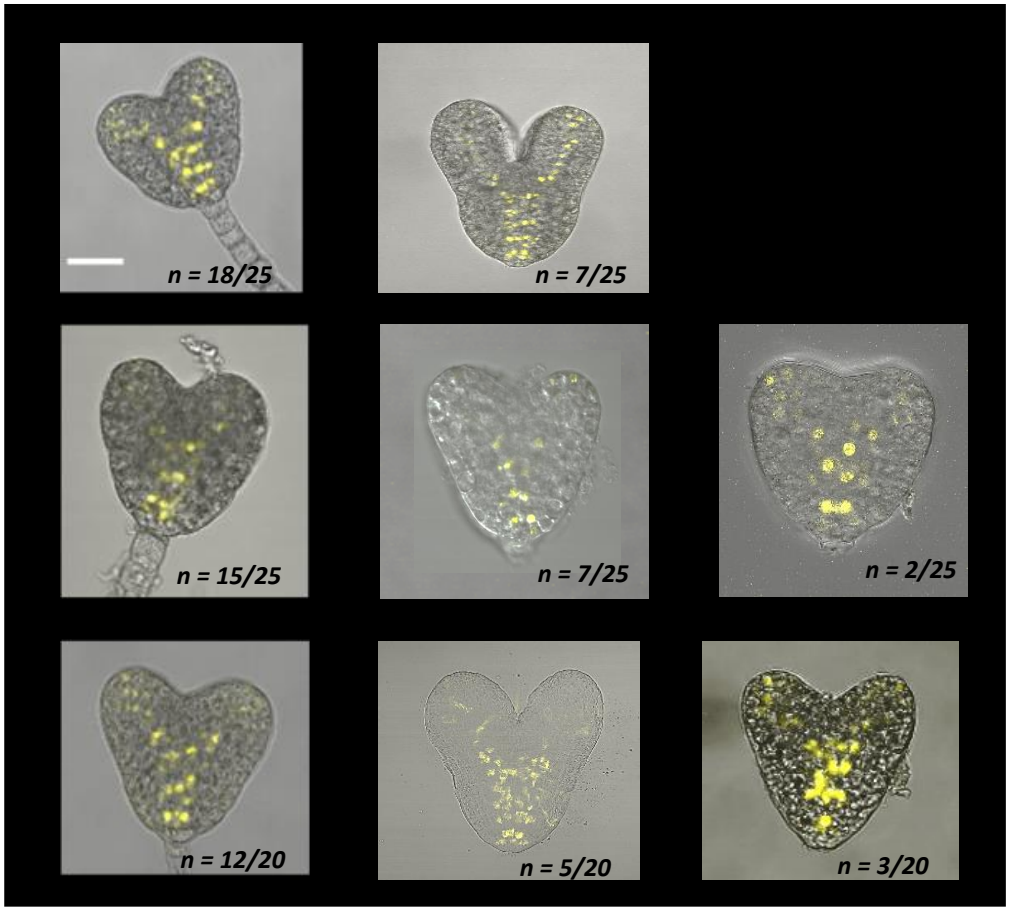

Figure 2-26. Representative images of embryo groups from non-Spd treated plants expressing AtHB8-NUC::YFP reporter.

The WT, *mtn1-1mtn2-5* and *mtn1-1mtn2-1*emrbyos excised from non-Spd-treated plants expressing AtHB8-NUC::YFP reporter. The embryos were grouped according to the variation observed in the expression pattern. Scale bar= 200 µM

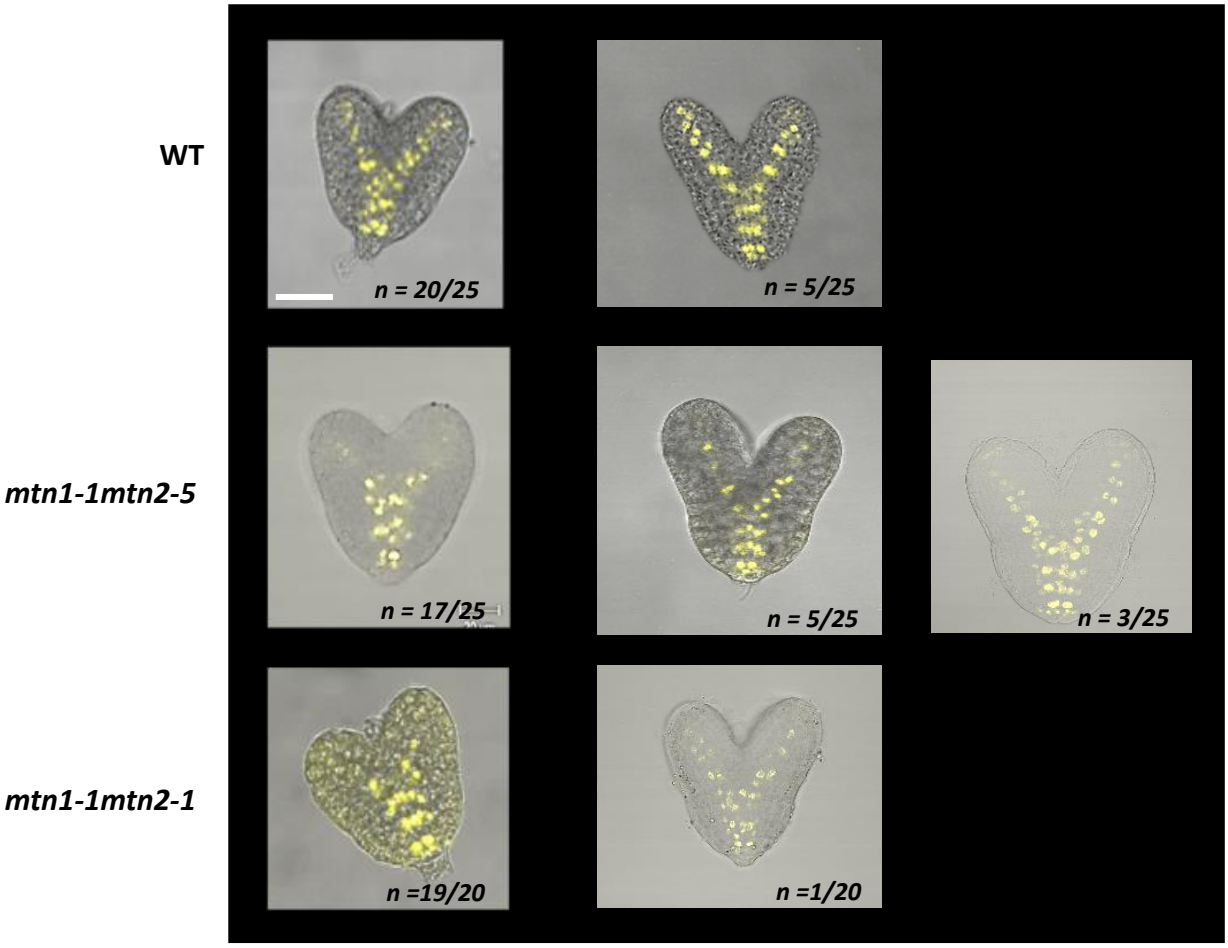

Figure 2-27. Representative images of embryo groups from Spd treated plants expressing AtHB8-NUC::YFP reporter.

The WT, *mtn1-1mtn2-5* and *mtn1-1mtn2-1*emrbyos excised from Spd-treated plants expressing AtHB8-NUC::YFP reporter. The embryos were grouped according to the variation observed in the expression pattern. Scale bar= 200 µM

Appendix VII

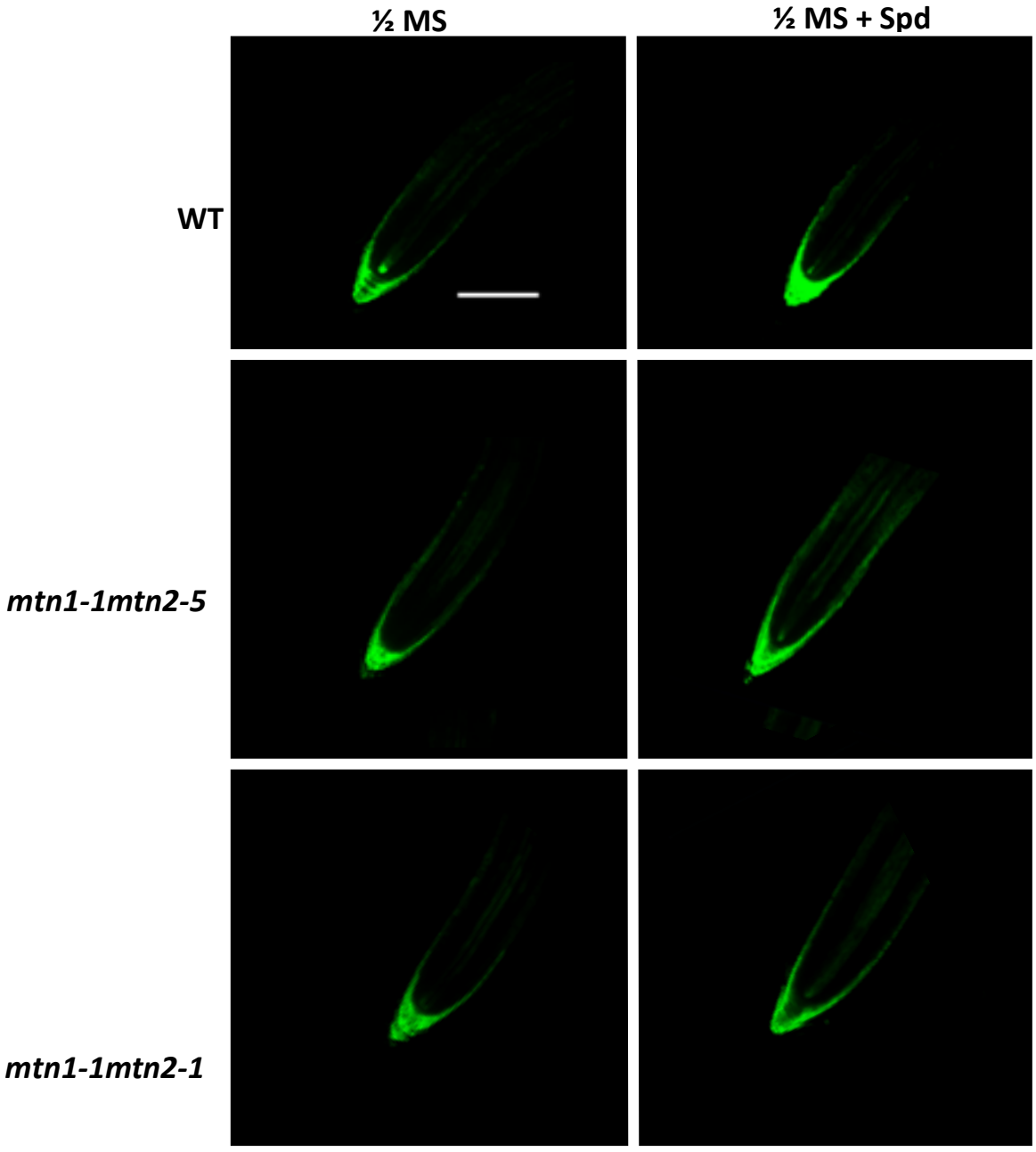

Figure 2-28. The expression pattern of CK reporter (TCSn::GFP) at root tips.

Spd treated and non-treated 5-day-old seedling roots of WT, *mtn1-1mtn2-5* and *mtn1-1mtn2-1* mutants

Scale bar = 200 μM

Appendix VIII

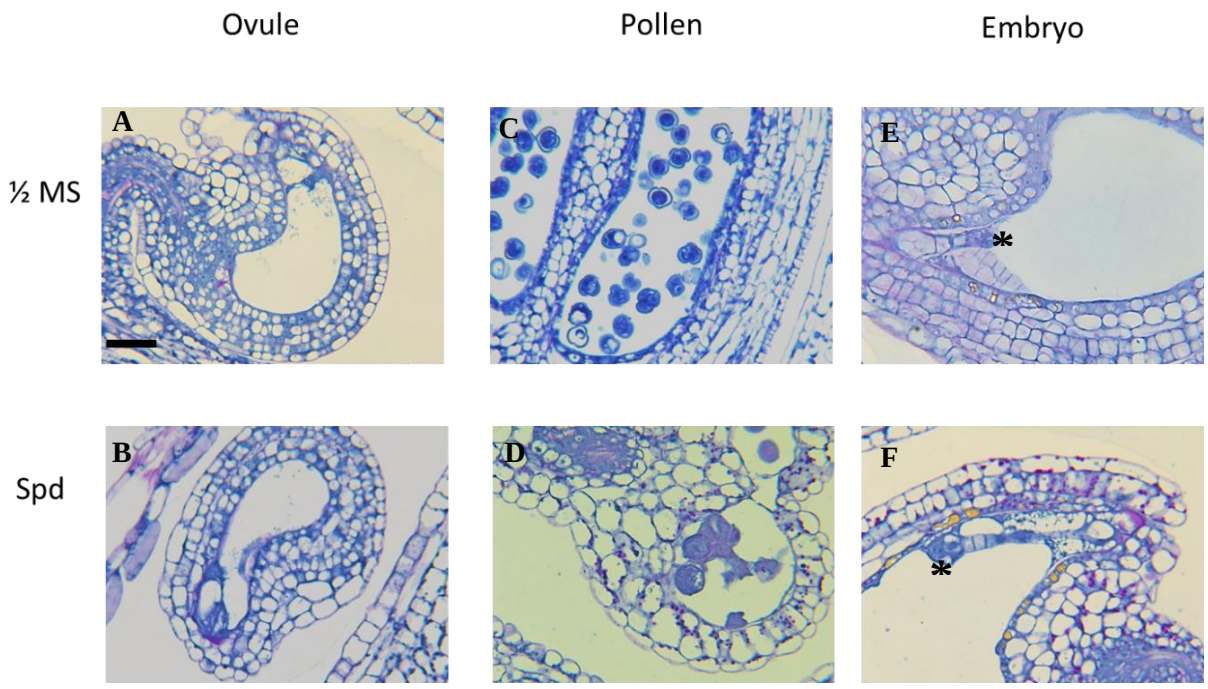

Figure 2-29. Ovule, pollen and developing seed sections from *mtn1-1mtn2-1* G2 generation plants

Representative images of ovules from non-Spd-treated and Spd treated Ovules (A and B, respectively), pollen (C and D, respectively) and developing seeds (E and F, respectively) of *mtn1-1mtn2-1* G2 generation plants. The developing seeds in both panles (E and F) carry a very young embryo (*).

Scale bar = 200 µM

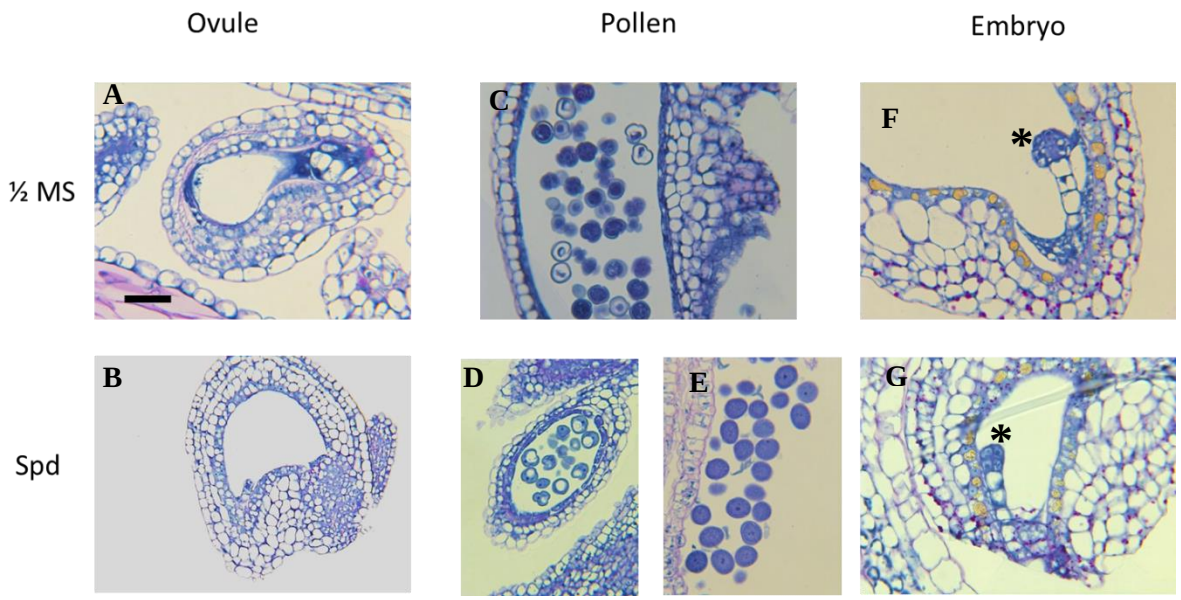

Figure 2-30. Ovule, pollen and developing seed sections from *mtn1-1mtn2-1* G3 generation plants

Representative images of ovules from non-Spd-treated and Spd treated Ovules (A and B, respectively), pollen (C, D and E respectively) and developing seeds (E and F, respectively) of *mtn1-1mtn2-1* G2 generation plants. The developing seeds in both panles (E and F) carry a very young embryo (*).

Scale bar = 200 µM